Proceedings of the Conference on Science in The National Parks

1986

Volume 3

Physical Processes and Water Resources

Marshall Flug
Editor

Colorado State University
Fort Collins, Colorado

July 13-18, 1986

Co•Sponsored by

The U. S. National Park Service and The George Wright Society

Conference on Science in The National Parks

The Fourth Triennial Conference on Research in The National Parks and Equivalent Reserves

July 13-18, 1986

Colorado State University
Fort Collins, Colorado

Managing Editors of the Conference Proceedings: Raymond Herrmann and Terri Bostedt-Craig; Associate Editor, Formatting: Christopher Linn; Publications Manager: Robert M. Linn; Electronic Communications Advisor: Kevin J. Kinnell.

Published by
The George Wright Society
and
The U. S. National Park Service

Printed in
The United States of America
1987

Toward the Year 2000

Conference on Science in The National Parks

—Proceedings—

Volume 3

Physical Processes and Water Resources

The Fourth Triennial Conference on Research in the National Parks and Equivalent Reserves

July 13-18, 1986

Marshall Flug
Editor

Colorado State University
Fort Collins, Colorado
USA

Co·Sponsored by

The U. S. National Park Service and The George Wright Society

Conference Chairmen

Raymond Herrmann and Calvin Cummings
Colorado State University, Fort Collins, CO

Program Planning Committee

Stanley Albright
National Park Service
Washington, DC

Destry Jarvis
National Parks and Conservation Assoc.
Washington, DC

Robert Stottlemyer
National Park Service
Houghton, MI

Boyd Evison
National Park Service
Anchorage, AK

William H. Key
University of Denver
Denver, CO

John T. Tanacredi
National Park Service
Brooklyn, NY

Jerry Franklin
U.S. Forest Service
Corvallis, OR

Bruce Kilgore
National Park Service
San Francisco, CA

James Thompson
National Park Service
Rocky Mtn. NP, CO

David J. Parsons
National Park Service
Sequoia NP, CA

Jack Morehead
National Park Service
Yosemite NP, CA

Arthur T. Wilcox
Colorado State Univ.
Fort Collins, CO

Glen E. Haas
Colorado State Univ.
Fort Collins, CO

Francis P. Noe
National Park Service
Atlanta, GA

Jim Wood
National Park Service
Atlanta, GA

The Triennial Conferences
on
Research in The National Parks
and Equivalent Reserves

1976—New Orleans, Louisiana
1979—San Francisco, California
1982—Washington, D. C.
1986—Fort Collins, Colorado

CONTENTS

PHYSICAL PROCESSES AND WATER RESOURCES

Marshall Flug[1]

ABOUT THE CONFERENCE

The 1986 Conference on Science in the National Parks was the fourth in a series conducted by the United States National Park Service (NPS) and the George Wright Society to discuss the role that science should play in supporting the understanding, management and preservation of park resources. The dialogue focused upon the special relationship between research and management that must succeed if appropriate information is to be available to the National Park Service decision process. The Conference highlighted the active regional science programs and displayed the results of many effective research and resources management projects.

The Conference provided the catalyst for productive discussions of the role of research in the National Park Service but just as important it stimulated important discussions and considerations about science issues. In some areas we have gained substantial knowledge, and must now learn how to apply it to innovative problem solutions. In other instances we remain ignorant and require directed research.

Many persons contributed their expertise and thoughts to the success of this Conference. There were over 400 attendees who gave approximately 325 poster presentations in 28 symposia and two plenary research panel discussions on the role of research with 12 plenary presentations on topics of importance to NPS researchers and resource managers. The Conference was attended by NPS Directorate, superintendents, researchers (natural, cultural and social sciences), resource managers, interpreters, representatives of university and other agency research, park service personnel of six foreign countries, and the public. The collection of papers in this volume were contributed principally from Symposium 25, Monitoring and Physical Processses of Water Resources. Papers presented describe impacts on natural resources relating to water, soils, air, and geology.

---

[1]National Park Service,
Colorado State University,
Fort Collins, Colorado 80523 USA

CONFERENCE SCOPE

The philosophical basis behind past thinking regarding NPS research weights on the purposes of the 1986 Conference on Science in the National Parks. It was once presumed that under ideal pristine conditions, an area might be left completely alone. But today we recognize some degree of protective management is required. The preservation of natural resources requires the active management of dynamic not static resources. The problems faced today by the NPS include all those resulting from rapid technological progress and resource development. Numerous resource conflicts can be cited; a few of the most commonly recognized are: destructive pollution effects; insularity, and the associated loss of species and their habitats; human/resource conflicts, including recreation and development both inside and at park boundaries; and, global climatic change (viz. warming and sea level rise). Taken together these concerns dictate a directed aggressive program of research to ascertain what management practices are feasible, what management tools should be utilized, what degree of management control should be exerted, and what timing is proper for management actions.

Resource studies often yield less-than-certain prescriptions and complicate work for park managers. Nevertheless, we must acknowledge uncertainties, and employ state of the art techniques and knowledge to support resource management actions in a decision arena often dominated by legal conflicts, politics and headlines.

Consideration of interacting social, cultural, technological, and biological forces change the process of resources studies and offers new possibilities for planning and programming of science activities. While our understanding of resources is often too narrow to encompass resource decisions, and we almost always lack up-to-date information, research priorities can be set to improve this imbalance. Promising new areas of inquiry will require the use of all the tools that technology can provide. It is argued in the plenary selection of papers that albeit complex, feasible approaches do exist to today's and tomorrow's resource analyses.

We each have our perceptions of what the role of research should be in the National Parks. The NPS research organization can provide strong and mandatory research support while continuing to support other mandated functions such as public education and understanding. Numerous discussions have occurred over the last year, and indeed before that, about the role that science should play in park management. The 1986 Conference on Science in the National Parks served to articulate the present relationship of science and management, and provide a forum about where science should be in the future.

SCOPE OF THIS MONOGRAPH

Park resources are experiencing ever increasing pressures, which include encroaching urban and industrial developments as well as growing visitor use with associated impacts. An enlightened awareness of our natural resources, particularly in this era of legal confrontations (e.g., mineral and water rights claims) require the proper arming of park management with facts to support actions for the continued preservation of both the quantity and quality of our trusted resources. These events emphasize the need for sound technical data and well documented methodology. Discussions throughout the 1986 Conference on Science in the National Parks addressed:

- How the National Park Service can actively participate in long-term basic data collection to quantitatively and qualitatively identify resources.
- How to best utilize available and forthcoming data for the detection of change and quantification of impacts.
- The need to develop methods to assess management alternatives that are tailored to natural resource preservation, concern for public health and safety needs.

Many of the authors of papers included in this monograph participated in a discussion entitled Monitoring and Physical Processes of Water Resources. The recurring comments from that discussion are identified here as they relate directly to the scope of events described in the research papers that follow. The applied research activities described in each paper emphasize the concern surrounding these comments.

Foremost among discussion participants is the need for the National Park Service to establish pre-impact and baseline information that will allow for the quantification of environmental changes at some time in the future. In conjunction with such efforts, a commitment to long-term (i.e., decades) and continuous (i.e., uninterrupted) data sampling are required. Both the long-term and continuous components are required in order to sample extreme events and impacts from both other natural and man-made causes that are typically random occurrences (i.e., non-scheduled). A big problem associated with field data collection in parks relates to the remoteness of many sites. Too often researchers and their crew spend several days or weeks hiking in and out only to collect a few isolated data samples. Some of these sampling problems can be overcome by utilizing base funding to establish data collection programs; and hiring permanent qualified technicians for assignment to data collection, as opposed to relying on seasonals, volunteers, or fill-in staff whenever available. These modifications will provide consistent and reliable data with a high degree of quality control. Experienced data collectors are prepared to document environmental conditions which can often help explain outliers, other unusual occurrences and provide uniformity from year to year. Other comments relating to data collection efforts apply to management's concern to sample only within a Park boundary. This aspect indicates a lack of understanding for our natural resource systems and the area of influence that can impact upon the land, water, and air. There was a feeling that our National Parks represent premier data sites and as such should be monitored and the information gathered then entered into a global data network.

As an extension of the concept for park service to establish base funding for data collection efforts belongs the attitude change from crisis management and emergency response to one of forward planning and commitment to projects over the long-term. If the data effort and research are base funded then they should continue even though a related controversial issue or project suddenly gets placed on hold (e.g., tar sands, energy development, nuclear waste) or conversely if some other park crisis arises. Another direct benefit from the recommended structural change is a move away from dependence on outside agency personnel and consultants that too often advise the National Park Service on what is needed. In-house employees that develop a long and close relationship with our natural resources are the best sources of quality advice. This recommended structural change also provides for consistency of sampling, maintenance of equipment, and dedication of equipment to the assigned data effort for the duration of the study effort. These changes will all help in providing quality controlled data that will contribute to the defining of interrelationships among environmental measurements (i.e., variables). As a direct result, researchers can advance and develop appropriate methods to detect and model both natural and man-induced changes.

The first paper in this monograph is contributed by John Elliott of the U.S. Geological Survey. His study to determine annual sediment loads transported by the Yampa River in Dinosaur National Monument was inspired by the need to quantify federal reserved water rights for the monument. A two year field data collection effort of sediment samples was combined with 43 years of flow discharge records for the river. Mean annual sediment load computations are based on sediment-transport relations developed from the two years of field data collected for this study. The second paper by Professor Thorne et al. also addresses sediment transport but focuses on meander processes in the Fall River within Rocky Mountain National Park. This study takes advantage of a unique field laboratory provided by the July 1982 failure of Lawn Lake Dam which massively increased the sediment supply to the Fall River. Field monitoring of flow and sediment has continued on a year by year basis since shortly after the flood. Research from this particular study site has provided some new insights into meander flow.

Moving away from rivers, the third paper by Carol Hill with the Cave Research Foundation investigates the dissolution of large cave passages in Carlsbad Caverns National Park. Her study supports the hypothesis that sulfuric acid rather than carbonic acid was primarily responsible for cave formation. Speleogenesis development in Guadalupe Mountains by sulfuric acid is related to reactions in the oil and gas fields of the Delaware Basin. Richard Spicer, author of the fourth paper researches the retreat of Blue Glacier on Mount Olympus in Olympic National Park. Written accounts and photographs dating back to 1899 document the early 20th century retreat of Blue Glacier. The National Park Service began field measurements in 1938 and repeated the program <u>nearly</u> every year through 1955, at which time the surveys were continued by the University of Washington and California Institute of Technology scientists. Papers three and four address natural events which are slow processes that occur over centuries and clearly require long-term monitoring.

A further emphasis on long-term data collection is evident by Gary Larson's limnologic study in Crater Lake National Park. This, the fifth paper, cites early short-term studies between 1913 and 1969.

However, the conclusions of a careful peer review found existing databases to be inadequate to draw definitive conclusions about changing lake water quality. As a result, Congress mandated a ten-year limnological study of the lake which began in 1982. Paper six authored by william Locke and Grant Meyer from Montana State University and the seventh paper by Robert Fournier of the U.S. Geological Survey deal with volcanic activity within the Yellowstone caldera in Yellowstone National Park. Locke and Meyer state that separation of short and long-term signals of pre-eruptive behavior is difficult, but critical for prediction. Long-term monitoring for vertical displacement is accomplished by surveying the raised shorelines of Yellowstone Lake. Patterns of deformation are related to historical (i.e., 55 years) and contemporary (i.e., 1 year) deformations. Estimates of average deformation over the past 2500 years is provided by carbon 14 dating of basal organic matter in abandoned lagoons. The seventh paper by Fournier investigates the relationship of water under hydrostatic pressure and thermal energy (i.e., heat) from past volcanic activity. Fournier states that hydrothermal activity appears to have been continuous for 10,000-70,000 years. He concludes that active crystallization and cooling are occurring while new magma also accumulates at other levels and therefore, there could be a slight potential for future explosive volcanic activity.

The last three papers in this monograph all relate to natural resource impacts from atmospheric derived inputs. In the eighth paper by Mary Lueking et al., a watershed study in Sequoia National Park is designed to evaluate the effects of acidic deposition on aquatic and terrestrial ecosystems. This ongoing study seeks to identify the major soil processes affecting nutrient cycling and the sensitivity of soils within the Emerald Lake Watershed to anthropogenic acid deposition. The ninth paper by Gail Baker et al. reports on another study in a rather unique field laboratory, the relatively pollutant free Hoh Rain Forest in Olympic National Park. These authors are documenting natural variation and assessing the impact of airborne pollutants on long-term ecosystem productivity using lichen and moss, litter fall and decay rates, and conifer needle analysis. Each ecosystem process is undergoing evaluation for use as an index of pollutant stress. In the tenth and final paper, Richard Keigley and Robert Porter make use of the National Atmospheric Deposition Program (NADP) data. This study compares the results from experimental treatment in Rocky Mountain National Park with potential real world changes on the growth of an alpine sedge as extrapolated from baseline data in the NADP dataset. All of these last three papers represent examples of: the premier quality of many National Park Service areas; the far reaching area of influence upon our natural resources; and the need for long-term study.

DETERMINATION OF ANNUAL SEDIMENT LOAD FOR THE YAMPA RIVER, DINOSAUR NATIONAL MONUMENT, COLORADO

John G. Elliott[1]

ABSTRACT

Discharge was measured and sediment samples were collected at streamflow-gaging station 09260050 Yampa River at Deerlodge Park during 1982 and 1983 to determine the mean annual sediment load of the Yampa River in Dinosaur National Monument, Colorado. Sediment-transport equations were derived for estimating total-sediment discharge, suspended-sediment discharge, bedload discharge, and the discharge of sand and gravel. Forty-three years of discharge records at two tributary sites upstream were combined to determine an average hydrograph and flow-duration curve for the Yampa River at Deerlodge Park. Mean annual sediment loads were determined by the flow-duration, sediment-rating-curve method. These computations indicate that mean annual suspended-sediment load was approximately 1.94 million tons, mean annual bedload was 0.1 million ton, and mean annual total-sediment load was 2.04 million tons for the period 1941-83. Sand- and gravel-size material comprised nearly 40 percent of the mean annual total-sediment load. Discharges greater than 9,900 cubic feet per second occur only 5 percent of the time but transport 38 percent of the mean annual total-sediment load.

INTRODUCTION

Channel morphology as well as the aquatic and riparian habitat of many reaches of the Yampa River in Dinosaur National Monument primarily are controlled by the prevailing streamflow regime and transported sediment. Water-resource development in the Yampa River basin could lead to substantial alteration of the Yampa River through Dinosaur National Monument. In 1982, a study was undertaken by the U.S. Geological Survey to determine prevailing streamflow of, and sediment load transported by, the Yampa River into Yampa Canyon in Dinosaur National Monument and to determine the relative quantity of annual sediment load transported by various ranges of discharge (Elliott and others, 1984). The results of that study are described in this paper.

[1]Hydrologist, U.S. Geological Survey, Water Resources Division, Box 25046, MS 415, Lakewood, CO 80225.

The Yampa River drains approximately 8,000 mi^2 of northwestern Colorado and south-central Wyoming and is a major tributary of the Colorado River (fig. 1). Mean-annual streamflow of the Yampa River at Deerlodge Park is approximately 1.5 million acre-ft. Elevation in the basin ranges from 5,065 ft at the river's mouth to greater than 12,000 ft in the headwaters in the Park Range. Precipitation varies from less than 12 in./yr in the western part of the basin to over 60 in./yr at higher elevations along the Continental Divide. Tertiary and Cretaceous sandstones, mudstones, and shales underlie a large part of the basin (Tweto, 1979) and are the source of most of the material transported by the Yampa River in its lower reaches. The Yampa River is incised into Permian and Pennsylvanian sandstones and limestones of the Uinta

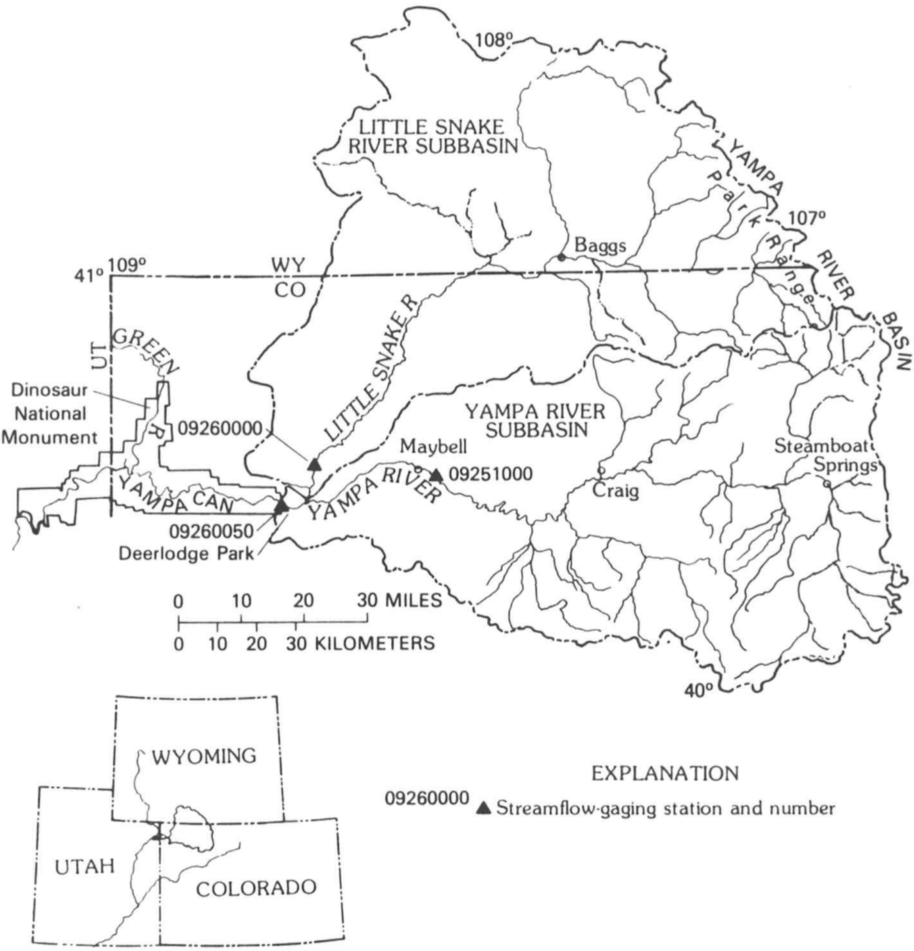

Figure 1.--Yampa River basin east of Dinosaur National Monument showing location of stream gages.

Mountain uplift for the last 45 mi of its course. With no major dams upstream and modest water consumption (approximately 10 percent of annual streamflow, Steele and others, 1979), the Yampa River in Dinosaur National Monument retains a relatively pristine character and is a unique feature in the Western United States.

Two streamflow-gaging stations upstream from Dinosaur National Monument have recorded discharge from a combined area that represents 89 percent of the entire Yampa River basin (fig. 1). Discharge data have been recorded since 1917 at station 09251000 Yampa River near Maybell, and since 1921 at station 09260000 Little Snake River near Lily. These gaging stations are located on rivers draining roughly equal areas, 3,410 mi^2 for the Yampa River basin upstream from the Maybell station, and 3,730 mi^2 for the Little Snake River basin upstream from the Lily station. The two subbasins, however, have striking differences in annual streamflow and sediment load. The Yampa River basin upstream from Maybell contributes approximately 73 percent of the annual streamflow (1.1 million acre-ft) and 27 percent of the annual sediment load of the entire Yampa basin. Conversely, the Little Snake River basin upstream from Lily contributes only 27 percent of the annual streamflow (0.4 million acre-ft) but nearly 69 percent of the annual sediment load (Andrews, 1978).

The size and quantity of sediment transported by the Yampa and Little Snake Rivers are reflected in the appearances of their channels. The Yampa River upstream from the confluence with the Little Snake River has a well-defined channel with cobble bed and point-bars; the banks are steep and composed of silt- and clay-size material. In contrast, the Little Snake River has a bed composed predominantly of sand-size material, and the channel has numerous braids and transverse channel bars that are exposed at intermediate and low flows. Downstream from the confluence with the Little Snake River and upstream from the beginning of Yampa Canyon in Dinosaur National Monument, the morphology of the Yampa River changes because of the large contribution of sediment from the Little Snake River. Along this 4.5-mi reach, the Yampa River has a shallow, anastomosing channel and a bed composed of sand-size material. Riverbanks in Yampa Canyon are predominantly bedrock or talus material. Sand, gravel, and cobbles are found locally in bars or along banks where the river gradient lessens or where the canyon width increases.

STREAMFLOW

A streamflow-gaging station and sediment-sampling site were established in 1982 in Deerlodge Park to obtain data for determining annual streamflow and sediment transport into Yampa Canyon. The gaging station is located approximately one-half mile upstream from the entrance to Yampa Canyon. River banks at the study site were vertical and resistant to erosion; whereas, most of the riverbed consisted of mobile sand-sized material. River stage at this station, 09260050 Yampa River at Deerlodge Park, was continuously recorded from April 1982 through September 1983, and 31 measurements of sediment discharge were made during this period. Daily mean water discharges for the Yampa River at Deerlodge Park were determined from continuously recorded river stage. The relation between water-surface elevation and discharge was determined from 35 discharge measurements made from a boat attached to a fixed cable or by wading. Measured discharge ranged from 646 to 17,600 ft^3/s.

Hydraulic-geometry relations were derived from the discharge measurements and are presented in table 1. The low value of the exponent (0.059) in the equation of channel width as a function of discharge resulted because banks at the study section were vertical; hence, channel width varied little with discharge. Most adjustment to increasing discharge occurred as change in mean depth and mean flow velocity. A large quantity of bed scour and fill was observed between discharge measurements (fig. 2); however, large R^2 and small SE values of most hydraulic geometry relations (table 1) indicate that responses of channel width, mean depth, mean velocity, and cross-sectional area to changes in discharge are predictable. Water-surface profiles were surveyed on 12 occasions at discharges ranging from 930 to 15,800 ft^3/s. Although the average water-surface slope of the reach varied from 0.00040 to 0.00087 ft/ft, no consistent relation between water-surface slope and discharge was apparent. Water-surface slope values varied about a mean of 0.00069 ft/ft with a standard deviation of 0.00014 ft/ft.

Table 1.--Hydraulic geometry relations at station 09260050 Yampa River at Deerlodge Park

[W, channel width in feet; $\bar{D}$, mean depth in feet; $\bar{u}$, mean velocity in feet per second; A_f, cross-sectional area in square feet; Q, instantaneous discharge in cubic feet per second; R^2, coefficient of determination; SE, standard error of estimate in percent; n, sample size]

Regression equation	R^2	SE	n
$W = 178\ Q^{0.059}$	0.18	12	35
$\bar{D} = 0.0227\ Q^{0.64}$	.96	13	35
$\bar{u} = 0.251\ Q^{0.30}$	.91	9	35
$A_f = 4.04\ Q^{0.70}$	.98	10	35

For 12 measurements, the water-surface slope varied about a mean of 0.00069 ft/ft, with standard deviation of 0.00014 ft/ft.

Daily mean discharges recorded for the Yampa River at Deerlodge Park were highly correlated with the sum of daily mean discharges recorded at the Maybell and Lily gaging stations (R^2=0.98). The concurrent period of record for these three gaging stations was 548 days and included peak-flow months for both 1982 and 1983. Consequently, historic discharges for the Yampa River at Deerlodge Park were estimated as the sum of historic discharges of the Yampa River near Maybell and the Little Snake River near Lily. An average hydrograph for the Yampa River at Deerlodge Park was computed from the daily sums of daily mean discharges recorded at the Maybell and Lily gaging stations for the period 1941 through 1983 (fig. 3). A flow-duration curve based on daily mean discharges for this 43-year period is presented in figure 4.

High peak discharges and greater-than-average annual streamflows occurred during water years 1982 and 1983. The 1982 instantaneous peak discharge for the Yampa River at Deerlodge Park was 16,500 ft^3/s, and the 1983 instantaneous peak discharge was 23,400 ft^3/s. In 1983, the flood plain at Deerlodge Park was inundated by floodwater for several days during the peak runoff. Recurrence intervals of annual maximum daily mean discharges for the Yampa River at Deerlodge Park were estimated for 1982 and 1983, using 43 years of discharge record and a Log Pearson Type III analysis (Interagency Advisory Committee on Water

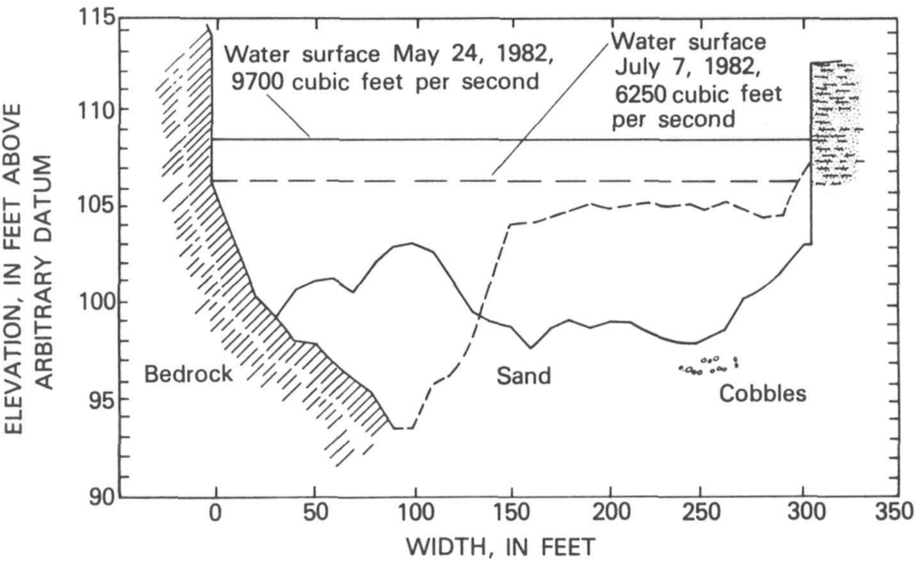

Figure 2.--Channel cross section showing magnitude of scour and fill of bed material.

Data, 1981). The 1982 maximum daily mean discharge had a recurrence interval of about 3 years, and the 1983 maximum daily mean discharge had a recurrence interval of about 20 to 25 years. The combined long-term mean annual streamflow of the Yampa River near Maybell and the Little Snake River near Lily is 1.5 million acre-ft (U.S. Geological Survey, 1982). In 1982, the combined annual streamflow of the Yampa River near Maybell and the Little Snake River near Lily was 1.9 million acre-ft, and in 1983, it was 2.3 million acre-ft.

SEDIMENT DISCHARGE

Suspended-sediment discharge and bedload discharge were measured 31 times in the Yampa River at Deerlodge Park during the spring and summer of 1982 and 1983. Suspended sediment was collected in verticals spaced every 15 ft across the channel with a DH-48 or D-74 depth-integrating sampler. Measured

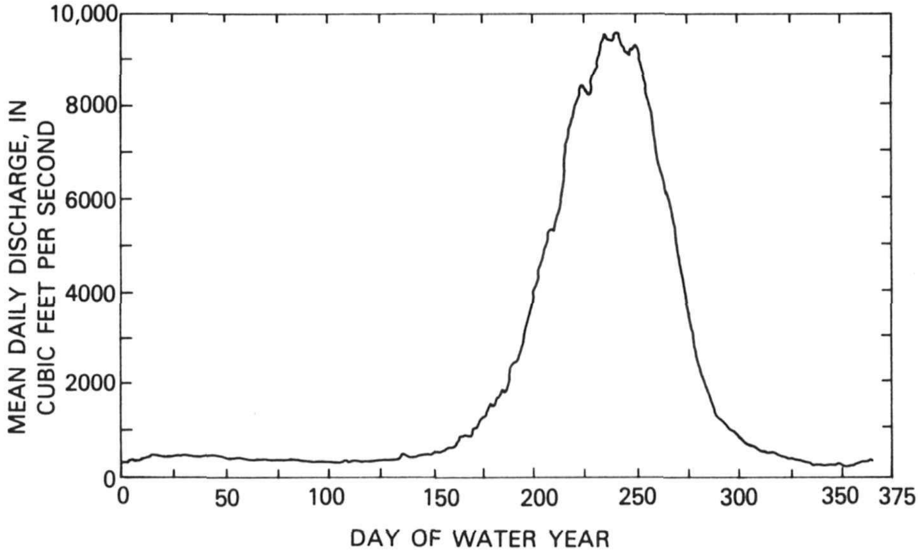

Figure 3.--Hydrograph of mean daily discharges for station 09260050 Yampa River at Deerlodge Park. Extrapolated from daily mean discharges at station 09251000 Yampa River near Maybell and station 09260000 Little Snake River near Lily, 1941-83.

suspended-sediment concentrations ranged from 137 to 5,600 mg/L. Bedload was collected at 15-ft intervals across the channel using a Helley-Smith bedload sampler (Helley and Smith, 1971; Emmett, 1980). In addition, bed-material samples were collected with a pipe dredge (6-in. diameter) at 50-ft intervals along the cross section.

Sediment discharges in the Yampa River at Deerlodge Park were computed from the 31 measurements made over a range of discharges. Suspended-sediment discharge was computed from the mean suspended-sediment concentration and measured water discharge. Bedload discharge was computed by dividing the dried sample weight by the total sample time and by the width of the Helley-Smith sampler orifice (0.25 ft), and multiplying by the channel width. Total-sediment discharge was determined as the sum of suspended-sediment discharge and bedload discharge.

Particle-size distributions of suspended sediment collected in the Yampa River at Deerlodge Park varied considerably. Silt- and clay-size material (sediment finer than 0.062 mm) comprised 10 to 92 percent of the

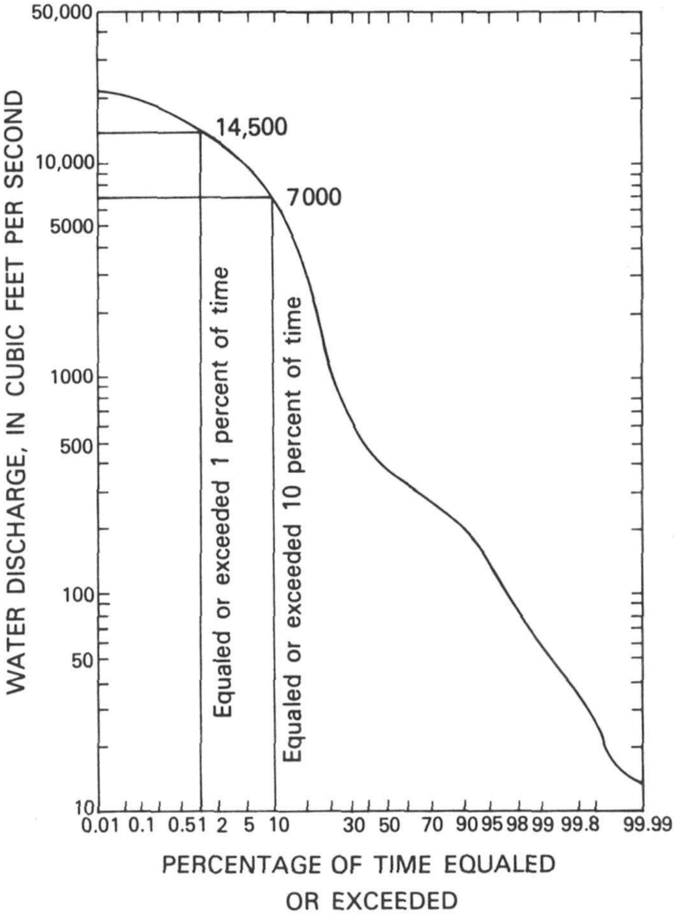

Figure 4.--Estimated flow-duration curve for station 09260050 Yampa River at Deerlodge Park for period 1941-83.

suspended sediment; the mean was 60 percent and the standard deviation was 23.7 percent. The remainder of suspended sediment was in the sand-size range (0.062 mm to 2.00 mm).

Particle-size distributions of bed material and bedload were similar. Both the bed material and bedload were predominantly medium-to-coarse sands; the average of median grain sizes (d_{50}) for bed-material samples was 0.61 mm (standard deviation = 0.17) and for bedload samples was 0.57 mm (standard deviation = 0.12). Gravel was included in some bed-material samples from the measurement section. Particle-size distributions of these bed-material samples were highly skewed. Silt- and clay-size material in bed-material samples averaged less than 1 percent by weight. Virtually all silt- and clay-size material in the Yampa River at Deerlodge Park was transported in suspension.

Sediment-transport equations were determined for total-sediment discharge, suspended-sediment discharge, bedload discharge, and for sediment coarser than 0.062 mm (mostly sand) (table 2). Neither nonlinear nor seasonal trends were apparent in the sediment-discharge and water-discharge data; therefore, sediment-transport equations that describe the variation in measured sediment discharge as a function of the water discharge were derived by a least-squares linear regression of the logarithms of all observations.

Table 2.--Sediment-transport equations derived from sediment discharges measured at station 09260050 Yampa River at Deerlodge Park

[Q_s, sediment discharge in tons per day; Q, instantaneous water discharge in cubic feet per second; R^2, coefficient of determination; SE, standard error of estimate in percent; n, sample size; mm, millimeter]

Type of sediment discharge	Regression equation	R^2	SE	n
Total------------	$Q_{st} = 0.290\ Q^{1.26}$	0.79	67	31
Suspended--------	$Q_{ss} = 0.125\ Q^{1.35}$	0.76	88	33
Bedload----------	$Q_{sb} = 0.702\ Q^{0.80}$	0.54	79	31
Material coarser than 0.062 mm--	$Q_{sg} = 0.0160\ Q^{1.48}$	0.82	73	31

Movement of bed material was observed over the entire range of discharges measured in 1982 and 1983 (fig. 2) and, from analysis of bedload samples, it seemed that all sizes of bed-material particles in the channel could be transported by the prevailing flow regime. A modification of the dimensionless shear stress relation (Shields, 1936) may be used to estimate bed material particle size at the threshold of movement for a given shear stress; therefore, the competence (maximum particle size transportable) of the Yampa River at Deerlodge Park may be estimated for various discharges. By definition:

$$d_c = \frac{\bar{D}\ S}{(\gamma_s/\gamma - 1)\ \tau^*_c}$$

where:

d_c = particle size of bed material in feet at threshold of movement,
$\bar{D}$ = mean channel depth in feet,
S = water-surface slope,
γ_s/γ = ratio of specific weights of sediment and water = 2.65, and
τ^*_c = dimensionless critical shear stress.

Neill (1968) determined the dimensionless critical shear stress (τ^*_c) be 0.03 for the median grain size (d_{50}) in uniform sand-sized materials. Using the average water-surface slope (S=0.00069), and the minimum observed mean channel depth ($\bar{D}$=1.80 ft), the threshold particle size (d_c) is equal to 7.69 mm. Sediment particles of this size on the bed are at the threshold of movement, and all smaller material is mobile under these flow conditions. The median grain size (d_{50}=0.61 mm) of bed material in the study reach is considerably smaller than d_c for this flow depth, and indicates that the majority of material that composes the streambed at Deerlodge Park is of a size capable of being transported at even the lowest flows.

ANNUAL SEDIMENT LOADS

Mean annual sediment loads for the period 1941-83 were computed for the Yampa River at Deerlodge Park by the streamflow-duration, sediment-rating-curve method described by Miller (1951). Sediment loads transported by increments of mean annual discharge were estimated by combining the relation between sediment discharge and water discharge (sediment-rating curve) with the midpoints of incremental discharge and weighing by the average frequency of discharge occurrence (flow-duration curve). Incremental sediment loads were summed to estimate the mean annual sediment loads.

The mean annual total-sediment load was 2.04 million tons, the mean annual suspended-sediment load was 1.94 million tons, and the mean annual bedload was 0.10 million ton (table 3). Material coarser than 0.062 mm, mostly sand, made up approximately 40 percent of the total-sediment load (0.79 million ton). Bedload, predominantly sand with some gravel, constituted about 5 percent of the total sediment load. Therefore, approximately 87 percent of the sand-sized material transported by the Yampa River was carried in suspension. This proportion for bedload as a percentage of total-sediment load seems reasonable based on instantaneous sediment-discharge measurements. Bedload discharge as a percentage of total-sediment discharge ranged from 1 to 32 percent and averaged 7 percent for 31 instantaneous sediment-discharge measurements.

Table 3.--Mean annual sediment loads, station 09260050 Yampa River at Deerlodge Park, 1941-83
[mm, millimeter]

Type of sediment	Mean annual sediment load (tons)
Total	2,040,000
Suspended	1,940,000
Bedload	100,000
Material coarser than 0.062 mm	790,000

The mean annual total-sediment load of 2.04 million tons based on 1982 and 1983 sediment measurements and 43 years of discharge data agrees with Andrews' (1978, p. 11) estimate of mean annual total-sediment load for the Yampa River at Deerlodge Park of 2.0 million tons. His estimate was based on suspended-sediment discharges measured at station 09251000 Yampa River near Maybell and station 09260000 Little Snake River near Lily, bedload estimates computed with the Meyer-Peter and Mueller (1948) formula, and an adjustment for the intervening ungaged drainage area.

Nearly all bed material particle sizes were mobile at the lowest discharges, and bed scour was observed between most discharge measurements (fig. 2). Although low discharges transport large quantities of sediment in the Yampa River at Deerlodge Park, intermediate and high discharges transport most of the annual total-sediment load. The relation of cumulative sediment load to discharge (fig. 5) illustrates the relative portion of annual total-sediment load transported by a specified discharge range, and indicates the significance of various discharge ranges in the annual sediment budget. Yampa River discharges greater than 9,900 ft^3/s occur 5 percent of the time (fig. 4), or an average of 18 days per year. These discharges transport 38 percent of the mean annual total-sediment load (fig. 5) and are, therefore, very important in the long-term sediment budget of the Yampa River. Large floods and discharges greater than the bankfull discharge, 17,600 ft^3/s, occur 0.15 percent of the time, an average of 1 day every 2 years, and transport only 2 percent of the mean annual total-sediment load. Whereas flood flows are a relatively minor component of the long-term sediment budget of the Yampa River, the extensive bed, bar, and bank scour that accompanies flooding is important in maintaining the riparian character in Deerlodge Park and Yampa Canyon (Elliott and others, 1984; Potter and others, 1983).

SUMMARY AND CONCLUSIONS

Discharge was measured and sediment data were collected at streamflow-gaging station 09260050 Yampa River at Deerlodge Park during 1982 and 1983 to determine the mean annual streamflow and the mean annual sediment load transported through Deerlodge Park and into the Yampa Canyon. Daily mean discharges recorded at this station correlated well (R^2=0.98) with the sum of daily mean discharges recorded during the same period at two streamflow-gaging stations in the drainage basin upstream: 09251000 Yampa River near Maybell and 09260000 Little Snake River near Lily. Mean annual streamflow for the Yampa River at Deerlodge Park was estimated to be 1.5 million acre-ft per year for the period 1941 through 1983.

Suspended sediment and bedload were measured 31 times throughout a range of discharges. Particle-size distribution of suspended sediment varied considerably. Silt- and clay-size material comprised 10 to 92 percent of suspended-sediment and averaged 60 percent. The remainder of suspended sediment was sand-size material. Bed material and bedload in the Yampa River at Deerlodge Park were mostly medium to coarse sand with some gravel. Movement of bed material was observed over the entire range of discharge measurements. An analysis of bed material particle size and shear stress indicated that nearly all sizes of material on the bed were transported at even the lowest discharges. The average of median grain sizes

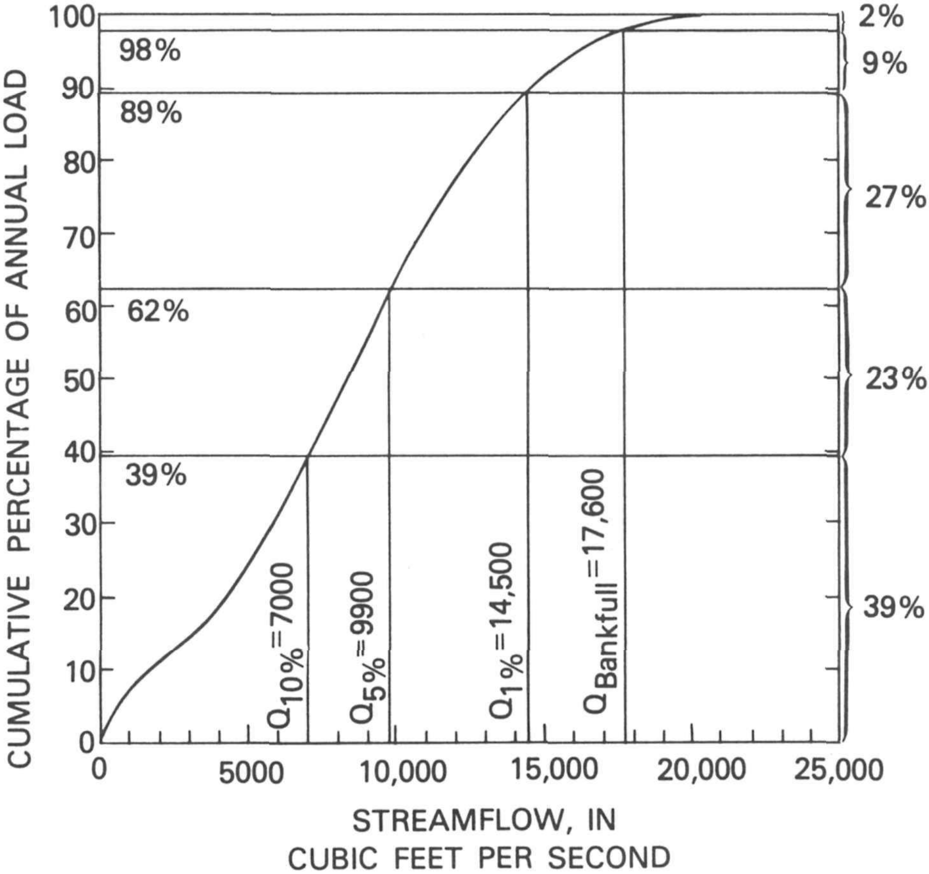

Figure 5.--Relation of cumulative sediment load to discharge, showing the percentage of annual total-sediment load transported by flows less than or equal to a given discharge, station 09260050 Yampa River at Deerlodge Park.

for bed-material samples (d_{50}) was 0.61 mm with a standard deviation of 0.17, and for bedload samples was 0.57 mm with a standard deviation of 0.12.

Daily sediment discharges were computed from instantaneous water discharge and suspended-sediment concentration measurements. Total-sediment discharge, suspended-sediment discharge, bedload discharge, and the discharge of sand and gravel material coarser than 0.062 mm were computed and are presented as power function relations of water discharge (table 2). Neither nonlinear nor seasonal trends were apparent in the data.

Mean annual sediment loads for the period 1941-83 were computed by the flow-duration, sediment-rating-curve method. Mean annual total-sediment load was 2.04 million tons, mean annual suspended-sediment load was 1.94 million tons, and mean annual bedload was 0.10 million ton. Sand and gravel load, material coarser than 0.062 mm, was 0.79 million ton. Virtually all silt- and clay-size material and approximately 87 percent of sand-size material was transported in suspension.

Nearly all bed-material particle sizes were mobile at the lowest discharges, and bed scour was observed between most discharge measurements (fig. 2). Although low discharges transport large quantities of sediment in the Yampa River at Deerlodge Park, intermediate and high discharges transport most of the annual total-sediment load (fig. 5). Streamflows greater than 9,900 ft^3/s occur 5 percent of the time (average 18 days per year) and transport 38 percent of the mean annual total-sediment load. In contrast, sediment transported by flood flows of the Yampa River is relatively insignificant in the long term. Flood flows greater than 17,600 ft^3/s occur 0.15 percent of the time (average 1 day every 2 years) and transport only 2 percent of the mean annual total-sediment load.

ACKNOWLEDGMENTS

Funding for this study was provided by the National Park Service. Paul Von Guerard provided invaluable assistance with logistical support and data collection. E.D. Andrews and J.E. Kircher offered thoughtful suggestions for analysis of the data. R.S. Parker, E.D. Andrews, and H.A. Martinson reviewed the manuscript.

LITERATURE CITED

Andrews, E. D., 1978. Present and Potential Sediment Yields in the Yampa River Basin, Colorado and Wyoming. U.S. Geological Survey Water-Resources Investigations Report 78-105, 33 pp.

Emmett, W. W., 1980. A Field Calibration of the Sediment-trapping Characteristics of the Helley-Smith Bedload Sampler. U.S. Geological Survey Professional Paper 1139, 44 pp.

Elliott, J. G., Kircher, J. E., and Von Guerard, Paul, 1984. Sediment Transport in the Lower Yampa River, Northwestern Colorado. U.S. Geological Survey Water-Resources Investigation Report 84-4141, 44 pp.

Helley, E. J., and Smith, W., 1971. Development and Calibration of a Pressure-difference Bedload Sampler. U.S. Geological Survey Open-File Report 73-108, 38 pp.

InterAgency Advisory Committee on Water Data, 1981. Guidelines for Determining Flood Flow Frequency (2d ed., revised) [editorial corrections made March 1982]. Reston, Va., U.S. Geological Survey Office of Water Data Coordination, Hydrology Subcommittee Bulletin 17B, appendixes 1-14, 28 pp.

Meyer-Peter, E., and Muller, R., 1948. Formulas for Bed-load Transport. In: International Association for Hydraulic Structures Research, 2nd Congress, Proceedings. Stockholm, Sweden, pp. 39-64.

Miller, C. R., 1951. Analysis of Flow-duration, Sediment-rating Curve Method of Computing Sediment Yield. U.S. Bureau of Reclamation, Project Planning Division, Hydrology Branch, Sediment Section, 15 pp.

Neill, C. R., 1968. A Reexamination of the Beginning of Movement for Coarse Granular Bed Materials. Wallingford, United Kingdom, Hydraulics Research Station Report No. INT 68, 37 pp.

Potter, L. D., Fischer, N. T., Toll, M. S., and Cully, A. C., 1983. Vegetation Along Green and Yampa Rivers and Response to Fluctuating Water Levels, Dinosaur National Monument. University of New Mexico, Albuquerque, New Mexico, 179 pp.

Shields, A., 1936. "Anwendung der Achnlichkeits-mechanik und Turbulenz forschung auf die Geschiebewegung," Mitteilung Preussischen Versuchanstalt Wasser, Erd, Schiffbau, Berlin, No. 26 (in German).

Steele, T. D., Bauer, D. P., Wentz, D. A., and Warner, J. W., 1979. The Yampa River Basin, Colorado and Wyoming--A review to Expanded Coal-resource Development and Its Impacts on Regional Water Resources. U.S. Geological Survey Water-Resources Investigations 78-126, 133 pp.

Tweto, Ogden, 1979. Geologic Map of Colorado. U.S. Geological Survey Special Geologic Map, Scale 1:500,000 (1 inch = about 8 miles), 1 sheet.

U.S. Geological Survey, 1982. Water Resources Data for Colorado, Water Year 1982--volume 3. U.S. Geological Survey Water-Data Report CO-82-3.

MEANDER PROCESSES IN THE FALL RIVER, ROCKY MOUNTAIN NATIONAL PARK, FOLLOWING LAWN LAKE DAM DISASTER

Colin R. Thorne[1], Lyle W. Zevenbergen[2] and John C. Pitlick[3]

ABSTRACT

Natural channels usually adopt a meandering course. Waterflow in meander bends is three-dimensional consisting of longstream and cross-stream velocities. The pattern of flow strongly affects the distribution of shear stress on the bed and banks of the channel. In turn the shear stress distribution controls the pattern of erosion and deposition which are responsible for the channel shifting and changing shape. Even today several important aspects of meander processes remain unexplained and further research is required especially on natural rivers rather than laboratory flumes. The Fall River in Rocky Mountain National Park provides an excellent opportunity to study active meanders. Following the July 1982 failure of Lawn Lake Dam on an upstream tributary, sediment supply to the Fall River has been massively increased. Field monitoring of flow and sediment processes on the Fall River began soon after the flood and has continued to the present. Many aspects have been covered but this paper deals particularly with the meander processes in a highly sinuous reach in Horseshoe Park. Measurements of bend flow show that helical flow is usually restricted to the deepest or thalweg portion of the channel. Flow at the inner bank is radially outwards while at the outer bank a small helix of reverse rotation is found. These results refute some earlier work on meander flow, but confirm the results of other recent studies. Point bar growth is found to be controlled by the flow pattern with lateral deposition on the point bar face

---

[1]Dept. Geography and Earth Science,
Queen Mary College, University of London,
London E1 4NS UK

[2]Engineering Research Center,
Colorado State University,
Fort Collins, Colorado 80523 USA

[3]Dept. Earth Resources,
Colorado State University,
Fort Collins, Colorado 80523 USA

between the radially outwards and helical inwards bed flow components being the primary bar building process. The outer bank reverse helix is very detrimental to bank stability and can cause severe erosion by undercutting. Taken together these observations of flow and sediment processes shed considerable light on the mechanisms of meander migration, and channel shifting.

BACKGROUND

On July 15th, 1982 Lawn Lake Dam in Rocky Mountain National Park failed catastrophically, sending a devastating flood down the valleys of the Roaring and Fall Rivers (Fig. 1). The flood took the lives of three people, destroyed a beautiful mountain valley and caused $36 million of damage to property. It was in human and natural terms a terrible disaster.

In the fall of 1982 the area was recognized as being of great scientific value to fluvial geomorphologists and river engineers interested in studying and quantifying the recovery of a mountain river system from a catastrophic event. Studies began in 1983 and have continued to date. All aspects of the river's recovery are being monitored, including both physical and ecological processes, by scientists from Colorado State University, University of Colorado and the National Park Service.

This paper deals with just one aspect of the study of physical processes in the Fall River following the flood. In Horseshoe Park the meander flow processes have been amplified and accelerated by the influx of sediment from the devastated Roaring River Valley. This provides an excellent opportunity to investigate flow-sediment interactions, to determine how sediment is either transmitted downstream or stored in an actively meandering river.

In the remainder of the paper, the current state of knowledge on meander flow is briefly reviewed, the study site is described and the method of data collection is outlined. The results are presented and discussed and the main findings are listed as a series of conclusions. Finally, acknowledgements to the sponsoring organizations and individuals are given.

FLOW PATTERNS IN MEANDER BENDS

Natural channels are seldom straight, but usually follow a meander course (Leopold et al., 1964). Flow

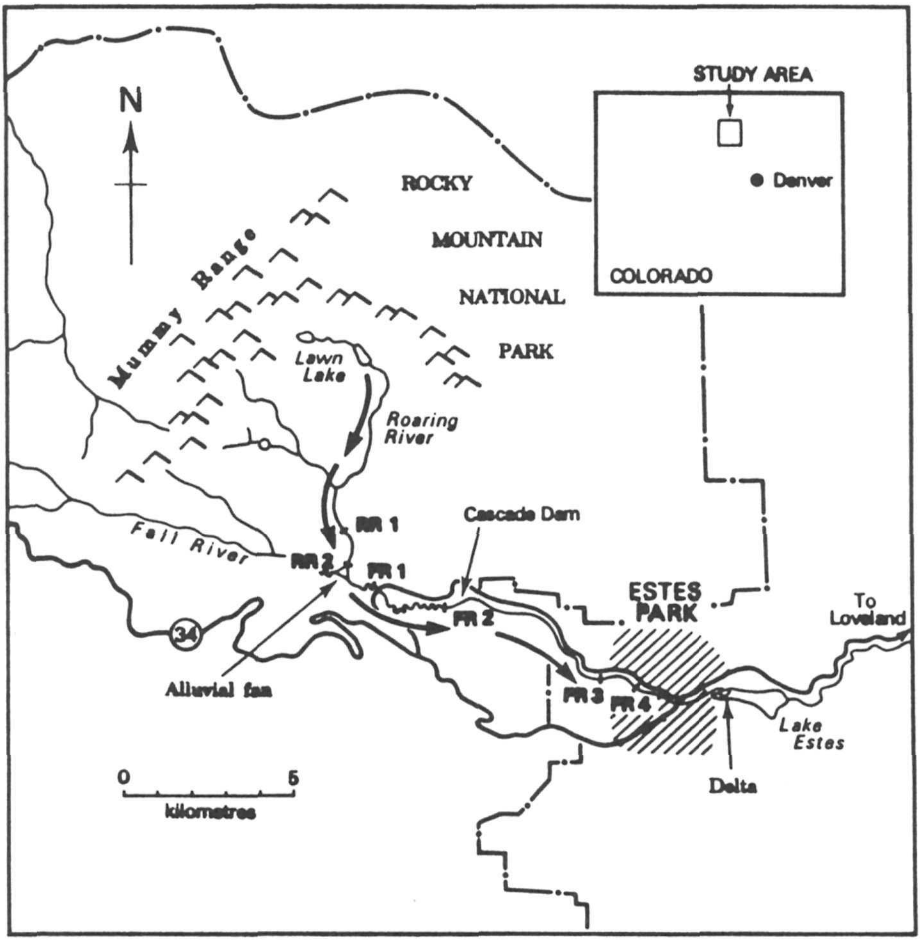

Figure 1. Location map for Fall River basin. Heavy arrows show course of Lawn Lake flood.

in a meandering channel is known to be three-dimensional, consisting of primary and secondary velocity components. Secondary velocities are defined as those that occur in a plane normal to the local axis of primary flow (Prandtl, 1952). In straight channels their existence is ascribed to nonuniform distribution of boundary shear stress and anisotropic turbulence, but in bendways they are caused by skewing of the flow (Prandtl, 1952; Perkins, 1970). Skewing creates a helical flow circulation, carrying fast surface water towards the outer bank and slower near-bed water towards the inner bank (Fig. 7a). The existence of helical flow in bends has been confirmed by many studies in natural rivers, canals and laboratory flumes (for example; Rozovskii, 1961; Leopold et al., 1964; Hey and Thorne, 1975; Bridge and Jarvis, 1976, among many others).

Helical flow strongly influences the distributions of primary velocity, boundary shear stress and sediment erosion, transport and deposition in bendways. Outward flow near the surface carries fast primary velocities close to the outer bank, where they generate high boundary shear stresses on that bank. Consequently, the bank is eroded and retreats. Near bed currents towards the inner bank sweep bedload inwards as it is transported down channel. Sediment accumulation as a point bar at the inner bank gives the channel an asymmetrical cross-section with a deep thalweg near the steep outer bank and a shallow point bar at the shelving inner bank. The balance between the inward sweeping of sediment by the helical flow and its tendency to roll outwards down the point bar under gravity has been used to model bed topography in bends (for example, Allen, 1970; and Bridge, 1984; among others).

However, in the 1970's and 1980's this somewhat simple picture of bend flow-sediment transport interaction has been questioned by researchers collecting data from natural river channels.

At the outer bank, observations seem to indicate that a small secondary flow cell may exist, with reverse circulation to that of the main skew-induced cell (Hey and Thorne, 1975; Bridge and Jarvis, 1976). This cell occupies the channel to a distance of one to two times the bank height away from the bank. This is a very small proportion of the channel cross-section in most rivers, but the outer bank cell is still important because it distorts the pattern of primary flow close to the outer bank hence influencing bank erosion processes.

At the inner bank, secondary velocities have been observed by some researchers to be directed radially outwards over the whole flow depth, with the helical flow confined to the deepest or thalweg portion of the channel (Dietrich and Smith, 1983) (Fig. 7b). As a result, bedload is concentrated in mid-channel, where the near-bed secondary currents converge, forming a steep transverse slope on the point bar, called the point bar face.

Bridge (1984) suggests that although this pattern of flow does exist at low flows, it is a product of point bar emergence at discharges below about two-thirds bankfull. He suggests that at higher, formative flows the helical flow expands from the thalweg to occupy the whole channel, and eliminate outward flow over the point bar.

Clearly, there is contention regarding the pattern of flow found in meander bends, its variation with discharge, and hence the nature of interaction between the flow pattern and the sedimentary processes responsible for channel evolution.

To help to resolve this contention a study of meander flow was undertaken on the meandering Fall River in Rocky Mountain National Park, Colorado. This river is ideally suited for such a study because it has a high sinuosity, a long series of tortuous bends, long periods of almost steady flow during spring snowmelt and a high sediment transport rate. This latter attribute is a result of the unlimited supply of sediment to the channel from an upstream area devastated by the 1982 Lawn Lake Dam disaster. It is essential to collect data from meanders with a high transport rate for a study of this kind, to ensure that the channel geometry and point bar shape have been adjusted to prevailing flow conditions by alterations in the dispositions of erosion, transport and deposition in the channel. Otherwise, channel form may well be inherited from an earlier flow and may be out of balance with the current pattern of primary and secondary currents.

HORSESHOE PARK STUDY REACH

Horseshoe Park is an old glacial lake bed in Rocky Mountain National Park, between FR1 and FR2 on the map in Figure 1. The Fall River flows through the Park with a low gradient of about 0.1 percent, in a series of highly tortuous meander bends. The sinuosity is 2.2, and bankfull capacity is about 4 $m^3 s^{-1}$. The river hydrograph is snowmelt dominated, with significant flows occurring between May and July each year. Prior to the Lawn Lake Dam failure the bed was formed in coarse gravel and cobbles with pronounced armouring making the bed static at all but the highest flows. The impact of the dam break flood itself was small here because the great width of the valley coupled with its low gradient minimized erosive activity. However, since the flood the supply of sand from the devastated Roaring River upstream has increased massively. Consequently, the bed is now formed in medium sand (D_{50} = 1 mm) moving in dunes, ripples and as suspended load. The relatively fine nature of the bed material compared to the original cobble bed, makes the bed mobile at all flows. Hence, the point bars in the bends can respond quickly to changes in discharge, maintaining equity between the imposed flow pattern and the bed morphology.

The channel banks are sandy-silt strongly bound by the roots of riparian vegetation - particularly willows (Salix). They are not easily eroded by inbank flows. Retreat takes place by undercutting below the root mat, followed by cantilever collapse of root-bound blocks. Failed blocks may remain in place at the bank foot for long periods, acting as natural riprap and retarding near bank flows. As a result, bank retreat rates are slow and rapid morphological changes are achieved by changes in bed topography and particularly adjustment point bar geometry.

These factors combine to make the reach an excellent one in which to study meander flow processes.

SEDIMENTATION

The first runoff season following the flood (1983) was remarkable in that it was the year of record for both discharge peak and duration. The combination sustained record flow magnitudes and unlimited sediment availability from areas devastated by the flood produced massive sediment production from the Roaring River and alluvial fan area, into Horseshoe Park. A detailed account of sediment supply, transport and storage in 1983 and 1984 may be found in a recent paper by Pitlick and Thorne (1986). Only a brief review is given here, to define the sediment transport conditions in the study reach.

The relatively low gradient of the Fall River in the Park coupled with high flow resistance to overbank flows due to vegetative effects meant that in 1983 the high transport rates could not be sustained and deposition occurred. A 2000 m long sedimentation zone developed in the Park, with the channel bed aggrading to floodplain level. At this time sediment transport rates out of the Park were very low. Late in the year the front of the sedimentation zone was entrenched and sediment transport downstream picked up. In 1984 the flows were much lower and sediment supply to the Park was greatly reduced. As a result, the upstream half of the sedimentation zone experienced degradation, back down to the preflood, cobble bed (Fig. 2). Downstream of the sedimentation zone, transport rates were high, but the highly sinuous channel was able to transmit the sediment without filling-in.

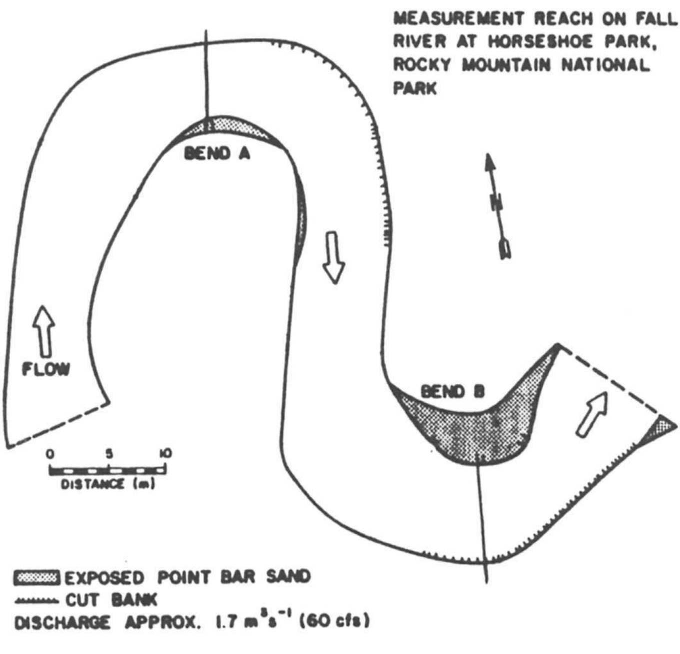

Figure 2. Study bends on the Fall River in Horseshoe Park high sediment transport reach.

The meander process measurements were made in this downstream reach, where sediment transport rates were high, but overall channel geometry remained stable. Here, there was no sediment starvation, but at reach scale input equalled output.

BEND MORPHOLOGY

Two consecutive bends were selected for the study. They are characteristic of bends throughout the reach. The first bend is relatively narrow and has an almost constant width at all in-bank flows. The second bend has a wide point bar and its width increases with discharge (Fig. 2).

Bed morphology is similar in the two bends. The outer banks are vertical, or overhanging and failed blocks of bank material may be found, mostly around the bend exits. The inner banks have a gently shelving point bar platform backed by a near vertical bank. The platform is much wider in the lower bend. The platform is separated from the deepest portion of the channel, the thalweg, by a steeply sloping point bar face. This is a mega-bedform scaled on the channel width rather than the depth and it is clearly distinguishable from the regular dunes found in the thalweg (Fig. 3). The point bar face is angled across the channel from the outer bank at the bend entrance to the inner bank at the bend exit. It is the salient feature of bed morphology in all the bends in the study reach and appears to be present at all discharges up to and including bankfull.

DATA COLLECTION

All measurements were made from temporary, portable bridges constructed from 15 m floor joists and five-ply boards. Seventeen sections were established and surveyed on a compass and tape map of the bend. The sections corresponded to the cross-over, bend entrance, apex and exit for each bend, plus intermediate sections.

Measurements in 1983 and 1984 consisted of the following parameters: bed and water surface topography by levelling, bed material size distribution by grab sampling, longstream and cross-stream velocity components by current metering. In 1985 the same measurements were made, plus bedload distribution by Helley-Smith sampler. The complete data sets are available in two Colorado State University reports (Thorne, et al., 1983 and Thorne,

Figure 3. Bend morphology in the high transport reach showing point bar platform at the inner bank, deep thalweg at the outer bank and point bar face between them. Note undercutting of outer bank and steep inner bank behind shelving point bar.

et al., 1985). Only the results for low flow and bankfull flow patterns at the bend apices are presented here. These are representative of the bend flow results in general.

The measurement of longstream and cross-stream velocities was undertaken using a Marsh-McBirney two component electromagnetic current meter. This device uses the Farraday principle of electromagnetic induction to measure purely unidirectional velocities. By having two sensors set at ninety degrees it is possible to measure mutually perpendicular velocity components simultaneously with an error of only about ±3 mm/s. At each point data were time averaged over a one minute period and recorded using a Hewlett-Packard 3421A Data Acquisition Unit and H-P 41CV hand-held calculator. The instrumentation is shown in Fig. 4.

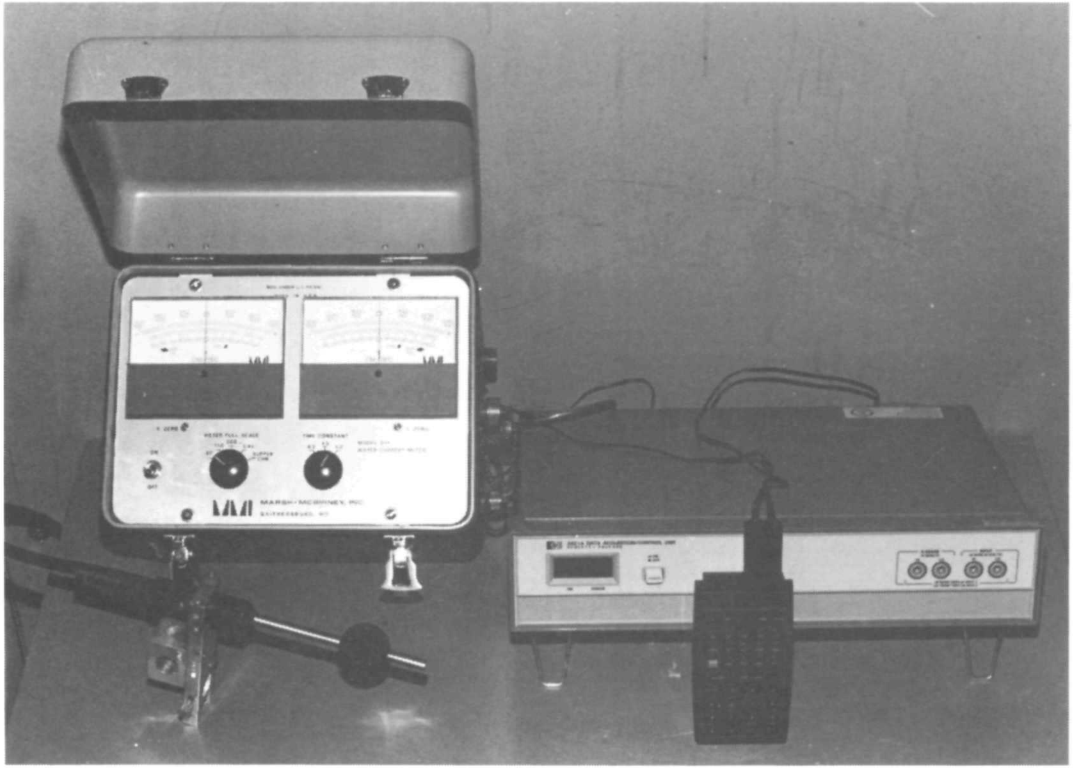

Figure 4. Instrumentation used to collect velocity data. Left, two-dimensional electro-magnetic current meter; and right, data logger and calculator.

In the field, the bridges were set perpendicular to the outer bank and the meter was oriented to measure velocities orthogonal and parallel to the bridge, corresponding to the longstream and cross-stream components. These are not necessarily the primary and secondary components, however, because the whole flow may itself be angled across the channel, particularly at low flow. Longstream and cross-stream velocities were resolved into primary and secondary components using the method proposed by Dietrich and Smith (1983) which is based on consideration of three-dimensional continuity between consecutive sections.

RESULTS

Figures 5 and 6 show the patterns of primary isovels and secondary velocities at the two bends at discharges of 1.7 m^3s^{-1} and 4.0 m^3s^{-1}. These flows correspond to about 40 percent and 100 percent of bankfull discharge for the reach. At low flow (Figs. 5a and 6a) secondary velocities over the point bar platform are directed radially outwards at all depths. This confirms the earlier results of Dietrich and Smith (1983) and is as expected from the comments of Bridge (1984) as the discharge is considerably less than 60 percent of bankfull. In the thalweg there is helical flow driving surface water outwards and bed water inwards. At the outer bank there is clearly a small cell reverse rotation in the second bend, but not so at the first bend although the strength of helical flow is much reduced. The primary isovels are distorted by the secondary flows. The velocity maximum is shifted towards the outer bank by the outward flow in the helical cell. The velocity gradient on the outer bank is steepened by this shifting and this increases the boundary shear stress on that bank. At the bank the small reverse cell appears to distort the isovels and depress the maximum velocity.

At the point bar face at center channel, secondary flow convergence at the bed, and upwelling of slow bed water retard the primary flow. Isovels are arched upwards here and the velocity gradient is reduced, decreasing shear stress on the point bar face. This contrasts sharply with the closely packed near-bed isovels over the point bar platform just inside the face, where there is a high bed shear.

The high flow results (Figs. 5b and 6b) show some similarities with low flow patterns, but also some important differences.

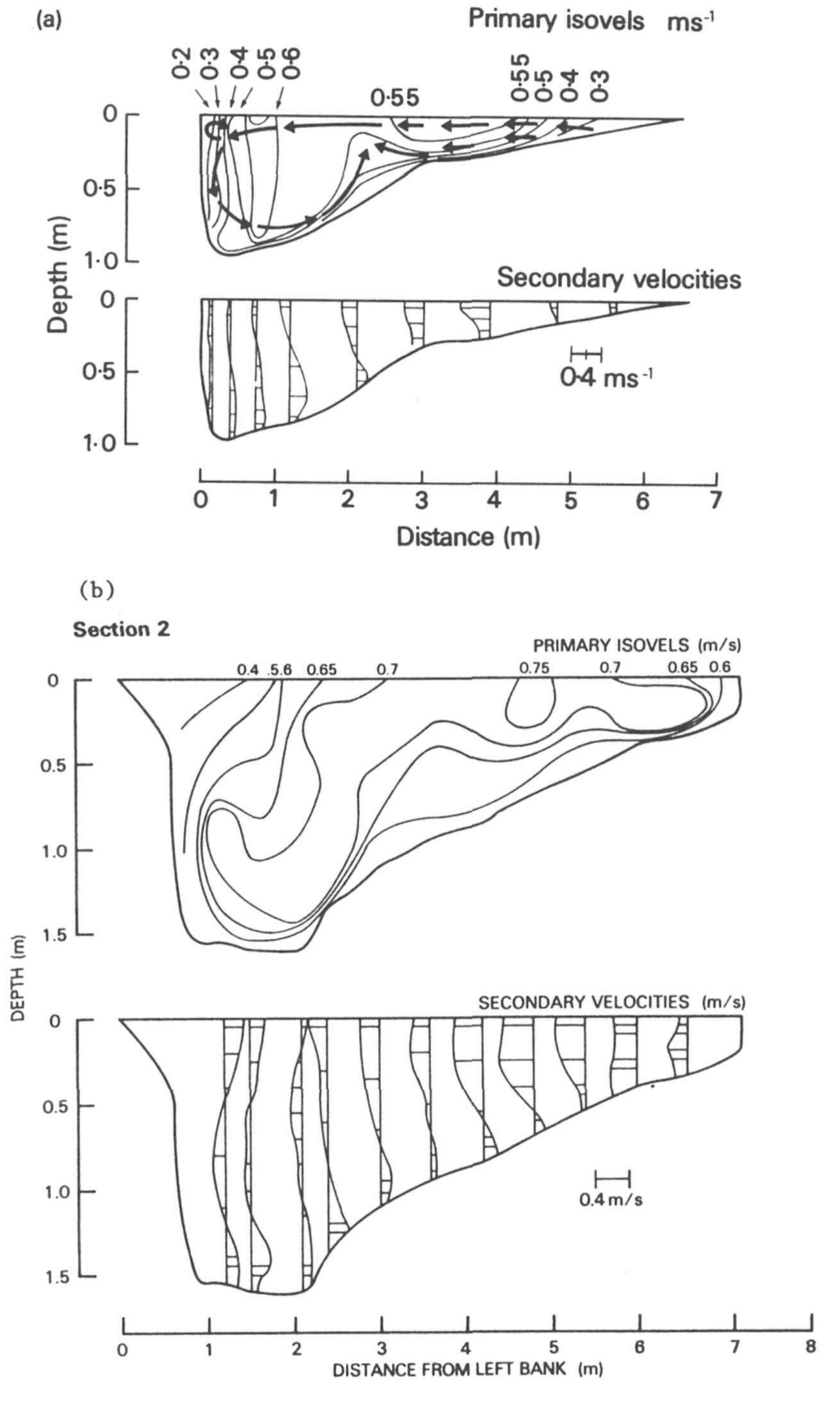

Figure 5. First bend apex flow patterns. (a) Low discharge. (b) Bankfull discharge.

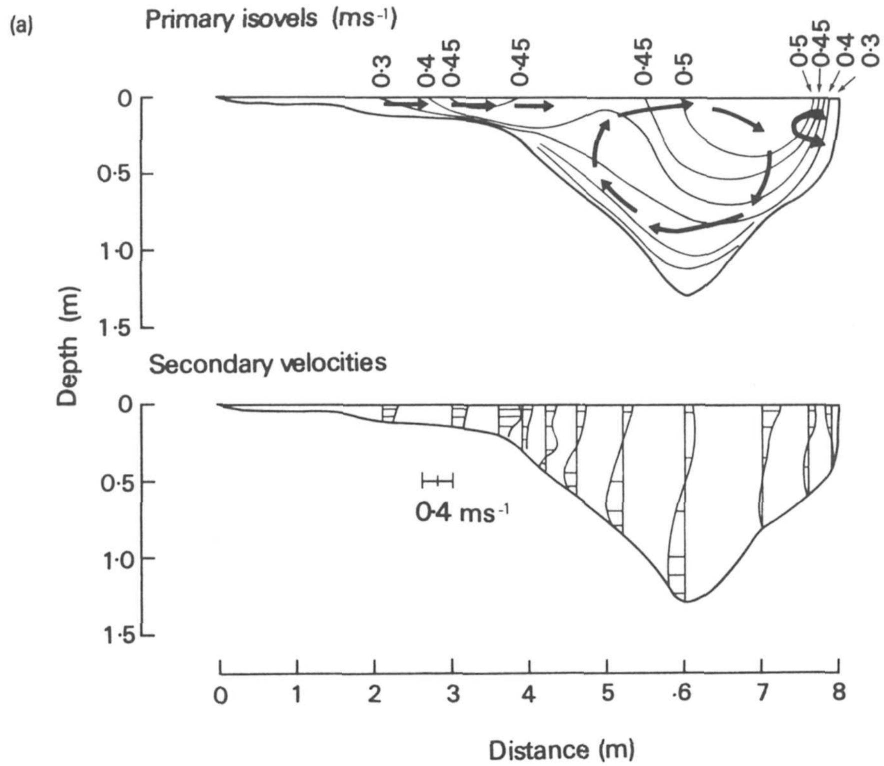

Figure 6. Second bend apex flow patterns. (a) Low discharge. (b) Bankfull discharge.

(b)

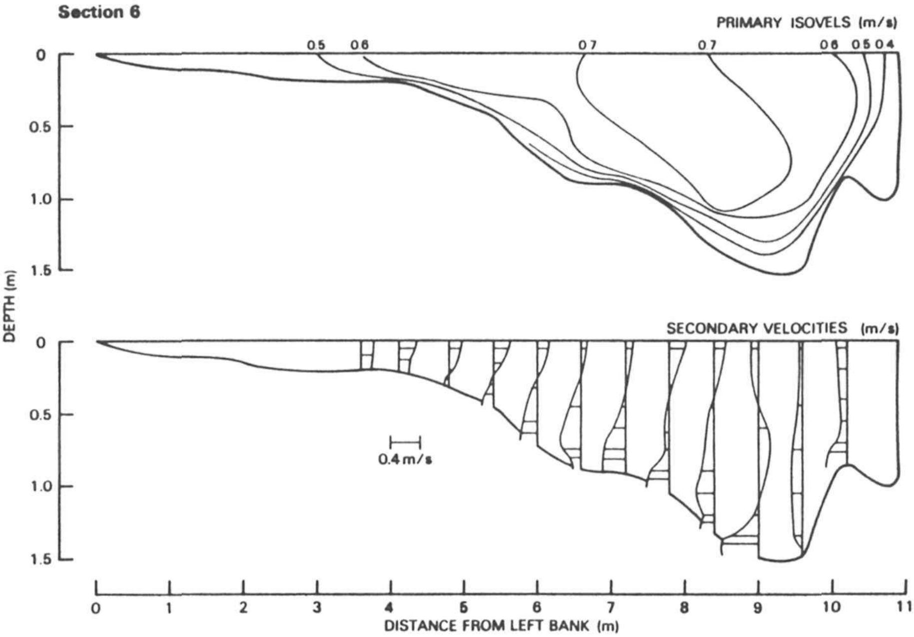

Figure 6. continued.

The zone of helical flow expands towards the inner bank as predicted by Bridge (1984), but it does not completely replace the zone of outward flow at the inner bank. It comes much closer to doing so at the first bend, but even here outward flow is found up to 2 m from the inner bank. The outer bank cell is much stronger at bankfull flow and is clearly present at both bends. At the second bend a failed block of bank material disrupts the somewhat orderly secondary flow cells. Clearly, the presence of such blocks can be important in determining local flow patterns. The primary isovels indicate that the velocity maximum shifts back towards the channel center at bankfull flow, as a result of the increased affect of downstream effects compared to cross-stream effects at the higher flow (Bathurst, et al., 1979). Shifting increases the velocity gradient and boundary shear stress on the point bar face, while generally high velocities and distortion caused by the outer bank cell maintain high shear stress on the outer bank. The highest stresses are found on the lower bank and the failed block in that location. Upwelling at the top of the point bar face reduces velocities and shear stresses there, but over the platform high stress are still found.

DISCUSSION

The results of this study are broadly in agreement with those of Dietrich and Smith (1983) and show that patterns of flow at the apex of a meander bend are more complicated than was previously realized.

The most contention concerns the existence of outward flow at the inner bank and here the results show that this does persist up to and including bankfull discharge. Earlier data for the site, reported in Thorne, et al. (1985) suggest that this is not necessarily a universal result. In those observations the zone of outward flow almost disappeared, with helical flow all across the channel at the first bend. The reason for this difference is unclear at present, but further studies are underway to resolve this issue, however, the bulk of our data to date support the view that outward flow is present at the inner bank at all in-bank flows. Helical flow is found in the thalweg, as expected from earlier studies and the presence of the outer bank cell is confirmed at least for high discharges.

The convergence of near-bed flows at the point bar face was observed to cause concentration of bedload in that area. At low flows material tended to deposit there due to the relatively low shear stresses, but at bankfull discharge high stresses tended to keep bedload in motion and also to erode the bar. Sediment sorting operated on the point bar face. A mixture of grain sizes moved off the point bar platform under the outward flow. On the face, coarse grains rolled downwards and outwards under gravity while fine grains were swept inwards and upwards by the helical flow. At the outer bank the high velocities and stresses low on the bank were observed to be effective in undercutting the bank below the vegetated layer, generating cantilever blocks which subsequently failed under gravity. This system of bank erosion has been described in detail elsewhere (Thorne and Tovey, 1981).

CONCLUSIONS

Flow Patterns

(i) Outward flow usually exists over the point bar at all discharges up to bankfull.
(ii) Helical flow is found in the thalweg and over the point bar face at all discharges.
(iii) Helical flow expands towards the inner bank as discharge increases.
(iv) An outer bank cell of reverse rotation often exists.
(v) The flow pattern in Fig. 7(c) should replace those previously proposed (Fig. 7(a) and (b)).

Meander Processes

(i) Sediment moves off the point bar platform due to outward flow there.
(ii) Bedload transport is concentrated on the point bar face.
(iii) Sorting occurs on the face where coarse grains roll outwards and fine ones are swept inwards.
(iv) The outer bank cell brings fast water close to the lower bank causing undercutting and rapid retreat.
(v) Models of meander processes which do not include and account for these phenomena cannot truly represent natural processes.

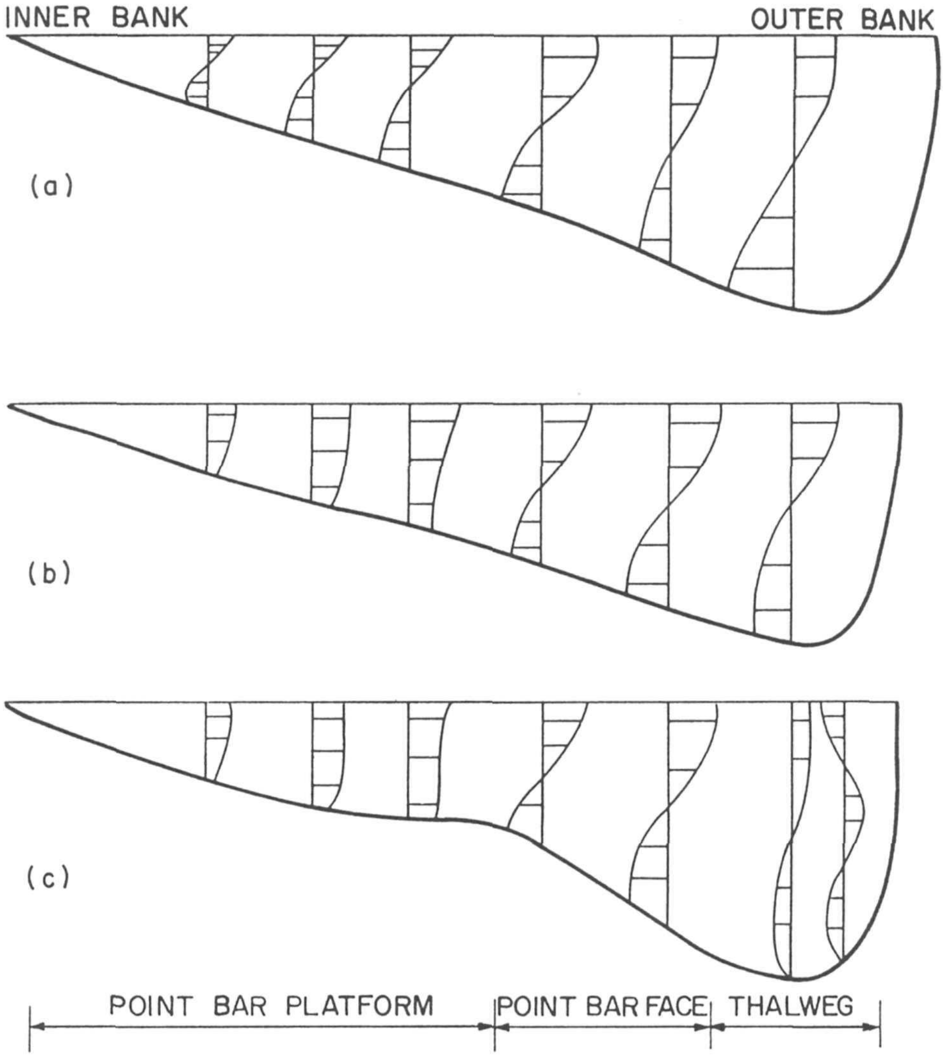

Figure 7. Idealized secondary flow patterns at a bend apex. (a) Simple helical flow. (b) Helical flow plus outward flow at the inner bank (after Dietrich and Smith, 1983) and (c) with both outward flow at the inner bank and an outerbank cell, as proposed here.

ACKNOWLEDGEMENTS

The research reported here was funded by the National Park Service through the Water Resources Field Support Laboratory at Colorado State University and through Rocky Mountain National Park. Their funding is gratefully acknowledged. We also thank Dr. Ray Herrmann and Dr. Marshall Flug of WRFSL and Dr. Dave Stevens and Mr. Jim Thompson of RMNP for their active support of the Fall River Project.

REFERENCES

Allen, J.R.L., 1970. Physical Processes of Sedimentation, Allen and Unwin, London, 248 pp.

Bathurst, J.C., C.R. Thorne, and R.D. Hey. 1979. Secondary flow and shear stress at channel bends. J. Hydraul. Div., ASCE, 105(10), 1277-1295.

Bridge, J.S. 1984. Flow and sedimentary processes in river bends: comparison of field observations and theory. In River Meandering, ASCE Special Publication, C.M. Elliott (Ed.) 857-872.

Bridge, J.S. and J. Jarvis. 1976. Flow and sedimentary processes in the meandering river South Esk, Glen Clova, Scotland. Earth Surface Processes, 1, 303-336.

Dietrich, W.E. and J.D. Smith. 1983. Influence of the point bar on flow through curved channels. Water Resources Research, 19(5), 1173-1192.

Hey, R.D. and C.R. Thorne. 1975. Secondary flows in river channels. Area, 7, 191-195.

Leopold, L.B., M.G. Wolman and J.P. Miller. 1964. Fluvial Processes in Geomorphology. Freeman, San Francisco, USA.

Perkins, H.J. 1970. The formation of streamwise vorticity in turbulent flow. Journal of Fluid Mechanics, 44, 721-740.

Pitlick, J.C. and C.R. Thorne. 1986. Sediment supply movement and storage in an unstable gravel-bed river. In Sediment transport in gravel-bed rivers, C.R. Thorne, J.C. Bathurst and R.D. Hey (Eds.), Wiley and Sons, Chichester, UK.

Prandtl, L. 1952. Essentials of Fluid Dynamics, Blackie, London, UK.

Rozovskii, I.L. 1961. Flow of water in bends of open channels. Israel Program for Scientific Translations, Jerusalem, Israel.

Thorne, C.R. and N.K. Tovey. 1981. Stability of composite river banks. Earth Surface Processes and Landforms, 6(5), 469-484.

Thorne, C.R., L.W. Zevenbergen, J.B. Bradley, and P.Y. Julien. 1983. Measurements of bend flow hydraulics on the Fall River at low stage, N.P.S. Water Resources Field Support Lab Report 83-9P, Fort Collins, 48 pp.

Thorne, C. R., L. W. Zevenbergen, J.B. Bradley, and J.C. Pitlick. 1985. Measurements of bend flow hydraulics on the Fall River at backfall stage, N.P.S. Water Resources Field Support Lab Report 85-3, Fort Collins, 69 pp.

A SULFURIC ACID SPELEOGENESIS OF CARLSBAD CAVERN

Carol A. Hill[1]

ABSTRACT

Sulfur isotope data and pH-dependence of the clay mineral endellite support the hypothesis that the large cave passages in Carlsbad Cavern and other caves in the Guadalupe Mountains, New Mexico, were dissolved primarily by sulfuric acid rather than by carbonic acid. Floor gypsum and native sulfur deposits in the caves have $\delta^{34}S$ values as low as -25.6. These values correspond to $\delta^{34}S$ values of H_2S gas and native sulfur in the Delaware Basin generated by oil and gas related reactions. The progressive eastward migration of the halite dissolution margin in the basin could have been a major factor controlling cave development in the Guadalupe Mountains. Where halite beds are intact, they may have acted as impermeable barriers, preventing hydrogen sulfide from rising to the surface in the basin; instead, the gas may have risen into the Capitan reef along fractures and other avenues, there dissolving out the caves by a sulfuric acid mechanism.

INTRODUCTION

The origin of Carlsbad Cavern and other caves in the Guadalupe Mountains is one of the great unsolved mysteries of speleogenesis. Geomorphically, Guadalupe caves bear little resemblance to other great cave systems of the world. Rooms are huge, yet passages are not long and they terminate abruptly. The caves seem unrelated to surface topography or to ground water flow routes, and caves seemingly "die with depth", even though water table conditions prevail below the lowest passages. Especially enigmatic are the deposits of massive gypsum and the colorful waxy clay in the caves.

For over 30 years the prevailing theory of speleogenesis has been that Guadalupe caves formed similar to other caves; that is, by carbonic acid dissolution at the water table. Within the past 10 years four new theories of origin have been proposed, all of which differ significantly from one another and from the earlier theory. The findings of this study support an unusual mode of speleogenesis for Guadalupe caves, one which involves sulfuric acid and which is related to the oil and gas fields of the Delaware Basin. This paper is a short synopsis of a large memoir on the geology of Carlsbad Cavern and other caves in the Guadalupe Mountains soon to be published by the New Mexico Bureau of Mines and Mineral Resources (Hill, in press).

1. Cave Research Foundation, Box 5444A, Route 5, Albuquerque, New Mexico 87123

Three types of cave deposits attest to a sulfuric acid speleogenesis for the caves of the Guadalupe Mountains: endellite, massive gypsum, and native sulfur. Endellite is a waxy, colorful mineral which, in all of its non-cave occurrences, forms in a sulfuric acid regime (pH 5 or below). In Guadalupe caves the endellite is associated with both montmorillonite and chert; montmorillonite, when exposed to acidic water, reacts to form endellite and silica (chert).

Massive floor deposits of gypsum up to 10 m high occur in Guadalupe caves, and these have $\delta^{34}S$ (sulfur isotope) values as low as -25.6. The gypsum formed as the by-product of the reaction of sulfuric acid with limestone:

$$H_2SO_4 + CaCO_3 + 2H_2O = CaSO_4.2H_2O + CO_2 + H_2O \quad (1)$$

The extreme enrichment of the gypsum in ^{32}S (leading to highly negative sulfur isotope values) can only be related to the biological oxidation and reduction of sulfur; such reactions have been proposed by Kirkland and Evans (1976) as having been generated by oil and gas-related reactions in the Delaware Basin.

It is interesting to compare $\delta^{34}S$ values obtained for the cave deposits with those reported by Kirkland and Evans (1976) for oil and gas-generated sulfur in the castile buttes of the Delaware Basin (Fig. 1). The castile sulfur has $\delta^{34}S$ values of +9.2 to -15.1 compared to the cave gypsum which has $\delta^{34}S$ values of +5 to -25.6. Both types of deposits fluctuate widely in their degree of fractionation; such large fluctuations over short distances are diagnostic of biologic systems because bacterial populations are always changing depending on nutrient levels and temperature.

Canary-yellow, rhombic sulfur crystals and pale-yellow, massive sulfur have been found in Cottonwood Cave, Carlsbad Cavern, and Lechuguilla Cave. In Carlsbad Cavern the sulfur occurs in three localities: in the Big Room, New Mexico Room, and Christmas Tree Room (near the Lake of the Clouds). The New Mexico Room sulfur coats the undersides of bedrock projections and it also covers secondary gypsum flowers and crusts. The Christmas Tree Room sulfur covers bedrock, cave rafts, popcorn, and flowstone. The sulfur formed by the subaerial oxidation of H_2S gas according to the equation:

$$2H_2S + O_2 = 2S + 2H_2O \quad (2)$$

The Big Room sulfur has a $\delta^{34}S$ value of -20 and the Cottonwood Cave sulfur a value of -14.6. This compares with $\delta^{34}S$ values for H_2S gas in the basin which average -14.4 and -20.5 at the WIPP (Waste Isolation Pilot Plant) and ERDA (Energy Reseach Development Administration) sites, respectively, located near Carlsbad, New Mexico. It also compares with the isotopic values of economic sulfur deposits in the basin ($\delta^{34}S$ values as low as -15).

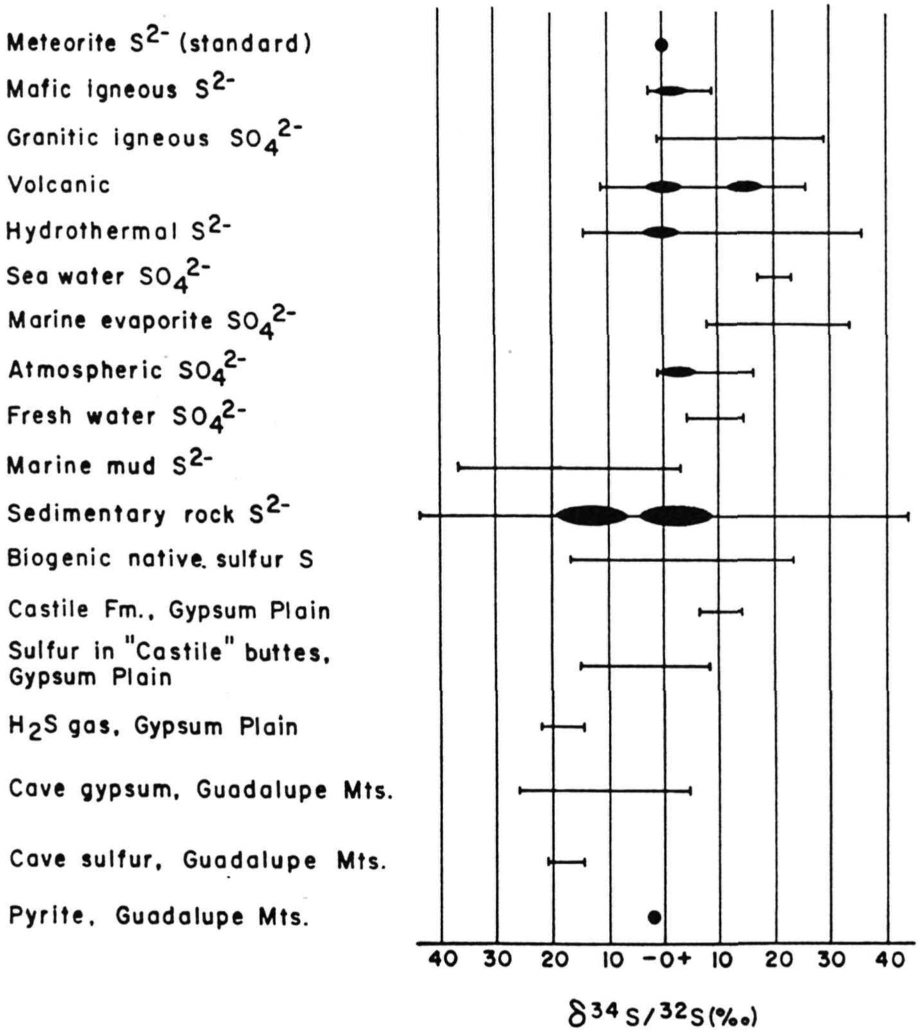

Figure 1. $\delta^{34}S$ values for various geologic environments. Note that the gypsum and sulfur in Guadalupe caves are significantly enriched in $\delta^{32}S$ compared to the gypsum and anhydrite of the Castile Formation in the Gypsum Plain.

RELATIONSHIP OF CAVES TO OIL AND GAS IN THE DELAWARE BASIN

The Delaware Basin of southeast New Mexico and northwest Texas is characterized by oil and gas fields, commercial sulfur deposits, limestone castile buttes, and caves in the buttes where H_2S gas is still degassing (Fig. 2). Where sulfur exploration companies drill below halite beds, they find plentiful H_2S gas, but no native sulfur (i.e., in the area to the right of the solid and dashed line in Fig. 2). The sulfur in the basin is found only at the edge of the halite margin (just to the left of the line), where the H_2S has been oxidized to sulfur by meteoric ground water.

According to the model proposed by Hill (in press) gas trapped beneath the halite beds moved from the basin into the reef along regional fractures and joints or along the Bell Canyon Formation (Fig. 3). Natural gas migrating updip from the oil fields to the east encountered anhydrite at the base of the Castile Formation. Reactions between the gas and the anhydrite produced hydrogen sulfide, carbon dioxide, and the castile limestone masses (Kirkland and Evans, 1976). The hydrogen sulfide and carbon dioxide continued updip along the Bell Canyon Formation into the Capitan reef where they mixed with oxygenated ground water moving downdip along backreef beds.

Vertical tubes, fissures, and pits in Guadalupe caves, according to this model, are interpreted as being developed along injection points for gas and/or ascending water, and horizontal cave levels are interpreted as being developed at the water table where dissolved oxygen is the most concentrated (Fig. 4). Cave rooms end abruptly in a horizontal direction because, away from gas injection points, the acid becomes neutralized by its interaction with limestone. Since the amount of dissolved oxygen decreases with depth below the water table, fissure passages and pits terminate in the vertical direction and do not possess bottom drains. With successive lowering of base level, new horizontal levels are connected to older horizontal levels by these pits and fissures.

Acidic solutions which dissolved out the caves also changed montmorillonite clay to endellite and chert, and massive gypsum was produced as a by-product of the acidic dissolution of the caves according to equation (1). Degassing of carbon dioxide, also a by-product of equation (1), produced atmospheric condensation-corrosion (gas weathering) of cave ceilings and walls, and the large cave passages grew further by stoping upward (Fig. 4). The native sulfur in the caves was produced when hydrogen sulfide degassed under atmospheric conditions according to equation (2).

The progressive eastward migration of the halite margin in the Delaware Basin could have been a factor controlling cave development in the Guadalupe Mountains. As the Guadalupe Mountains and Delaware Basin uplifted and tilted to the northeast in the Pliocene-Pliestocene, halite beds in the basin became progressively eroded from west to east. This erosion created a salt dissolution zone or margin which, according to Bachman and Johnson (1973), has had a horizontal rate of erosion

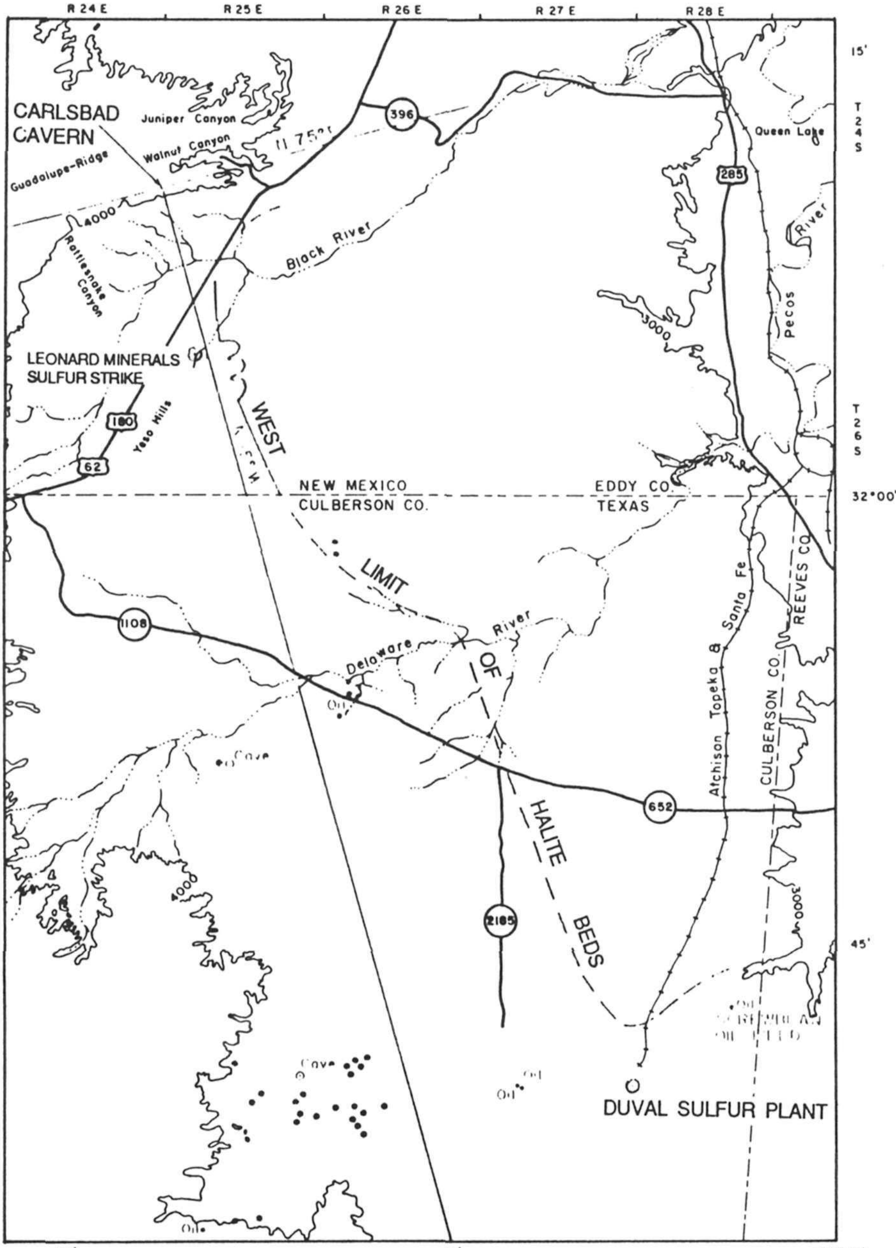

Figure 2. Location of Carlsbad Cavern with relationship to oil, sulfur, and the castile buttes (circular dots) of the Gypsum Plain. Line is the extenstion of the trend of the Big Room, Carlsbad Cavern (N15°W). Caves in the Gypsum Plain are tubular caves with degassing H_2S.

Location of the west limit of Halite 1 beds and Leonard Minerals sulfur strike courtesy of Leonard Minerals, Albuquerque, Mew Mexico. Scale: 1 cm = 1 km.

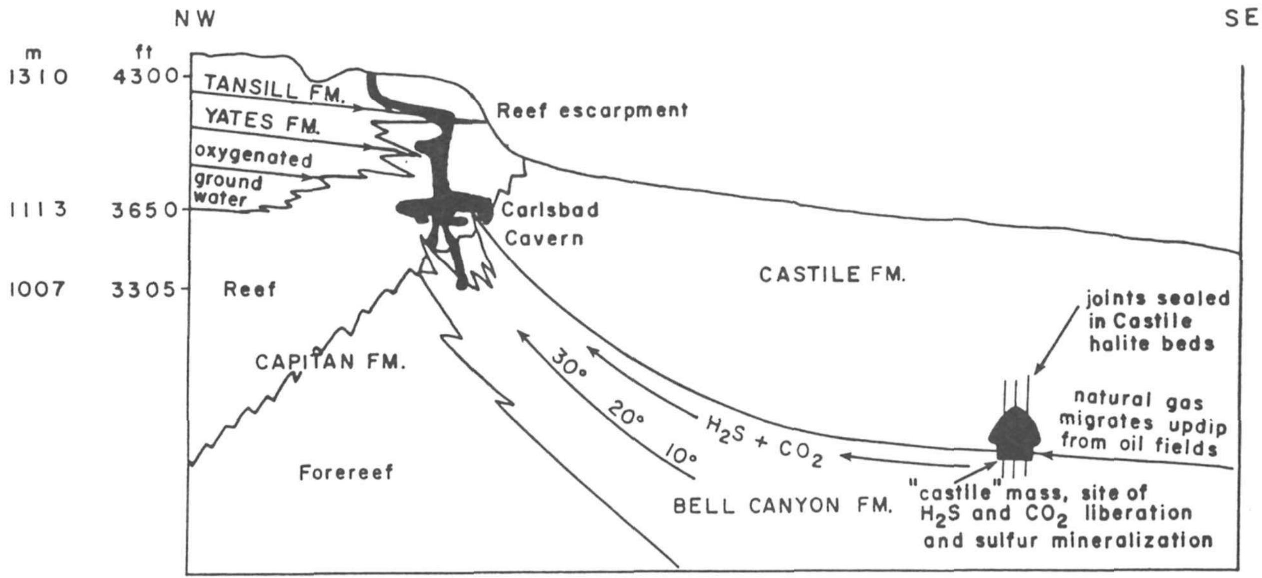

Figure 3. Model of gas ascension from the basin into the reef along the Bell Canyon Formation.

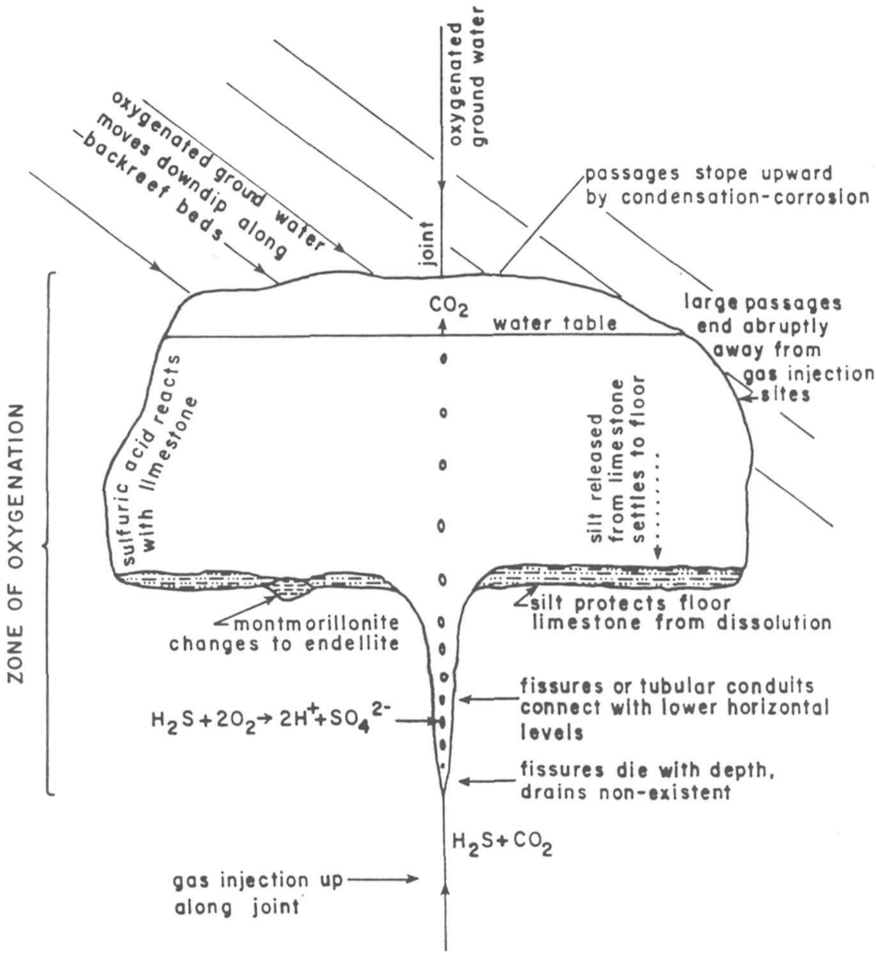

Figure 4. Model of hydrogen sulfide reaction with dissolved oxygen near the water table.

of about 10-13 km/million years. Using this rate and the fact that the halite margin has moved 0.5-0.65 km to the east of Carlsbad Cavern (see Fig. 2), it can be calculated that the halite margin passed the location of Carlsbad Cavern about 50,000 years or so ago, which date signifies the time when gas could no longer move into the reef at this location and the development of Carlsbad Cavern stopped. Cave raft-cones on the Balcony of the Lake of the Clouds (the lowest passage in Carlsbad Cavern) have U-series dates of about 50,000 yrs BP, and sulfur overlies comparable cave rafts in the Christmas Tree Room off the Lake of the Clouds Passage. Flowstone highly modified by condensation-corrosion drippage has been dated at 150,000 yrs BP in the nearby Bell Cord Room. Thus, the youngest speleogenesis events in Carlsbad Cavern, as recorded in the Lake of the Clouds area, correlate in time with the movement of the halite margin past the location of the Carlsbad Cavern.

ACKNOWLEDGEMENTS

I would like to thank the Cave Research Foundation for field support and the National Park Service, Carlsbad Caverns National Park, for administrative support and permission to collect samples. Derek Ford, McMaster University, performed the U-series dating analyses, and Geochron Laboratories performed the sulfur isotope analyses.

LITERATURE CITED

Bachman, G. O., and Johnson, R. B., 1973, Stability of salt in the Permian salt basin of Kansas, Oklahoma, Texas, and New Mexico: U. S. Geol. Surv. Open File Rept., 4339-4.

Hill, C. A., in press, Speleogenesis of Carlsbad Cavern and other caves in the Guadalupe Mountains: New Mexico Bureau of Mines and Mineral Resources, Memoir 44.

Kirkland, D. W., and Evans, R., 1976, Origin of limestone buttes, Gypsum Plain, Culberson County, Texas: Am. Assoc. Petrol. Geol. Bull., v. 60, no. 11, p. 2005-2018.

RECENT VARIATIONS OF BLUE GLACIER, OLYMPIC MOUNTAINS, WASHINGTON

Richard C. Spicer[1]

ABSTRACT

Blue Glacier is located on Mount Olympus in the Olympic Mountains, Washington, and is unusual among North American glaciers for its association with a long record of historic observation and scientific research and its sensitivity to small climatic change. Compilation of terminus variation data for Blue Glacier therefore provides a useful record as a rough indicator of local climatic variations from the early 19th century to the present.

The maximum Neoglacial positions reached by Blue Glacier in the early 19th century are marked by moraines and trimlines, which Heusser (1957) mapped and dated by dendrochronology. Later use of lichenometry in the same regions to refine the recessional chronology proved unsuccessful, however (Spicer, 1983).

Written accounts and mountaineering photographs from 1899 onward document the early 20th century retreat of Blue Glacier. At that time, the glacier descended as a spectacular icefall into the Glacier Creek valley some 500 m below. Snow and ice avalanched with "great, booming crashes," audible more than 20 km distant by an 1899 account, and ascribed more fancifully by local Indian legend to the moving about of the Thunderbird in its nest in a dark hole under the glacier. Photographs from the mid-1920's show that the glacier then began rapidly to withdraw from avalanche cones amassed in previous decades, thereby exposing the ice-worn cliff face above them; significant avalanche activity ceased probably soon after 1934, and the cones gradually melted away.

In order to record the glacier's rapid retreat, National Park Service staff began field measurement of the Blue Glacier terminus in 1938 and repeated the program nearly every year through 1955; since then, University of Washington and California Institute of Technology scientists have continued the surveys. A summary of measurements made from 1938 to 1982 shows that significant glacier recession, totaling 248.5 m, occurred until 1953 and was anomalously great in 1941 (56.5 m) and in 1951 (22.9 m). As a result of cooler and moister climatic conditions that had prevailed since the late 1940's, however, more than three decades of glacier retreat came to an end when the terminus stablized in 1954 and advanced a short distance (3 m) in 1955; but the trend was short-lived. By 1959, the terminus had receded another 15 m, most of which probably occurred during the same long, hot, and dry summer of 1958 that caused widespread glacier recession throughout the Pacific Northwest. In 1960, Blue Glacier retreated to the

1. National Park Service, National Natural Landmarks Program, P.O. Box 37127, Washington, D.C. 20013-7127.

farthest up-valley position reached at least since the early 19th century and then remained relatively stationary for the next four years.

Despite the glacier's apparent stability during the early 1960's, mass balance calculations from 1958 to 1964 increased by an average of 0.4% each year, and contemporaneous photographs betrayed observable thickening of ice in upper portions of the glacier. Blue Glacier began noticeably to advance in 1965 as a result, and the trend continued until 1980. The terminus advanced a total distance of 164.0 m between 1960 and 1980, most of which (122.9 m) occurred between 1975 and 1978, as a result of additional snow accumulation during the cool and wet years of the late 1960's and early 1970's. The total distance gained was far greater than that gained by Hoh or Black Glaciers, the only other Olympic glaciers to have advanced at the same time. Drought conditions that prevailed from 1977 to 1981, however, caused an almost immediate cessation of glacier advance, and since 1980, the Blue Glacier ice front has remained relatively stable, about 15 m up-valley of the 1941 position.

Photography of the Blue Glacier terminus was begun in 1953, when the Chief Park Naturalist established a photo station on a high bedrock knoll below the ice front. Pictures of the terminus have been taken from that location in every year of measurement since then. In addition, aerial photography of the Mount Olympus area has been taken intermittently from 1955 to 1982, principally by the U. S. Geological Survey and Olympic National Park. That photographic data, along with earlier mountaineering photographs and Blue Glacier maps surveyed in 1939, 1952, 1957, and 1979, enabled construction of a variation map for Blue Glacier, from which measurements of glacier length, area, and altitude were made for various years from 1899 to 1982.

INTRODUCTION

Records of glacier variation are common in the European Alps (e.g., Messerli et al., 1978), where historical data of various kinds extend back many centuries, but are rare in glacierized regions of the United States, few of which were explored, photographed, and mapped prior to the 19th century. Blue Glacier, however, the largest of 266 glaciers in the Olympic Mountains, Washington (Spicer, 1986), affords an unusual exception; for, unlike other North American glaciers, Blue Glacier is associated with an exceptionally long and varied record of observation and research.

Located on the northeast slope of Mount Olympus (2424 m), the highest peak in the Olympics, Blue Glacier descends from 2377 m to 1234 m in altitude, is 4.3 km long and 1 km wide at the firn line, and covers an area of 5.32 km^2 (Fig. 1). The terminus remains perched on a high bedrock cliff overlooking the Glacier Creek valley some 500 m below, where a bouldery ground moraine and visible trimlines separating an old-growth conifer forest from more recent slide alder thickets mark the glacier's 19th century extent.

Nineteenth century variations of Blue Glacier can be reconstructed from glacial geologic evidence dating to about 1820 and from mountaineering observations late in the century. Heusser (1957) mapped and dated by dendrochronology the deposits defining the glacier's Neoglacial limit. Although situated in the heart of a rugged mountain wilderness not easily traversed, Blue Glacier also earned the interest and recognition of early explorers and adventuresome climbers, who provided useful historical accounts and photographs of the glacier from 1899 onward. Of glaciers in the Pacific Northwest, perhaps only those on Mount Rainier and Mount Hood offer longer and more detailed 19th century records.

More recently, the National Park Service began measurement of the glacier terminus in 1938 and annual ground photography of the same in 1953; both Olympic National Park and the U. S. Geological Survey also executed programs of aerial glacier photography intermittently from 1959 through 1982. In addition, during the International Geophysical Year of 1957-58, Blue Glacier became the focus of annual glaciological investigation that since then has generated the longest record of summer climate and annual mass balance data of any glacier in the United States.

Finally, although Mount Olympus receives the greates precipitation of any area in the lower 48 states, Blue Glacier also experiences the high rates of summer ablation typical of strongly maritime conditions and so is highly sensitive to climatic change (LaChapelle, 1965). The relationship among climatic records, mass balance data, and terminus variations is therefore perhaps more interesting than for other glaciers, and so a compilation of variation data for Blue Glacier provides a useful scientific record as a rough indicator of local climatic change since the early 19th century.

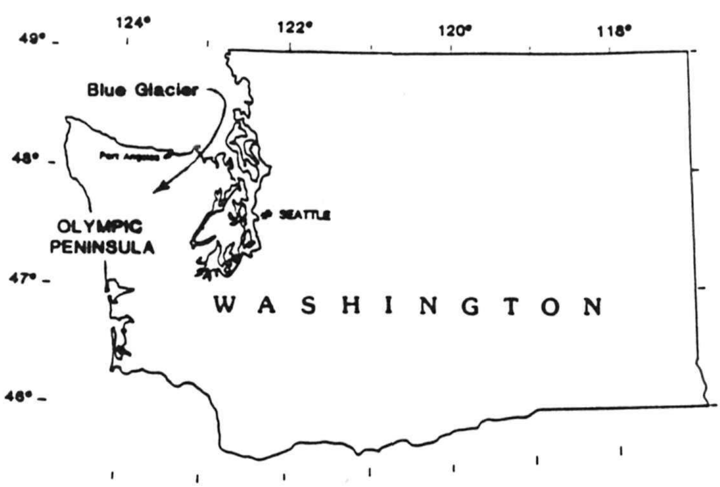

Fig. 1. Map of Washington State, showing the Olympic Peninsula and the location of Blue Glacier.

GLACIAL GEOLOGIC EVIDENCE

Heusser (1957) mapped and dated by dendrochronology the maximum Neoglacial positions reached by Blue, White, and Hoh Glaciers in the early 19th century, as well as earlier, less-extensive positions of Blue Glacier recorded in its compound right-lateral moraine. The ages of two outer lateral-moraine segments bordering Blue Glacier were indeterminable, but were thought to pre-date 1250 A.D.; the earliest datable moraines were constructed about 1650. An old-growth forest bordering both moraine sequences was found to be more than seven centuries old, and so its margin defines the limit of ice for at least as long.

Blue Glacier reached its farthest and lowest position in the early 19th century, when it cascaded as a steep icefall into the Glacier Creek valley and possibly coalesced with adjacent White Glacier and its tributary, Black Glacier. Moraines marking that maximum advance stabilized about 1815. At the same time, two lateral ice tongues along the northeastern margin deposited large quantities of boulder and glaciofluvial sediment in the forest below and then withdrew from a moraine constructed between about 1817 and 1820. As a result, earlier deposits of the 1650 advance were obliterated or obscured in all but one location.

Rapid retreat of glacier ice from those maximum positions, punctuated by brief stillstand or minor readvance, characterized the late 19th and early 20th centuries. No recessional moraines were deposited in the valley below the Blue Glacier icefall, but four are evident above the 1817-1820 moraine near the glacier's northeastern margin. Approximate dendrochronologic dating of those moraines indicated stabilization during the 19th century, about 1900, and in the 1920's.

Spicer (1983) attempted to refine the recessional chronologies of Blue, White, and Black Glaciers by lichenometry, but found the technique unsuitable for dating recent glacial deposits in the Mount Olympus area. Distinct recessional deposits of the three glaciers are scarce due to the nature of ice retreat in the Glacier Creek valley, and many of those remaining are unstable, often covered by seasonal snow well into the summer, and therefore lacking in vegetation. In addition, correlative deposits of Blue Glacier and Black and White Glaciers are separated by more than 350 m in altitude and so occur in different climatic environments, where rates of lichen growth probably differ.

In any case, a lichen growth curve for the Mount Olympus area could not be constructed, owing to the lack of lichen-bearing substrates datable by independent means. Recent rockfalls on Hoh and White Glaciers and an ablation till deposit below Black Glacier were the only distinct surfaces datable by bracketing photographs, but all three deposits were found to bear scant lichen cover. Incipient forestation by Sitka alder (<u>Alnus sinuata</u>) and other less prevalent species in the absence of significant lichen growth on two of the deposits showed, in addition, that in the

Mount Olympus area lichen colonization does not necessarily precede establishment of forest species on newly stabilized deposits, contrary to recent observations at Mount Rainier (Porter, 1981).

Maximum Neoglacial and older moraines dated previously by dendrochronology also were examined for lichen growth, but the results proved unreliable for development of a growth curve. Much lichen growth on those moraines occurs in streaks and patches unsuitable for measurement. In addition, Rhizocarpon geographicum in the Mount Olympus area appears restricted to sandstone substrates, which on older moraine segments bordering Blue Glacier are altered by thin, pinkish (1 mm) weathering rinds, to the apparent detriment of lichen growth, and at lower altitudes in the montane forest below Black and White Glaciers are covered extensively by mosses. It is doubtful that further refinement of the recent recessional histories of Mount Olympus glaciers will be achievable.

EARLY OBSERVATIONS OF BLUE GLACIER

Until the late 19th century, the Olympic Moutains remained an unexplored wilderness that defied penetration, fostered fanciful legend, and intrigued the adventuresome. Forays into the rugged interior by white settlers and Indians alike did occur throughout the mid-19th century (Majors, 1981a), but few early explorations reached areas of glacial activity, and of those that did, no useful accounts or photographs of glaciers appear to have remained.

The first party organized specifically to traverse the Olympic Peninsula across the mountains was the well-publicized Press Expedition, encouraged by Washington State's new governor and sponsored by the Seattle Press to report upon the untold wonders of America's last frontier (Wood, 1976a). The six expedition members chose to make their journey during the severe winter of 1889-90, however, a season characterized by excessive snowfall that was still much evident in the primitive expedition photographs taken in early spring 1890 (Majors, 1981b).

The unusual conditions seriously hindered the party's progress, threatened its very survival, and, in any case, obviously obscured the glaciers throughout the trip. It was for that reason, when expedition historian Captain Charles A. Barnes sought to verify a report "that Olympus cradled a glacier on its eastern sides," that he ventured up the "Belle River Canyon" (Long Creek) on March 29, 1890, in search of secondary proof:

> We had examined every stream draining [the] northern slopes [of Olympus] without finding in their waters any evidence of [the glacier's] existence. By this stream [Long Creek], then, if by any, the glacier must drain, and I wished to examine it.

I arrived late in the afternoon, at a large mountain torrent, which came down between the two great eastern spurs of Olympus. This was the only possible glacial stream. Its waters were clear as crystal and gave no evidence of glacial origin. (Seattle Press, July 16, 1890, p. 3)

His search was misguided, however. Not only did Barnes fail to realize that the relative contribution of sediment-laden glacial meltwater at that time of year would be negligible, but he also mistook nearby Mount Carrie for Mount Olympus and so examined the wrong drainage.

Misadventure notwithstanding, first-hand accounts of the interior Olympics by Press Party members did serve at last to dispel the mystery and disprove the mythology of the mountains; but further observations soon thereafter verified that at least one Indian legend was grounded in glacial truth. Although hunters from the numerous Indian tribes that inhabited the coastal lowland of the Olympic Peninsula are now known to have frequented the mountainous interior long before the arrival of European man (Berglund, 1983), long-standing lore had it that the natives feared and avoided the mountains as the mythical dwelling of the dreaded Thunderbird:

The Indians believe that in time of stormy weather a bird of monstrous size soars through the heavens and by the opening and shutting of his eyes it produces the lightening and by the flapping of its wings it produces the thunder and the mighty winds. This bird, they say, has its nest in a dark hole under the glacier at the foot of the Olympic glacial field and that its moving about in its home produces the "thunder-noise" there. (Reagan, 1909)

Professor D. G. Elliott, Chairman of the Zoology department at the Field Columbia Museum in Chicago, spent three summer months in the Olympics in 1899 and was the first correctly to surmise the nature of the phenomenon that gave rise to the widespread Thunderbird legend:

While in the vicinity, perhaps fifteen miles away, during September, strange and unaccountable noises were heard coming from [the] direction of [Mount Olympus]. The professor likens them to low, rumbling incessant sounds, followed at irregular intervals by great, booming crashes, which he explains on the theory of glacial action. He thinks that somewhere on the mountain is a rapidly moving glacier which is constantly hurling gigantic bergs into some great abyss below. (Northwest Magazine, 1899, p. 39)

Photographs taken from 1899 to 1919 verify that Blue Glacier continued to cascade into the Glacier Creek valley during that time and extended to the cliff base now exposed below the present terminus. The active ice front remained relatively stationary throughout those years and merged with massive accumulations of avalanched snow and ice derived from above. Indian agent and geologist Albert B. Reagan described the spectacular glacial scene:

> The ice mass seems to be several thousand feet in thickness, and in its downward movement is caused to project out far over the canon walls of Glacier Creek and Hoh River, leaving a dark holelike space beneath it. . . . A fissure loosens a great block of this snow-field now and then and it plunges to the bottom of the canon, 2,000 feet below, with a terrible crash. (Reagan, 1909, p. 147)

Early photographs of Blue Glacier are rare, however, because the principal objective of most mountaineering parties at the turn of the century was not the glacier, but Mount Olympus itself; and until the Hoh trail was completed in 1926 (M. Lewis, pers. comm., 1985), most parties approached the highest peak along the Elwha River, through Queets Basin, over Humes and Hoh Glaciers, and thus from the back side of Blue Glacier. Only a few adventuresome natives of the peninsula managed to capture a view of the impressive Blue Glacier icefall from High Divide or from the closer Falls Creek ridge to the north. Chief among these early photographers were Theodore Rixon (1899), who surveyed Olympic National Forest with Arthur Dodwell for the U. S. Geological Survey from 1898 to 1900; George C. Welch (1906), an insurance salesman from Port Townsend, who roamed the eastern Olympics in particular, and from 1907 to 1916 took a valuable series of good photographs still retained by his family; and members of the Huelsdonk family (ca. 1915 and 1920), renowned pioneer settlers of the Hoh valley.

In 1924, the Aberdeen Chamber of Commerce hired Seattle photographer Asahel Curtis to photograph various scenes from the Olympic Peninsula for promotional distribution. Asahel was the brother and business partner of famed North American Indian photographer Edward Curtis, and also was active as an enthusiastic outdoorsman in the Seattle Mountaineers; in fact, he had accompanied the first Mountaineers summer outing to the Olympics in 1907 and 1913. His 1924 tour happened to include a venture up the Glacier Creek valley to photograph the Blue Glacier from directly below the icefall. The illustrative series of eight pictures resulting shows in sharp detail that active ice by then had already separated from basal avalanche cones amassed in previous decades and so had exposed the ice-worn cliff face above them. Another picture taken from the Hoh trail by Olympic National Forest ranger F. W. Cleator in September 1927 provides a verifying profile view.

Thus had begun a phase of rapid retreat that was to last for more than 30 years. Glacier ice disappeared quickly at first, as the slender, hanging terminus receded up steep portions of the lower cliff face. By the late 1930's, avalanched snow and ice had long since disappeared, and the snout had receded above a relative break in slope to the approximate location it occupies today. Although eventual superintendent of Mount Olympus National

Monument Preston P. Macy noted as late as 1934 that "at times great chunks of ice breaks off and goes tumbling, bouncing, and flying through space as it catapaults to the creek bed far below" (Macy Papers), it is unlikely that such avalanche activity continued long thereafter.

RECENT GLACIER RESEARCH

Scientific and administrative interest in monitoring Olympic glaciers was first prompted by the organizational transfer of Olympic National Monument from the Forest Service to the National Park Service in 1933. For several years thereafter, the monument was managed by rangers at Mount Rainier National Park, owing to a lack of funds for independent Olympic staff. It was thus to Naturalist C. Frank Brockman of Mount Rainier National Park that F. W. Mathias, manager of the Grays Harbor Chamber of Commerce, wrote on September 14, 1934, to propose that an inventory of Olympic glaciers be undertaken, in order to provide "some authentic data to give to the public" for due recogition of the Olympics (Glacier Files).

The governing authorities of Olympic National Monument received the idea with interest, but the lack of permanent personnel precluded proper implementation of the proposal. Macy had marked "one or two of the important Olympic glaciers for future measurement" in the summer of 1934 (O. A. Tomlinson, letter to F. W. Mathias, September 19, 1934, Glacier Files) and with Mount Rainier National Park Superintendent O. A. Tomlinson marked Blue Glacier in 1935 (O. A. Tomlinson, letter to F. W. Mathias, September 17, 1935, Glacier Files), but no records of those observations remain. In addition, although a geologist was assigned to undertake certain studies of the Monument in 1935, he did not have time to make detailed study of the glaciers. It is also unclear whether Macy's intentions ever were realized to mark all of the larger glaciers in the Monument in 1936 and to enact a U. S. Geological Survey recommendation that his engineers begin annual water surface elevation records for the stream issuing from White Glacier during the same summer (P. P. Macy, letter to O. A. Tomlinson, February 25, 1936, Glacier Files).

Contemporaneous retreat of most glaciers in the western United States during the late 1920's had prompted naturalists of Yosemite, Mount Rainier, Rocky Mountain, and Glacier National Parks to establish a coordinated field program of glacier study in 1931 (C. M. Bauer, "Glacier Measurements," February 8, 1949, Glacier Files). Upon establishment of Olympic National Park in 1938, its naturalist division began annual measurement of the rapidly retreating Blue Glacier terminus as a contribution to that program. Blue Glacier was selected probably as the most accessible of the largest glaciers in the park. Ranger reports dating back to 1935 indicate that the position of the Blue Glacier terminus was first marked on August 30, 1938 (W. B. Augustine, memorandum for the files, July 29, 1944, Glacier Files), and annual measurements were made thereafter through 1948, except in

1942, when park personnel were employed to install aircraft warning sevice posts (W. B. Augustine, letter to F. E. Matthes, December 7, 1944, Glacier Files). Triangle-shaped marks aligned with the glacier front were painted with red lead along the left-lateral rock wall to record the receding terminus locations during those years; although glacier ice now covers most of the marks, a few of the earliest remain visible today.

Instructions for uniform procedures for glacier measurement in national park areas were issued from the Director's office in February 1949 (C. M. Bauer, "Glacier Measurements," February 8, 1949, Glacier Files). Accordingly, when Park Naturalist Gunnar O. Fagerlund conducted the next Blue Glacier survey in 1950, he established a baseline extending from the 1948 mark, from which measurements were made that year and in 1951, 1953, and 1955 (Fig. 2; Table 1). Fagerlund also marked a photo station on a high bedrock knoll below the ice front in 1953, from which photographs of the terminus have been made in every year of measurement since then. The resulting photographic time series illustrates from the same perspective the change in both the ice front and surface profile of the lower glacier during those years.

Blue Glacier became the focus of extensive glaciological inestigation during the International Geophysical Year of 1957-1958. In order to compare the mass and energy exchange of a temperate, maritime alpine glacier with that of a polar alpine glacier, the United States Northern Hemisphere Program in Glaciology selected Blue Glacier and Alaska's McCall Glacier as the respective type examples of each for a dual program of comprehensive glacier research. For the Blue Glacier Project, scientists from the University of Washington under the direction of Edward R. LaChapelle constructed a field station on the upper glacier in 1957 and occupied it continuously for 14 months from July 1957 through September 1958.

After 1958, glaciologic investigations on Mount Olympus continued during summer months only and included not only annual determination of glacier mass balance and surface energy exchange experiments, but also a hot-point drilling program, ice movement surveys, time-lapse photography of the icefall, ice tunnel studies, and daily meteorological observations. Significant results of that research were summarized by LaChapelle (1959, 1960, 1965). Although most of the studies were completed during the first decade of the program, the collection of mass balance and summer weather data has continued each year to the present, except from 1974 to 1979.

California Institute of Technology scientists joined University of Washington researchers from 1957 to 1980 with a complementary program of field study that focused on the structure and flow of lower Blue Glacier (e.g., Allen et al., 1960; Corbato, 1965; Meier et al., 1974; Echelmeyer, 1983). The two institutions together also assumed responsibility from the park in 1959 for monitoring the glacier terminus. Single-point measurements made

TABLE 1. FIELD MEASUREMENTS FROM 1950 BASELINE (1948 MARK) TO BLUE GLACIER TERMINUS								
Year	Distance from Baseline to Ice Front (m) at Specified Points (m) along Baseline (South End = 0 m)							
	15.2	22.9	26.7	30.5	33.5	45.7	61.0	Unspec
1950	23.2	----	----	8.2	----	21.3	34.1	----
1951	68.0	----	31.1	35.1	----	44.8	70.4	----
1953	73.1	----	----	43.9	43.0	55.5	73.8	----
1955	----	----	----	40.8	----	54.3	----	----
1959	----	----	----	55.8	----	----	----	----
1960	----	----	----	58.5	----	----	----	----
1961	----	57.0	----	----	----	----	----	----
1962	----	----	----	----	----	----	----	53.6
1963	----	----	----	----	----	----	----	54.1
1964	----	----	----	----	----	----	----	53.3
1965	----	----	----	----	----	----	----	48.8
1970	----	----	----	----	----	----	----	29.3
1970	----	----	----	----	----	----	----	23.5

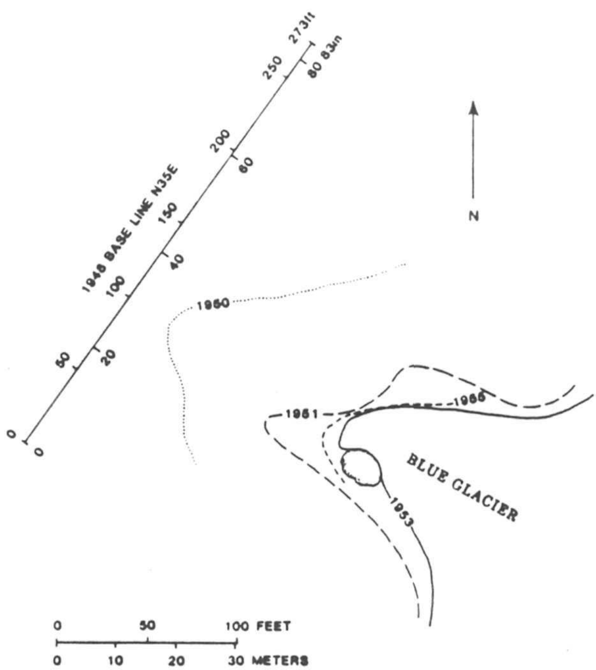

Fig. 2. Positions of the Blue Glacier terminus in 1950, 1951, 1953, and 1955, relative to the 1948 baseline, as compiled from 1953 and 1955 reports by Gunnar O. Fagerlund.

from 1959 to 1967 (R. P. Sharp, unpubl. repts., 1959, 1960, and 1961; C. R. Allen, unpubl. repts., 1962, 1963, and 1964; and E. R. LaChapelle, letter to D. Karraker, November 21, 1967; Glacier Files) and from 1970 to 1971 (W. B. Kamb, unpubl. data) were made from Fagerlund's base line. From 1975 to 1981, however, measurements were recorded in reference to early paint marks (K. A. Echelmeyer and W. B. Kamb, unpubl. data), because the glacier advanced beyond the 1948 position and coincident base line sometime between 1971 and 1975. A new base line extending from the 1941 mark was constructed in 1982 by Blue Glacier Project scientists and used for the 1982 and 1983 measurements (Table 2). Measurements taken in 1984 were rough estimates only.

A summary of measurements made from 1938 to 1982 (Table 3) shows that significant glacier recession, totaling 248.5 m, occurred until 1953 and was anomalously great in 1941 (56.5 m) and in 1951 (22.9 m). As a result of cooler and moister climatic conditions that had prevailed since the late 1940's, however, more than three decades of glacier retreat came to an end when the terminus stablized in 1954 (R. C. Hubley, letters to G. O. Fagerlund, October 21, November 8, and November 16, 1954, Glacier Files), and advanced a short distance (3 m) in 1955; but the trend was short-lived. By 1959, the terminus had receded another 15 m, most of which probably occurred during the same long, hot, and dry summer of 1958 that caused widespread glacier recession throughout the Pacific Northwest (Harrison, 1961). In 1960, Blue Glacier retreated to the farthest up-valley position reached at least since the early 19th century and then remained relatively stationary for the next four years.

Despite the glacier's apparent stability during the early 1960's, mass balance calculations from 1958 to 1964 increased by an average of 0.4% each year (LaChapelle, 1965), and contemporaneous photographs betrayed observable thickening of ice in upper portions of the glacier. Blue Glacier began noticeably to advance in 1965 as a result, and the trend continued until 1980. The terminus advanced a total distance of 164.0 m between 1960 and 1980, most of which (122.9 m) occurred between 1975 and 1978, as a result of additional snow accumulation during the cool and wet years of the late 1960's and early 1970's. The total distance gained was far greater than that gained by Hoh or Black Glaciers, the only other Olympic glaciers to have advanced at the same time (Spicer, 1986). Drought conditions that prevailed from 1977 to 1981, however, caused an almost immediate cessation of glacier advance, and since 1980, the Blue Glacier ice front has remained relatively stable, about 15 m up-valley of the 1941 position.

A more detailed summary of the measurement and photography of the Blue Glacier terminus was compiled by Spicer ("History of measurement of the Blue Glacier terminus, April 1982, Glacier Files).

TABLE 2. FIELD MEASUREMENTS FROM 1982 BASELINE (1941 MARK) TO BLUE GLACIER TERMINUS

Year	Distance from Baseline to Ice Front (m) at Specified Points (m) along Baseline (South End = 0 m)								
	West Margin of Glacier (?)	7.5	10	20	30	40	50	60	East Margin of Glacier (62)
1982	19.2	18	19	25.8	31	32	25	25	25.8
1983	----	--	14	----	--	--	--	--	----

TABLE 3. FIELD MEASUREMENT OF THE BLUE GLACIER TERMINUS: 1938-1983

Date of Measurement (day-mo-yr)	Terminus Variation (m)	Meters from 1960 Position	Date of Measurement (day-mo-yr)	Terminus Variation (m)	Meters from 1960 Position
20-08-38	---	264.0	31-08-61	+ 1.5	1.5
1-09-39	- 8.4	255.6	23-08-62	+ 3.4	4.9
5-09-40	-25.3	230.3	13-08-63	- 0.5	4.4
28-10-41	-56.5	173.8	10-08-64	+ 0.8	5.2
5-10-43	-42.4	131.4	27-08-65	+ 4.6	9.8
26-09-44	-23.8	107.6	11-09-67	+ 8.7	18.5
2-10-45	-18.1	89.5	11-09-70	+10.7	29.2
18-09-46	- 9.7	79.8	19-08-71	+ 5.8	35.0
9-09-47	-12.5	67.3	30-08-75	+48.4	83.4
9-09-48	- 8.8	58.5	7-08-76	+35.2	118.6
14-09-50	- 8.2	50.3	15-07-77	+16.5	135.1
11-09-51	-22.9	27.4	22-07-78	+22.8	157.9
13-09-53	-11.9	15.5	22-07-79	+ 2.9	160.8
27-09-54	0.0	15.5	11-07-80	+ 3.2	164.0
6-09-55	+ 2.1	17.6	??-??-81	- 1.2	162.8
25-08-59	-14.9	2.7	??-??-82	- 7.0	155.8
27-08-60	- 2.7	0.0	??-??-83	+ 4.0	159.8

No measurements made in 1942, 1949, 1952, 1954, 1956-1958, 1966, 1968-1969, and 1972-1974; 1954 figures based upon qualitative observations by Richard C. Hubley.

Negative variation indicates glacier retreat; positive variation indicates glacier advance.

VARIATION MAP OF BLUE GLACIER

A map of Blue Glacier showing variations from 1899 to 1982 was produced by compilation of data from ground photographs of the Mount Olympus area dating back to 1899 and sets of aerial photographs taken in 1939, 1952, 1955 to 1957, 1959 to 1971, 1973, 1974, 1976, 1979, 1981, and 1982 (Fig. 3). Most ground photographs used were views of mountain scenery taken before 1945 by amateur photographers. Aerial photography used included sets of vertical aerial photographs covering wide portions of the Olympic Mountains (1939, 1952, 1976, 1981, 1982), coverage of the Mount Olympus area by the University of Washington from 1955 to 1957, oblique photography of Olympic glaciers taken intermittently by Olympic National Park from 1959 to 1976, and both oblique and vertical photography of Olympic glaciers taken by the U. S. Geological Survey from 1960 to 1971 and 1977 to 1979.

Glacier outlines traced from vertical photographs were transferred by use of a Bausch and Lomb Zoom Transfer-Scope to base photographs and then to sections of 15' topographic maps enlarged to 1:10,000; ice-front positions from oblique photography were estimated visually by comparison of adjacent vegetation and bedrock features. Blue Glacier maps from 1939, 1952, 1957, and 1979 aided the alignment of photographic data.

Variation data tabulated for each year of record included glacier length, measured along a central flow line shown on the map; terminus altitude; and glacier area, determined by planimetry (Table 4; Fig. 4). Several sources of error somewhat reduced the accuracy of map measurement, however. Photographic distortion imparted cumulative error through transferral of data from one photograph to another and then to a planimetric base, especially for map areas characterized by steep topography. Instrument error, standard map error, and the limits of measurement from 1:10,000 maps contributed further. In addition, it was necessary to estimate certain ice marginal positions from photographs showing excessive snow cover, for lack of better data.

An estimate of measurement accuracy was determined by comparison of variation data, derived as above, with field survey measurements taken from 1938 to 1983 (Table 5). By such means, the maximum error in length measurement was determined to be ±29 m. The error in area measurement was obtained as the product of length measurement error and glacier width, or ±0.27 km^2. The error in terminus altitude varies as the product of length measurement error and the gradient of slope; for Blue Glacier, where cliffs below the present terminus average 60% in slope, an altitude error of ±17 m results.

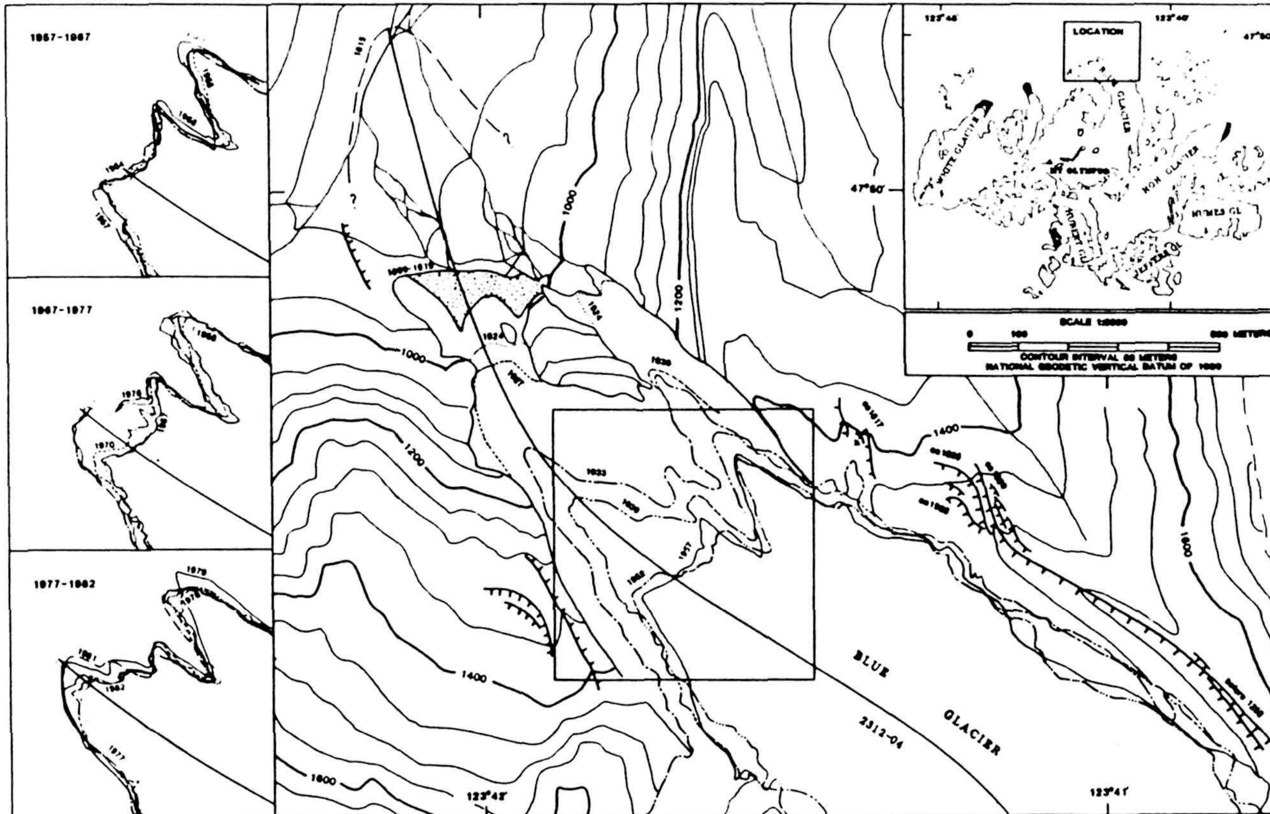

Fig. 3. Variations of Blue Glacier from 1899 to 1982.

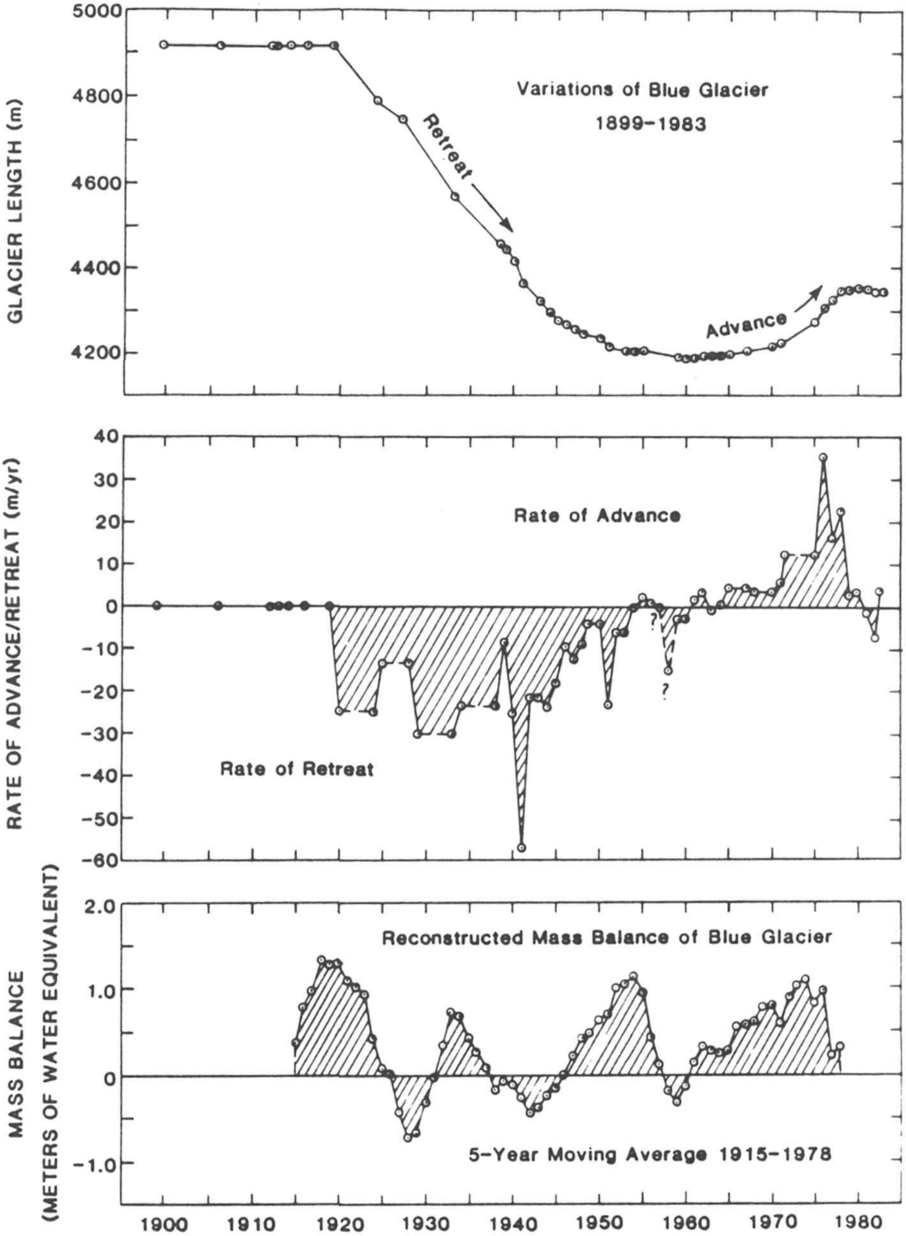

Fig. 4. Variations and rate of advance/retreat of Blue Glacier from 1899 to 1983, and variations of 5-year moving averages of reconstructed mass balance of Blue Glacier from 1915 to 1978 (A. Fountain, unpubl. data).

TABLE 4. VARIATIONS OF BLUE GLACIER FROM 1815 TO 1982.

†Glacier area indeterminable because 1927 photograph shows western terminus only.

Year	Glacier Length (m)	Length Change (m)	Length / 1939 L	Terminus Altitude (masl)	Change in TA (masl)	Mean Gl. Altitude (masl)	Change in MGA (masl)	Glacier Area (km^2)	Area Change (km^2)	Area / 1939 A	Photo Number
1815	5450	--	1.23	*850	--	1614	--	5.98	--	1.13	Heusser (1957)
1899	4915	-535	1.11	925	+ 75	1651	+ 37	5.61	-0.37	1.06	2312-04-1,2
1906	4915	0	1.11	925	0	1651	0	5.61	0.00	1.06	2312-04-3
1912	4915	0	1.11	925	0	1651	0	5.61	0.00	1.06	2312-04-4
1913	4915	0	1.11	925	0	1651	0	5.61	0.00	1.06	2312-04-5,6,7
1915	4915	0	1.11	925	0	1651	0	5.61	0.00	1.06	2312-04-8,9,10
1919	4915	0	1.11	925	0	1651	0	5.61	0.00	1.06	2312-04-11,12
1924	4790	-125	1.08	1000	+ 75	1689	+ 38	5.57	-0.04	1.05	2312-04-13-->23
1926	--	--	--	--	--	--	--	--	--	--	2312-04-24
1927	4750	- 40	1.07	1025	+ 25	1701	+ 12	†	†	†	2312-04-25,26
1930	--	--	--	--	--	--	--	--	--	--	2312-04-27
1933	4570	-180	1.03	1130	+105	1754	+ 53	5.38	-0.19	1.01	1935 Olympus
1936	--	--	--	--	--	--	--	--	--	--	2312-04-28,29
1939	4435	-135	1.00	1190	+ 60	1784	+ 30	5.31	-0.07	1.00	1939 map
1941	--	--	--	--	--	--	--	--	--	--	2312-04-30,31
1942	--	--	--	--	--	--	--	--	--	--	2312-04-32
1952	4230	-205	0.95	1260	+ 70	1819	+ 35	5.21	-0.10	0.98	1952 map
1957	4210	- 20	0.95	1270	+ 10	1824	+ 5	5.23	+0.02	0.98	1957 map
1964	4210	0	0.94	1270	0	1824	0	5.22	-0.01	0.98	V641-089
1965	4195	- 15	0.94	1275	+ 5	1826	+ 2	5.22	0.00	0.98	V654-225
1966	4210	+ 15	0.95	1270	- 5	1824	- 2	5.23	+0.01	0.98	V664-1064
1967	4210	0	0.95	1270	0	1824	0	5.23	0.00	0.98	V675-1331
1968	4205	- 5	0.95	1275	+ 5	1826	+ 2	5.23	0.00	0.98	V684-1229
1970	4230	+ 25	0.95	1260	- 15	1819	- 7	5.24	+0.01	0.99	70V1-112
1976	4295	+ 65	0.97	1240	- 10	1809	- 10	5.30	+0.06	1.00	OL-C-75/62-21
1977	4300	+ 65	0.97	1240	0	1809	0	5.30	0.00	1.00	77V6-193
1978	4305	+ 5	0.98	1235	- 5	1806	- 3	5.30	0.00	1.00	78KV1-69
1979	4350	+ 45	0.98	1201	- 34	1789	- 7	5.31	+0.01	1.00	O.P.'79-62*
1981	4355	+ 5	0.98	1200	- 1	1789	0	5.31	0.00	1.00	OSI-81/1-17-4
1982	4320	- 35	0.98	1225	+ 25	1801	+ 12	5.30	-0.01	1.00	ONP 82-3-3

TABLE 5. COMPARISON OF MAP AND FIELD MEASUREMENTS OF BLUE GLACIER VARIATIONS FOR ESTIMATION OF MEASUREMENT ERROR

Year	map measurement: Glacier Length (m)	map measurement: Length Change (m)	field survey: Glacier Length (m)	field survey: Length Change (m)	Error
1815	5450	--	--	--	--
1899	4915	-535	--	--	--
1906	4915	0	--	--	--
1912	4915	0	--	--	--
1913	4915	0	--	--	--
1915	4915	0	--	--	--
1919	4915	0	--	--	--
1924	4790	-125	--	--	--
1927	4750	- 40	--	--	--
1933	4570	-180	--	--	--
1938	--	--	4453.2	--	--
1939	4435	-135	4444.8	- 8.4	- 9.8
1940	--	--	4419.5	-25.3	--
1941	--	--	4363.0	-56.5	--
1943	--	--	4320.6	-42.4	--
1944	--	--	4296.8	-23.8	--
1945	--	--	4278.7	-18.1	--
1946	--	--	4269.0	- 9.7	--
1947	--	--	4256.5	-12.5	--
1948	--	--	4247.7	- 8.8	--
1950	--	--	4239.5	- 8.2	--
1951	--	--	4216.6	-22.9	--
1952	4230	-205	--	--	+ ?
1953	--	--	4204.7	-11.9	--
1954	--	--	4204.7	0.0	--
1955	--	--	4206.8	+ 2.1	--
1957	4210	- 20	--	--	+ ?
1959	--	--	4191.9	-14.9	--

Year	map measurement: Glacier Length (m)	map measurement: Length Change (m)	field survey: Glacier Length (m)	field survey: Length Change (m)	Error
1960	--	--	4189.2	- 2.7	--
1961	--	--	4190.7	+ 1.5	--
1962	--	--	4194.1	+ 3.4	--
1963	--	--	4193.6	- 0.5	--
1964	4210	0	4194.4	+ 0.8	+15.6
1965	4195	- 15	4199.0	+ 4.6	- 4.0
1966	4210	+ 15	--	--	--
1967	4210	0	4207.7	+ 8.7	+ 2.3
1968	4205	- 5	--	--	--
1970	4230	+ 25	4218.4	+10.7	+11.6
1971	--	--	4224.2	+ 5.8	--
1975	--	--	4272.6	+48.4	--
1976	4295	+ 65	4307.8	+35.2	-12.8
1977	4300	+ 5	4324.3	+16.5	-24.3
1978	4305	+ 5	4347.1	+22.8	-42.1
1979	4350	+ 45	4350.0	+ 2.9	standard
1980	--	--	4353.2	+ 3.2	--
1981	4355	+ 5	4352.0	- 1.2	+ 3.0
1982	4320	- 35	4345.0	- 7.0	-25.0
1983	--	--	4349.0	+ 4.0	--
1984	--	--			--

Maximum positive error = +15.6 m
Maximum negative error = -42.1 m

Estimated average error = ±29 m

ACKNOWLEDGEMENTS

I am grateful to Dr. W. Barclay Kamb of the California Institute of Technology, Rich Marriott and Ed LaChapelle of the University of Washington's Blue Glacier Project, and the staff of Olympic National Park for assistance in bringing together the Blue Glacier record. Construction of the variation map was enabled by the U. S. Geological Survey - Glaciology Project Office, Tacoma, Washington.

REFERENCES CITED

Allen, C. R., Kamb, W. B., Meier, M. F., and Sharp, R. P., 1960. Structure of the lower Blue Glacier, Washington. Journal of Geology 68(6):601-625.

Berglund, E., 1983. Summary prehistory and ethnography of Olympic National Park, Washington. National Park Service, Pacific Northwest Region, Division of Cultural Resources, Seattle, Washington, 119 p.

Corbato, C. E., 1965. Thickness and basal configuration of lower Blue Glacier, Washington, determined by gravimetry. Journal of Glaciology 5(41):637-650.

Echelmeyer, K. A., 1983. Response of Blue Glacier to a perturbation in ice thickness: theory and observation. California Institute of Technology, Pasadena, California, unpublished thesis, 342 p.

Glacier Files. Pioneer Memorial Museum, Olympic National Park, Port Angeles, Washington.

Harrison, A. E., 1961. Fluctuations of the Coleman Glacier, Mount Baker, Washington. Journal of Geophysical Research 66(2):649-650.

Heusser, C. J., 1957. Variations of Blue, Hoh, and White Glaciers in recent centuries. Arctic 10(3):139-150.

LaChapelle, E. R., 1959. Annual mass and energy exchange on the Blue Glacier. Journal of Geophysical Research 64(4):443-449.

_____1960. The Blue Glacier Project, 1959 and 1960. University of Washington, Department of Meteorology and Climatology, Seattle, Washington, 54 p.

_____1965. The mass budget of Blue Glacier, Washington. Journal of Glaciology 5(41):609-623.

Macy, P. P., Papers. University of Washington Libraries, Seattle, Washington.

Majors, H. M., 1981a. Early Knowledge of the Olympic Mountains. Northwest Discovery 2(2): 71-82.

_____1981b. The Press Party photographs. Northwest Discovery 2(3): 138-162.

Meier, M. F., Kamb, W. B., Allen, C. P., and Sharp, R. P., 1974. Flow of Blue Glacier, Olympic Mountains, Washington, U.S.A. Journal of Glaciology 13(68):187-212.

Messerli, B., Messerli, P., Pfister, C., and Zumbuhl, H. J., 1978. Fluctuations of climate and glaciers in the Bernese Oberland, Switzerland, and their geoecological significance, 1600 to 1975. Arctic and Alpine Research 10(2):247-260.

Porter, S. C., 1981. Lichenometric studies in the Cascade Range of Washington: establishment of _Rhizocarpon geographicum_ growth curves at Mount Rainier. Arctic and Alpine Research 13:11-23.

Reagan, A. B., 1909. Some notes on the Olympic Peninsula, Washington. Transactions of the Kansas Academy of Science 22:131-238.

Spicer, R. C., 1983. Lichenometry in the Mount Olympus Area, Olympic Mountains. _In_: Annual Report of the Regional Chief Scientist, Pacific Northwest Region, National Park Service, CY 1982. National Park Service, Seattle, Washington, pp. 78-80.

Spicer, R. C., 1986. Glaciers in the Olympic Mountains, Washington: present distribution and recent variations. University of Washington, Seattle, Washington, unpublished thesis, 158 p.

Wood, R. L., 1976a. Across the Olympic Mountains: the Press Expedition, 1889-90: Mountaineers, Seattle, Washington, 220 p.

LIMNOLOGICAL STUDIES OF CRATER LAKE CRATER LAKE NATIONAL PARK

Gary L. Larson[1]

ABSTRACT

Independent studies of Crater Lake during the late 1970s and early 1980s suggested that the lake had decreased in transparency and that the phytoplankton community had changed relative to earlier short-term studies between 1913 and 1969. After a careful peer review found that the existing databases were inadequate for developing any definitive conclusions about changing lake water quality, the National Park Service initiated a limnological study of the lake in 1982. That fall, Congress mandated (Public Law 97-250) a ten-year limnological study of the lake.

The emphasis in 1983 to 1985 was on developing an adequate monitoring program. Field work was limited to the summer-early fall period because of access problems the rest of the year. The results have indicated that the lake is very oligotrophic and that water clarity is still high. Secchi disc transparency readings were generally in the high 20 to low 30 m range (much less than a 40 m reading in August 1937). Nonetheless, a reading of 37.2 m was recorded in early July, 1985. With the monitoring program in place, program direction has shifted toward the interrelationships among environmental, terrestrial, cultural, and aquatic aspects of the ecosystem. A conceptual model has been developed from which specific research objectives have been established and areas needing additional study identified. These are discussed. Changing lake conditions will be addressed from trend analysis on lake monitoring data, repeating earlier studies of lake color and optical properties, and paleolimnological studies.

INTRODUCTION

Crater Lake is well known for its blue color, nearly pure optical properties, and extreme water clarity (Pettit, 1936; Smith et al., 1973). These characteristics exist for many reasons, but some important ones are the lake's great mean depth, a lack of influences from inflowing streams, a small watershed, and its National Park status which helps protect it from local anthropogenic disturbances. Limnological studies from 1978-81 suggested that lake

---

1. Cooperative Park Studies Unit, College of Forestry, Oregon State University, Corvallis, Oregon

clarity had declined (Larson, 1984). Much concern was voiced by park management, scientists, and the public about this suggestion, and in early 1982 the National Park Service convened two workshops to evaluate the situation. Because no adequate data base existed, a thorough analysis of the problem could not be made, but a monitoring program was initiated in the summer of 1982. The lack of an adequate baseline of data to evaluate the possible decline of clarity led Congress to mandate (PL-97-250, October 8, 1982) a ten-year study of the lake in September 1982 to be initiated by the Secretary of the Interior. The goals of this program were to i) develop a reliable limnological data base for the lake for future comparison; ii) develop a better understanding of physical, chemical, and biological characteristics and processes of the lake; and iii) establish a long-term monitoring program to examine the characteristics of the lake through time. This investigation will study lake conditions and if changes are detected, studies to identify the cause(s) will be carried out and mitigation measures developed if necessary.

The purposes of this paper are i) to define the objectives of the present program; ii) to summarize the development of the program and findings from 1983-85; and iii) to describe the objectives and approach for the remainder of the ten-year study.

STUDY AREA

Crater Lake covers the floor of the Mt. Mazama caldera that formed about 6600 years ago (Fryxell, 1965). The lake reached its present level (1882 m) about 700-1000 years ago (Nelson, 1967) and has an area of 48 km^2, a maximum depth of 589 m, and a mean depth of 325 m (Byrne, 1965). As with many formations of this type, steep caldera walls form a high rim around the lake, resulting in a large lake area to watershed area (flat map) ratio of about 3.6:1. A secondary intracaldera volcanic cone forms Wizard Island, the largest island in the lake (Fig. 1). Surface inflow comes from numerous small caldera wall springs and streams (Nelson, 1967), while most water input is believed to come from precipitation falling directly on the lake surface. There is no surface outlet; however, ground water seepage from the lake is suspected (Phillips and Van Denburgh, 1968).

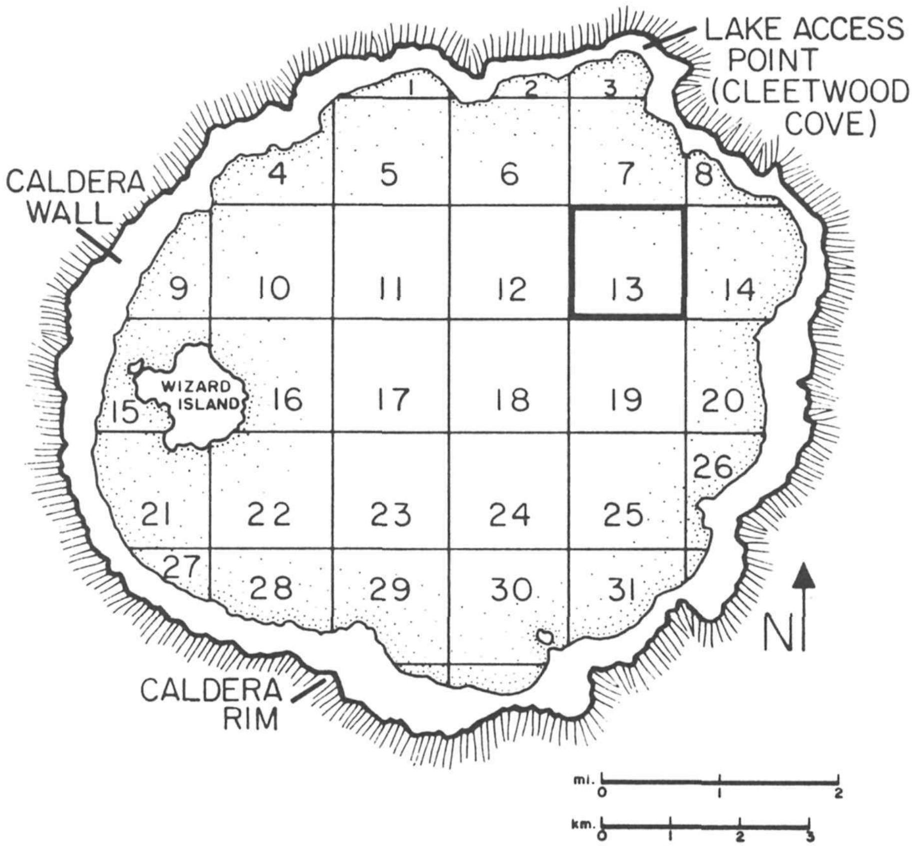

Figure 1. Crater Lake, Crater Lake National Park. The sampling station grid system is shown with the main station (13) highlighted.

THE TEN-YEAR LIMNOLOGICAL RESEARCH AND MONITORING PROGRAM

1983-1985

Field work was necessarily limited to the summer-early fall season (late June-middle of July to September) owing to sampling difficulties during the rest of the year. Work boats were either lifted to and from the lake by helicopter or by wench. Data collected included temperature, transparency (Secchi disc), light transmission and spectral sensitivity (photometer), nutrients (orthophosphate, nitrate-N, ammonium-N and silica), chlorophyll-a (in-vitro and in-vivo), primary production, phytoplankton, and zooplankton. Furthermore, most caldera wall springs and streams were sampled for nutrients and bacteria. Details of the methods have been described by Larson (1986).

Two sampling stations were used most of the time following the grid system developed by Hoffman (1967). Grid Sections 13 and 23 (Fig. 1) were emphasized in 1983 and 1984 because they were located in two of the three deep basins of the lake and because they had been used the most in past studies. Measurements of temperature and transparencies were obtained three times per week, and for nutrients and phytoplankton once every two weeks. In 1985, the number of main trend stations were reduced from two to one (Station 13), and the sampling frequency was reduced to once every four weeks. The 1985 program is outlined in Table 1.

Construction of a building on Wizard Island to house the research boats during winter was nearly completed in 1985. Only minor interior construction remains to be done (Jon Jarvis, Crater Lake National Park, personal communication). The last boat was hauled into the building in early October.

Water quality data indicates that the lake is still very oligotrophic and that water clarity is high. Secchi disc readings have generally been in the high 20 to low 30-m range, although a reading of 37.2 m in early July, 1985 was near record levels. Lake pH ranged from about 7 to 8. Conductivity, as micromhos/cm, had a range of about 100 to 125, while alkalinity ranged from about 25 to 30 mg/l. Phosphate was low in concentration with a range of about 9 to 20 µg/l. Nitrate was below detection limits in the upper 200 m of the water column, but reached up to 17 µg/l in the lower strata. Chlorophyll-a was less than 1 µg/l and deep water maxima were observed. Primary production

Table 1. Components of the Crater Lake Baseline Limnological Monitoring (Station 13)

---

1. Lake Program

   A. Temperature

      Record temperature profiles to 250 m (maximum length of Thermister cable) at:

         1 m intervals from 0 to 20 m
         5 m intervals from 20 to 100 m
         20 m intervals from 100 to 200 m, and
         25 m intervals from 200 to 250 m

   B. Optical

      1. Secchi disc (20 cm)

      2. Photometer

   C. Chemical

      Determine pH, alkalinity, specific conductance, dissolved oxygen, total phosphorus, orthophosphate, nitrate-nitrogen, total Kjeldahl nitrogen, ammonium-nitrogen and silica at all or selected depths from the following depth sequence:

         5 m intervals from 0 to 10 m
         20 m intervals from 20 to 200 m
         25 m intervals from 200 to 300 m
         50 m intervals from 300 to 550 m

   D. Biological

      1. Chlorophyll

         Determine the in-vivo and in-vitro chlorophyll at all chemical sampling depths.

      2. Phytoplankton

         Determine species, density and biovolume from samples collected at all chemical sampling depths.

Table 1. (Continued)

3. Zooplankton

Determine species, density and biomass. Preliminary work in 1985. Samples taken with a vertical haul .75 m diameter number 25 closing net.

2. Springs

A. Location

Each spring identified by a numbered tag

B. Physical and chemical water quality and bacteria

Record temperature and take samples for pH, conductivity, alkalinity, nutrients and bacteria (total coliforms, fecal coliforms and fecal streptococcus).

---

estimates were made in 1983 and 1984, and the results are being analyzed. Phytoplankton (1983-85) and zooplankton (1985) samples are being analyzed as part of two Master's degree programs.

Caldera springs and streams have been sampled since 1983, and some below the developed area on the caldera rim have consistently had elevated concentrations of nitrate. Other water quality measures, such as phosphate, pH, conductivity, and bacteria, have not shown any unusual features for these springs relative to the others (Larson, 1986).

1986-1992 Program Development and Planning

The goals established by Congress can be summarized into three broad program objectives. First, baseline data will be collected to characterize the conditions of the lake from 1982 to 1992. Second, studies of lake organization and structure will be instigated to develop reliable relationships among physical, chemical, and biological components of the lake ecosystem. Third, lake conditions will be evaluated for possible change and, if changes are detected, special studies will be initiated to determine the amount of change, and the possible causes; and if change is determined to be anthropogenic in nature, appropriate mitigation measures will be recommended.

The first two objectives are designed to understand the present lake conditions, structure, and organization. The heart of objective 3 is to assess these baseline data to determine if the water quality of Crater Lake has changed. We plan to repeat key studies that were conducted prior to the apparent change of lake clarity, and by conducting a paleolimnological study to help reconstruct the history of the lake's water quality. Establishment of a permanent boat house on the lake will enable limnological studies to be conducted year round.

These three objectives are useful for general discussion but are too broad to be practical and are not focused into a meaningful conceptual model. For these reasons the conceptual model shown in Figure 2 was developed to identify important aspects and interactions of the lake ecosystem which require further study. The lake characteristics are broadly defined as physical, chemical, and biological, plus the sedimentation and loss (leakage). Since hydro-thermal activity may occur at the lake bottom (Williams and VonHerzen, 1983), this phenomenom is also included. Future research will emphasize the interrelationships among environmental (e.g., atmospheric deposition, solar radiation, temperature, and chemical inputs), terrestrial (e.g., geology, siltation, surface and ground water, and nutrients), cultural (e.g., local disturbances, pollution, and contaminated atmospheric deposition), and lake aspects of the ecosystem.

With this model as our working platform, a set of specific objectives was developed for the program which can be divided into the following categories: (1) baseline studies; (2) lake structure and organization research; and (3) examination of the water quality data for potential changes, optical characteristics, lake color and paleolimnology (Table 2). New projects will be started or ongoing ones modified where needed as the results of our work are analyzed. Our approach will attempt to determine how much variation in the transparency can be explained from an analysis of the baseline limnological data and the structure and organization of the lake.

The lake program from 1982 to 1985 evaluated the quality and types of baseline data necessary to adequately characterize the limnological characteristics of the lake. Based on these data the current program was established. The next phase of the monitoring program will be to extend the sampling into late fall, winter, and spring (samples were taken in March and May 1986, but will be reported elsewhere), and to improve quality assurance. For water quality

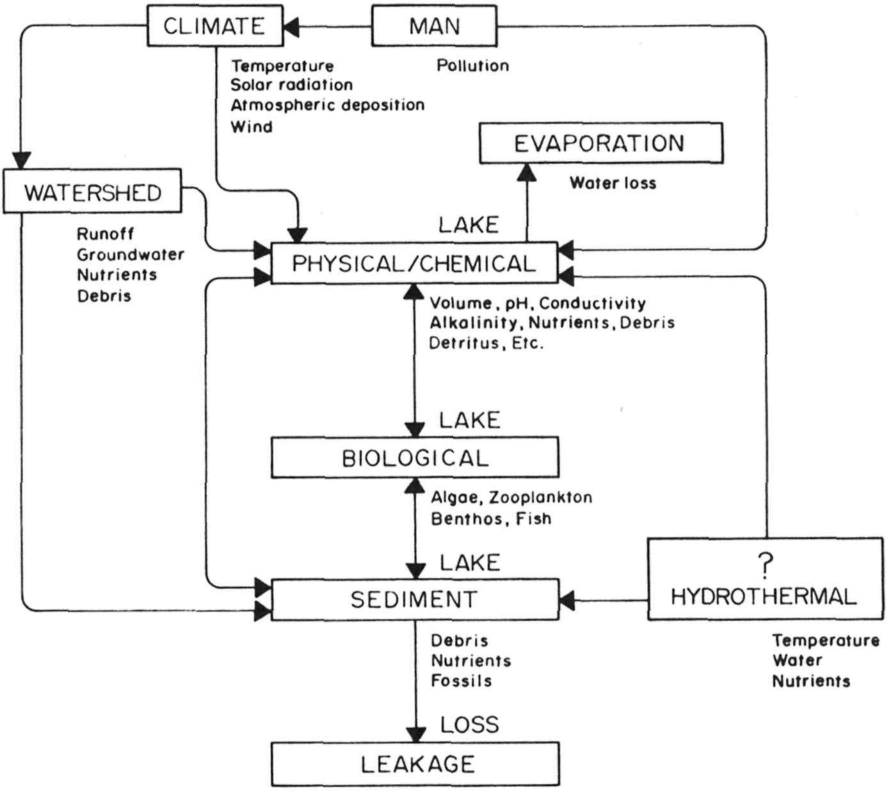

Figure 2. Conceptual Model of the Crater Lake Ecosystem.

tests, duplicate water samples will be analyzed and, where appropriate, test solutions with known concentrations, e.g., nutrient samples, will be submitted with the lake samples. The representativeness of the trend station will be examined by the replicate analyses mentioned earlier. Other improvements to the monitoring program will be the use of a photometer at monthly intervals, monthly primary production estimates, and weekly Secchi disc readings. Anions and cations will also be determined at seasonal intervals from selected depths of the lake. Zooplankton and fish sampling effort and procedures will be based on the results from the two presently ongoing Master's projects.

Studies of lake structure and organization could involve many areas of investigation. Our highest priorities are to refine Phillips and Van Denburgh's (1968) water budget, estimate loading levels of nutrients from the atmosphere into the caldera, and define the dynamics of the sedimentation process. Water budget analyses will include estimates of water input and developing a model for predicting lake levels. Nutrient loading will be determined by collecting samples at different locations around the caldera rim. This work will complement the ongoing particle input, settling, and sedimentation study by Drs. Jack Dymond and Robert Collier, Oceanography Department, Oregon State University, plus their appraisal of hydrothermal conditions and new work on the chemical characteristics of the lake sediment. Furthermore, the results will allow an assessment of how these components are interrelated and how biological lake components and lake clarity respond.

The biological components under study include phytoplankton, zooplankton, benthos, and fish. The former includes algal species, distribution, biomass, abundance, and production. Zooplankton studies will include species, distribution, abundance, biomass, size, and egg numbers. Fish studies will begin in 1986 and will include species, distribution, age, growth, feeding habits, and fecundity, but the details of the work have not been determined at this time. Studies of the benthos will be limited to defining the distribution and abundance of the dominant species.

The assessment of possible changes in lake conditions will be accomplished by repeating two early projects and conducting a paleolimnological study. We plan to repeat Pettit's (1936) early study of lake color and the Smith, Tyler, and Goldman (1973) study of the optical properties of the lake. If changes have occurred, these studies will help provide direction for

Table 2. Working Objectives of the Crater Lake Limnological Studies.

---

1. Baseline data base

   A. Describe the general physical, chemical and biological characteristics of the lake for ten years.

      1. Determine the amount of seasonal and annual variation of each parameter.

      2. Determine how each parameter varies with lake depth.

      3. Determine the amount of spatial variation of each parameter.

      4. Evaluate lake clarity data relative to the physical, chemical and biological conditions of the lake.

   B. Compare current data with those from previous studies of the lake.

2. Lake organization and structure through time.

   A. Lake volume.

      1. Quantify water input into the caldera and lake evaporation.

      2. Document relationships between input and changing lake levels.

   B. Nutrients.

      1. Estimate loading of atmospheric inputs into the caldera and compare with past conditions.

      2. Estimate loss of nutrients to sedimentation and leakage.

      3. Evaluate nutrient levels in the lake through time relative to inputs and losses.

Table 2. (Continued)

C. Biological features

1. Describe the relationships of phytoplankton species, abundance, biovolume, distribution and production relative to physical and chemical lake features and zooplankton.

2. Describe the relationships of zooplankton species, abundance, biomass, and distribution relative to physical and chemical lake features, phytoplankton and fish.

3. Describe the relationships of fish species, abundance, biomass and distribution relative to physical and chemical lake features and zooplankton, benthic macro-invertebrates and terrestrial insects.

3. Optical characteristics, lake color and paleolimnology.

A. Color and Optical Properties.

1. Determine color and optical properties of the lake.

    a. Compare with the 1935 lake color study (Pettit, 1936).

    b. Compare with the 1969 optical study (Smith et al., 1973).

2. If changes are observed from element 3.A1 above, interprete these relative to modern lake clarity conditions as found in element 1.A4 above.

B. Paleolimnology.

1. Evaluate historic lake conditions from analyses of sediment from the lake.

    a. Determine selected physical sediment characteristics through time.

    b. Determine selected chemical sediment characteristics through time.

Table 2. (Continued)

c. Examine the fossil record through time.

2. Determine relationships between the characteristics of surface sediments and settling materials.

4. Evaluate the System for Change (from 1, 2, and 3).

A. Determine if any parameter understudy shows signs of change that is greater than would be expected from modern annual variations.

B. Determine if any detected changes could result in a loss of lake clarity.

C. To the extent necessary, identify and conduct special studies to evaluate factors which may be impacting lake water quality.

---

determining why such changes have occurred and a course of action. The lake color project is being conducted by Dr. Peter Fontana, Physics Department, Oregon State University. The optical study will be conducted when funds become available.

The paleolimnological project has the potential to provide evidence of changing lake conditions. Some of this work will be started in 1986 as part of the nutrient budget study from analyses of chemical features of the lake cores by Dymond and Collier. Additional work will include analyses, through time (i.e., depth in the sediment cores), of diatom species assemblages and crustacean zooplankton species assemblages. In this evaluation an assessment will be made concerning how well the modern phytoplankton and zooplankton species in the lake today are represented in the surface sediments. This information will aid our assessment of changing biological conditions. The work by Dymond and Collier will fill this important gap in our data base.

A major task of this program is to determine if any components of the project show signs of change that would be greater than expected from normal annual variations. This evaluation will involve both the baseline data and data from the special studies. We will rely heavily on statistical and modeling procedures to accomplish these tasks. If changes are found, then special studies will be recommended to evaluate why these changes have occurred.

ACKNOWLEDGMENTS

The support and contributions of the peer review group has been appreciated. Thanks are also extended to Jim Larson, Shirley Clark, and the staff of Crater Lake National Park for their support and dedication to the lake program.

LITERATURE CITED

Byrne, J.V. 1965. Morphometry of Crater Lake, Oregon. Limnology and Oceanography. 10:462-465.

Fryxell, R. 1965. Mazama and Glacier Peak volcanic ash layers, relative ages. Science 147:1288 1290.

Hoffman, F.O. 1969. The horizontal distribution and vertical migration of the limnetic zooplankton in Crater Lake, Oregon. Masters thesis, Oregon State University, 60p.

Larson, D.W. 1984. The Crater Lake study: Detection of possible optical deterioration of a rare, unusually deep caldera lake in Oregon, U.S.A. Verh. Internat. Verein. Limnol. 22:513-517.

Larson, G.L. 1986. Crater Lake limnological studies, 1985. Annual Report, 73p.

Nelson, C.H. 1967. Sediments of Crater Lake, Oregon. Bulletin, Geological Society of America 78:833-848.

Pettit, E. 1936. On the color of Crater Lake water. National Academy of Science 22(2):139-146.

Phillips, K.N. and A.S. Van Denburgh. 1968. Hydrology of Crater, East and Davis Lakes. U.S. Geological Survey, Water Supply Paper 1859-E, 60p.

Smith, R.C., J.E. Tyler, and C.R. Goldman. 1973. Optical properties and color of Lake Tahoe and Crater Lake. Limnology and Oceanography 18:189-199.

Williams, D.L. and R.P. Von Herzen. 1983. On the terrestrial heat flow and physical limnology of Crater Lake, Oregon. Journal of Geophysical Research 88:1094-1104.

LATE HOLOCENE VERTICAL DEFORMATION IN THE YELLOWSTONE LAKE BASIN

William W. Locke[1] and Grant A. Meyer[2]

ABSTRACT

Volcano-tectonic deformation has been shown to be an integral part of the pre-eruptive behavior of basaltic and intermediate volcanoes. The separation of short-term variation from the long-term signal is critical to the use of such deformation as a predictive precursor. Signal separation is particularly difficult for large rhyolitic eruptive centers such as Yellowstone, where major eruptions may not occur over 0.1 m.y. Long-term monitoring of vertical displacement in the Yellowstone caldera is addressed through surveying of raised shorelines of Yellowstone Lake. Nearly continuous segments and correlative fragments of postglacial shorelines have been identified around the north and west shores of the lake. The pattern of deformation of those shorelines is broadly comparable to that of historical (55 yr) and contemporary (1 yr) deformation, but significant differences are present. These differences include areas of local up- and down-warping and evidence of changes in the direction of vertical deformation. Changes in the rate of deformation are potentially important eruptive precursors. Carbon 14 dates on basal organic matter in abandoned lagoons allow the tentative estimation of average deformation over the past 2500 years. The rates between 2500 and 1400 B.P. are less than between 1400 B.P. and the present, which in turn are about two-thirds those determined by historical survey. All are within the range of values determined by comtemporary survey. Present resolution does not allow us to use deformation rates as a predictive precursor.

INTRODUCTION

The Yellowstone region is one of the most studied volcanic areas in the world, yet there is much which is not known about it. Foremost among the questions relating to Yellowstone is its risk of future eruption. The eruptive activity over the past 2 m.y. is certainly indicative of the potential of future eruptions

---

1 and 2. Department of Earth Sciences, Montana State University, Bozeman, MT 59717

(Christiansen, 1984), but the lack of historical eruptions gives us no data base from which to predict future activity. The last minor eruption in the region occurred about 70,000 years ago, thus any consideration of future eruptions will require detailed monitoring, preferably with proxy data to establish a baseline of thousands of years.

The prediction of volcanic eruptions has been confined largely to basaltic vents, and has utilized the monitoring of seismic activity, ground deformation, and changes in gas chemistry, heat flow, magnetism, gravity, and electrical properties (Costa and Baker, 1981). The 1980 eruption of Mount St. Helens, although a human tragedy, was a scientific triumph in terms of the application of monitoring to a volcano of intermediate composition. The emplacement of sensitive equipment only two months prior to the climactic eruption, however, limited the baseline data, thus the recognition of significant changes (Lipman and Mullineaux, 1981).

No major rhyolitic eruption has occurred within historic times, although many such eruptive centers have shown the potential for major eruptions (Newhall et al., 1984). Within the United States the Long Valley caldera, California (Hill and Bailey, 1985) and the Yellowstone caldera (Smith and Braile, 1984) have shown evidence of significant ongoing unrest.

Evidence of unrest in the Yellowstone caldera such as seismic activity, gravity anomalies, teleseismic P-wave delays and interpreted seismic wave velocities, high heat flow, and crustal deformation indicate the presence of magma and the potential for eruption (Iyer et al., 1981; Smith and Braile, 1984). Among this evidence only crustal deformation has the potential of being preserved in the geologic record, thus of use as a long-baseline monitor of change within the caldera. This paper discusses the late Holocene (past 2500 years) record of vertical deformation within the southeast quadrant of the Yellowstone caldera.

VERTICAL DEFORMATION OF THE YELLOWSTONE CALDERA

In the late 1970's, Pelton and Smith (1982) resurveyed the first- and second-order benchmarks established in Yellowstone National Park in 1923. Vertical uplift was recognized throughout the area of the 0.6 m.a. caldera, with a maximum value of about 700 mm along the Yellowstone River north of the outlet of Yellowstone Lake. The deformation was interpreted as roughly symmetrical about the two resurgent domes. The maximum rates of deformation are comparable to those determined in tectonically active areas (Fig. 1).

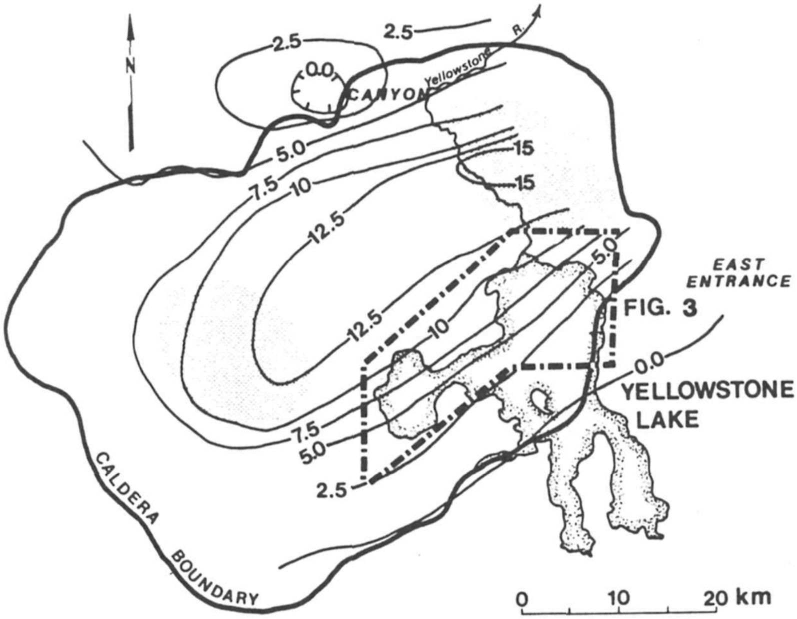

Figure 2. Location of surveyed profiles, measured shoreline angles, and their tentative correlation projected to nearly linear lakeshore segments. Segments F through V after Meyer and Locke (in press). Shaded areas indicate present and former lake cliffs. Solid lines indicate continuous terraces and dashes, dots, and numbered shorelines indicate possible correlation of fragments. Locations of radiocarbon dates (see text) are shown on Figure 3.

Pelton and Smith (1982) caution that their data were constrained to the Park roads, and that the data are consistent with the interpretation of a dome rather than being uniquely interpretable as indicating domal uplift.

Annual releveling across the axis of the dome between Canyon and the caldera rim on the East Entrance road (Dzurisin, 1986) (Fig. 1) confirmed the axially symmetric pattern of uplift and documented annual rates of uplift up to 23 mm/yr. Year-to-year variability, however, is great.

The presence of Yellowstone Lake and its shoreline terraces across the southeast quadrant of the caldera allows the determination of the post-glacial history of deformation within that part of the caldera. Lake shorelines define originally horizontal surfaces; their deviation from horizontal represents the net deformation since formation. Richmond (1973, 1974, 1976, 1977) has mapped post-glacial terraces which lie within 65 feet (20 m) above the present lake level.

Meyer and Locke (in press) have reported on preliminary studies of terrace deformation. Profiles were surveyed to ± 2 cm accuracy across terrace sequences using lake level (recorded daily) as a datum. The elevations of individual terraces were estimated as the intersection of the steepest portion of the former lake cliff with the former wave-cut platform ("the shoreline angle"; Kern, 1977). The accuracy of this estimation varies, but is believed to be better than ±0.3 m. Terraces were correlated between surveyed profiles by walking them out where possible; gullies and lake bluffs disrupt terrace sequences in many areas.

Their data (Fig. 2) allow many interpretations of which only one is shown. Correlation across major erosional gaps was accomplished through limited interpolation of tilt, degree of terrace development, and the assumption of local parallelism of consecutive shorelines. These assumptions affect the complexity of possible interpretations. The origin of the terraces can be interpreted in terms of lake outlet lowering by erosion and outlet raising or lowering through deformation. Terrace deformation can be discussed on both a local scale, involving tectonic stresses and geothermal activity, and a regional scale, resulting primarily from volcano-tectonism (Meyer and Locke, in press). This paper discusses only the origin of the terraces and the magnitude, timing, and rates of regional deformation.

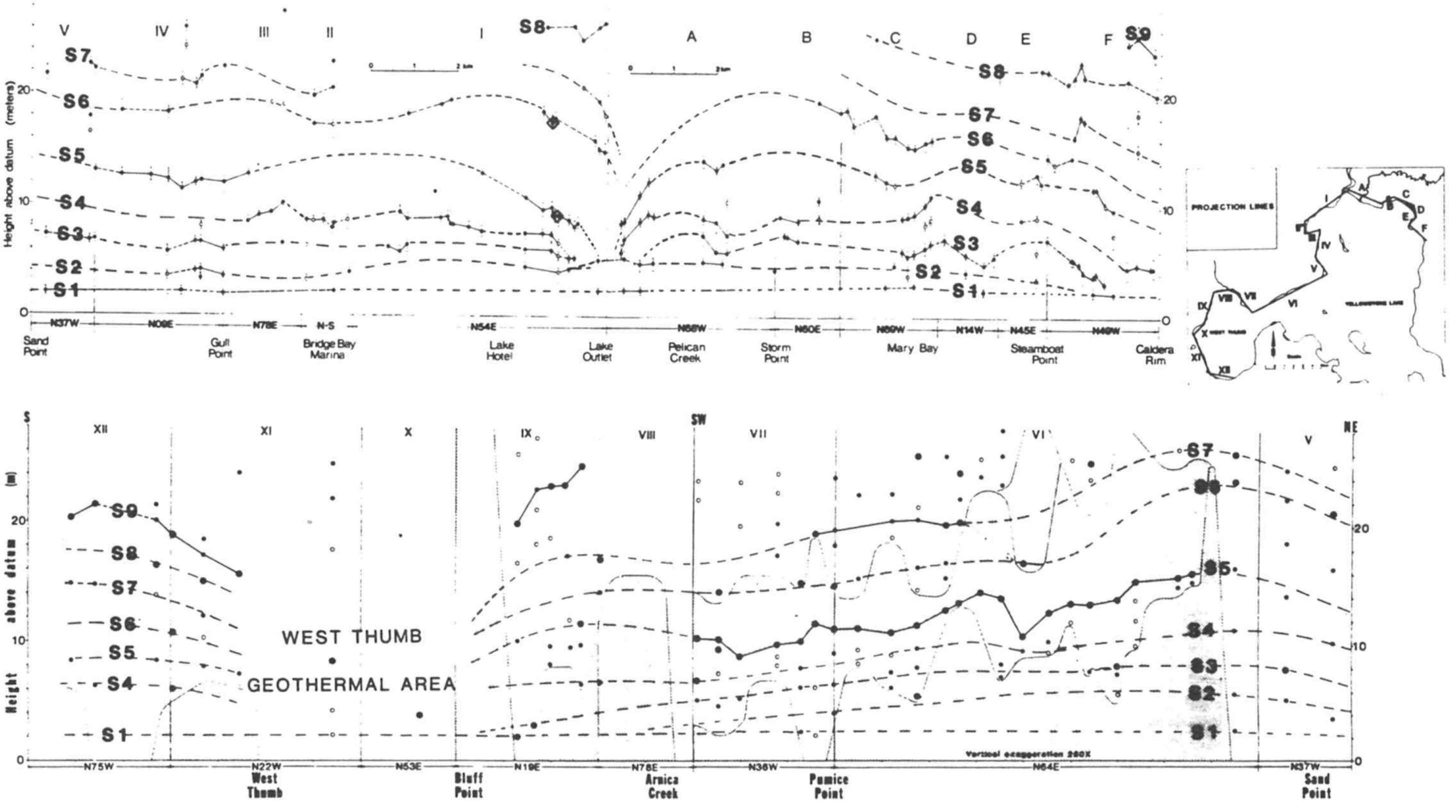

Figure 2. Location of surveyed profiles, measured shoreline angles, and their tentative correlation projected to nearly linear lakeshore segments. Segments F through V after Meyer and Locke (in press). Shaded areas indicate present and former lake cliffs. Solid lines indicate continuous terraces and dashes, dots, and numbered shorelines indicate possible correlation of fragments. Locations of radiocarbon dates (see text) are shown on Figure 3.

ORIGIN OF THE TERRACES

Terraces are not a common feature on lakes with outlets. The best analog for terrace formation at Yellowstone Lake is glacial Lake Agassiz, where episodic lowering of the outlet and isostatic uplift of the lake basin led to the preservation of a series of abandoned shorelines. In the Yellowstone Lake basin, assuming the rate of uplift exceeds that of erosion, continued uplift in the pattern documented by Pelton and Smith (1982) (Fig. 1) should result in a series of drowned, rather than raised shorelines as the outlet rises. The explanation for this anomaly probably lies in the local downwarping evident near the lake outlet (Fig. 2). As caldera inflation occurs, local extensional faulting is necessary to conserve crustal mass. Such faulting is implied 1-2 km south of the lake outlet in the form of a graben cutting Holocene sediments (Otis et al., 1977). According to this model lake level will rise slowly as the caldera inflates, drowning former shorelines and cutting deeply into sedimentary shores. The lake cliffs and wave-cut platforms so formed will then be abandoned during rapid, perhaps nearly instantaneous outlet lowering during relatively rare faulting events. The few 14C dates available (below) suggest periodicities of hundreds of years for such earthquakes. The major difficulty with this model is the lack of observed subaerial fault scarps in the outlet area.

MAGNITUDE OF DEFORMATION

The magnitude of deformation at any point can be crudely estimated as the difference between former and present lake level. This is only a first approximation, because it cannot allow for changes in lake level because of erosion and deformation at the outlet. Hamilton (1984) has documented ongoing erosion at the outlet at approximately 1.4 mm/yr; this rate is subject to change through time as units of differing resistance to erosion are exhumed. In addition, the observed local deformation in the outlet area suggests major changes in lake levels. The best measure of true lake level change would be shoreline elevations on a stable shore. Pelton and Smith (1982) inferred that the east shore of Yellowstone Lake was unaffected by volcano-tectonic deformation, thus terraces formed on that shore may record only changes in water level. Unfortunately, we have not been able to continue our surveys south of the East Entrance road, and the terraces are still markedly tilted (up to the northwest) at the east limit of survey (Fig. 2). The difference between the minimum and maximum recorded elevations on a given terrace yields a minimum magnitude of deformation of that surface.

TIMING OF DEFORMATION

The ages of two of the terraces have been estimated through radiocarbon dating. The datable material is basal organic matter from former lagoons along the lakeshore. These lagoons are easily recognized as broad, shallow, closed depressions with a grass cover. The lagoon floors are commonly beveled onto lake sediment or tills during rising water levels, thus are readily identifiable by digging or coring. Disseminated organic matter which accumulated during the partial draining of the lagoons during falling water levels was collected and dated. The thin late Holocene lagoon fills (<50 cm) allow the penetration of modern rootlets, thus contamination is a problem. (Two of the contracted dates, one on charcoal, are modern.) The two dates cited here (2495 ±130 B.P. [GX-10751] and 1410 ±160 B.P. [GX-10750]) should be viewed with suspicion although they are in correct stratigraphic succession. Assuming that they are close approximations of the ages of the terraces allows the calculation of rates of deformation.

RATES OF FORMATION

The average rates of deformation are the minimum estimates of accumulated deformation divided by the minimum age estimates by radiocarbon dating. These rates can be calculated as point values (in mm/yr) or as differences (tilt, in µrad/yr), and can thus be compared to published values.

Shoreline S-6 maintains a height of about 20 m above present lake level along the northline shore of the lake, showing at least 10 m of net uplift. If the ≈2500 B.P. date is accurate, an average rate of uplift of about 4 mm/yr is implied. The historical rate of uplift inferred by Pelton and Smith (1982) in that region ranges from 8 to 12 mm/yr. The same shoreline shows a maximum net tilt of about 0.7 µrad/yr along the north shore of the lake, compared with historic tilting at about 1 µrad/yr. At Rock Point, the 16 m height above lake level of shoreline S-5 implies net uplift of at least 8 m in ≈1410 years, thus an average rate of nearly 6 mm/yr, comparable to that inferred by Pelton and Smith (1982). In both this study and that of Pelton and Smith (1982), data in the West Thumb area are too fragmentary for significant comparison.

Figure 3 summarizes the interpreted deformation of shorelines S-5 and S-6 across the study area, and compares that deformation with the results of Pelton and Smith (1982). The rates of deformation between 2500 and 1400 years B.P. are computed using an assumed lake level

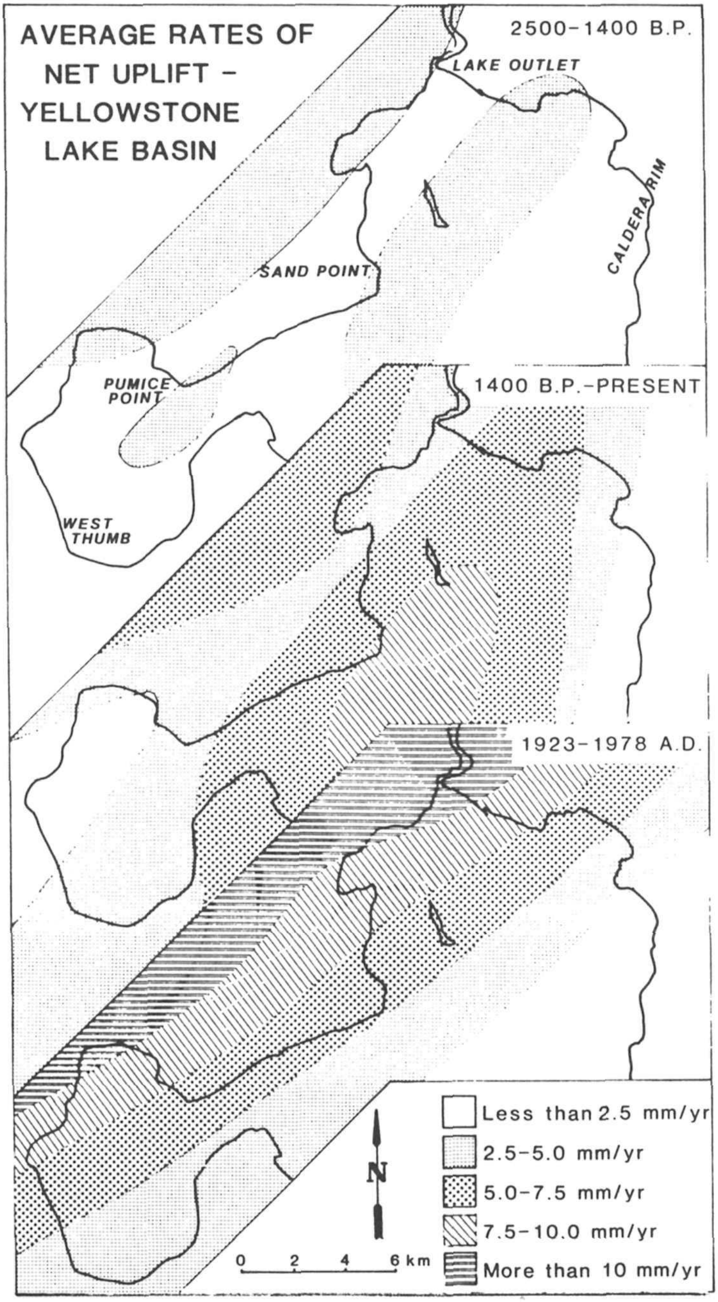

Figure 3. Approximate uplift rates in the Yellowstone Lake basin as indicated by the differences in altitude between shorelines S6 and S5 and between S5 and present water level, corrected for assumed outlet lowering. See text for discussion of assumptions and implications.

lowering (due to erosion and downwarping at the outlet) of 10 m, and were noticeably lower than rates observed subsequently. Rates of uplift over the last 1400 years, calculated using an assumed lake level lowering of 5 m, are greater than those over the preceding 1100 years but in general only about two-thirds those over a 55-yr period. This conclusion is in accordance with observations of a number of geophysical phenomena, which are normally episodic, and is in agreement with the annual data of Dzurisin (1986), which show marked variation in deformation rates from year to year. The late Holocene deformation record is also clearly more complex spatially than the documented historical record.

SUMMARY

From these data we cannot conclude that the rate of uplift in the Yellowstone caldera is increasing; nor can we conclude to the contrary. We can conclude that:

1) Volcano-tectonic uplift in the caldera is not only an historical phenomenon, but has been active for at least the past 2500 years.

2) Uplift centered on the caldera axis is accompanied by local uplift (unexplained) and downwarping (grabens?).

3) The local deformation complicates the pattern of caldera-wide deformation such that a direct compilation of deformation rates is not possible, but it appears that late Holocene rates of deformation have averaged about one-half to two-thirds those recorded in historic time, and that the rates of deformation may be increasing.

4) Further surveys along the east lakeshore are required to determine the absolute magnitude of net uplift within the lake basin.

5) Further dating of terraces is required to accomplish a) confident correlation of terrace fragments, b) confident assignment of ages to individual shorelines, and c) confident calculation of average rates of deformation since and between episodes of shoreline formation.

ACKNOWLEDGEMENTS

The authors wish to acknowledge productive discussion with many individuals, especially Drs. Wayne Hamilton and Dan Dzurisin, which influenced the evolution of this study. Funding in support of this project was received from the Research/Creativity

Committee and Earth Science Department of Montana State University and from the Yellowstone Library and Museum Association. Able field assistance was provided by Edward Spotts and Ralph Wanner.

LITERATURE CITED

Christiansen, R. L., 1984. Yellowstone Magmatic Evolution: Its Bearing on Understanding Large-Volume Explosive Volcanism. In: Explosive Volcanism: Inception, Evolution, and Hazards, National Research Council, Geophysics Study Committee, pp. 84-95.

Costa, J.E. and V.R. Baker, 1981. Surficial Geology: Building with the Earth. John Wiley and Sons, New York, 498 pp.

Dzurisin, D. and K.M. Yamashita, 1986. Implications of Historical Unrest at Yellowstone Caldera, Wyoming. Program and Abstracts. Conference on Science in the National Parks. Fort Collins, CO, 1986, pp.233.

Hamilton, W.L., 1984. Applying Lake Level Gaging Records to the Investigation of Uplift Within the Yellowstone Caldera, Yellowstone National Park (abs.). EDS (American Geophysical Union Transactions) 65: 192-193.

Hill, D.P., R.A. Bailey, and A.S. Ryall, 1985. Active Tectonic and Magmatic Processes Beneath Long Valley Caldera, Eastern California: An Overview. Journal of Geophysical Research 90: 11,111-11,120.

Iyer, H.M., J.R. Evans, G. Zendt, R.M. Stewart, J.M. Cookley, and J.N. Roloff, 1981. A Deep Low Velocity Body Under the Yellowstone Caldera, Wyoming: Delineation using Teleseismic P-Wave Residuals and Tectonic Implications: Summary. Geological Society of America Bulletin 92: 792-798.

Kern, J.P., 1977. Origin and History of Upper Pleistocene Marine Terraces, San Diego, California. Geological Society of America Bulletin 88: 1553-1566.

Lipman, P.W. and D.R. Mullineaux (eds.), 1981. The 1980 Eruptions of Mt. St. Helens, Washington. United States Geological Survey Professional Paper 1250, 844 pp.

Meyer, G. A. and W.W. Locke, in press. Origin and Deformation of Holocene Shoreline Terraces, Yellowstone Lake, Wyoming. Geology.

Newhall, C.G., D. Dzurisin, and L.S. Mullineaux, 1984. Historical Unrest at Large Quaternary Calderas of the World. United States Geological Survey Open-File Report 84-939: 714-742.

Otis, R.M., R.B. Smith, and R.J. Wold, 1977. Geophysical Surveys of Yellowstone Lake, Wyoming. Journal of Geophysical Research 82: 3705-3717.

Pelton, J.R. and R.B. Smith, 1982. Contemporary Vertical Surface Displacements in Yellowstone National Park. Journal of Geophysical Research 87: 2745-2761.

Richmond, G.M., 1973. Surficial Geologic Map of the West Thumb Quadrangle, Yellowstone National Park, Wyoming. United States Geological Survey Miscellaneous Investigations Map I-643.

Richmond, G.M., 1974. Surficial Geologic Map of the Frank Island Quadrangle, Yellowstone National Park, Wyoming. United States Geological Survey Miscellaneous Investigations Map I-642.

Richmond, G.M., 1976. Surficial Geologic History of the Canyon Village Quadrangle, Yellowstone National Park, Wyoming, For Use with Map I-652. United States Geological Survey Bulletin 1427.

Richmond, G.M., 1977. Surficial Geologic Map of the Canyon Village Quadrangle, Yellowstone National Park, Wyoming. United States Geological Survey Miscellaneous Investigations Map I-652.

Smith, R.B. and L.W. Braile, 1984. Crustal Structure and Evolution of an Explosive Silicic System at Yellowstone National Park. In: Explosive Volcanism: Inception, Evolution, and Hazards, National Research Council, Geophysics Study Committee, pp. 96-109.

HYDROTHERMAL ACTIVITY IN RELATION TO LATE HOLOCENE DYNAMICS IN THE YELLOWSTONE CALDERA, WYOMING

Robert O. Fournier[1]

ABSTRACT

Within the Yellowstone caldera, water at hydrostatic pressure convects to a depth of about 4-5 km and attains a temperature of 350-450°C. The heat discharged by the hydrothermal system is about 4×10^{16} cal/yr. Hydrothermal activity appears to have been continuous for 10,000-70,000 years. The thermal energy that drives the hydrothermal convection may be derived entirely from cooling of already crystalline rocks (subsolidus cooling by 350°C of about 0.2 km^3/yr of granite), entirely from the latent heat of crystallization of silicic magma (about 0.2 km^3/yr with no decrease in temperature of the total system), or a combination of the above. The recent uplift of the Yellowstone caldera, about 0.012 km^3/yr, suggests that the injection of magma into the system and/or liberation of fluid from a crystallizing magma are processes that are presently active. At this time the most plausible model is one in which the thermal energy carried to the surface by the advecting hot-spring water comes in part from crystallizing silicic magma and in part from cooling already crystalline rock. It is likely that crystallization and cooling are occurring at some levels while new magma accumulates at others. If water is becoming concentrated in residual silicic melt that is slowly crystallizing, and/or if expelled magmatic fluid is becoming trapped in regions where the pore-fluid pressure is lithostatic, there could be a high potential for future explosive volcanic activity.

DISTRIBUTION AND COMPOSITIONS OF HYDROTHERMAL FLUIDS

Waters from the hot springs and geysers in Yellowstone National Park have been repeatedly collected and analyzed over a 100-year interval (Gooch and Whitfield, 1888; Allen and Day, 1935; Rowe and others, 1973; Kennedy and others, 1985). A few representative analyses of thermal waters from Yellowstone are shown in Table 1. Within the analytical uncertainty, many of the major hot springs and geysers in the Park show no change in water composition with time. The major factors that control fluid compositions are the kinds of rock through which the waters flow, temperature-dependent water-mineral reactions, and underground boiling and mixing with dilute water.

---

[1]U.S. Geological Survey, Menlo Park, CA 94025

Within the Yellowstone caldera, prior to decompressional boiling the deepest and hottest waters that convect to the surface are dilute, pH neutral, chloride-rich solutions containing about 0.06 wt percent dissolved salts. Chloride-poor and sulfate-rich waters result from condensation of steam above the water table and subsequent transformation of H_2S to sulfuric acid that attacks the surrounding rock, such as the sample from Hot Springs Basin, shown in Table 1. The waters at Mammoth are rich in calcium bicarbonate as a result of interaction with sedimentary rocks that include limestone.

The stable isotopes of oxygen and hydrogen in the hydrothermal waters show that the most likely source of the deepest fluids is outside of the caldera in mountains to the north and northwest (Truesdell and others, 1977). However, as the deep fluids convect upward they mix with waters derived locally within the caldera. Hydrothermal fluids emerge especially along the main rim fracture, fractures at the margins of resurgent domes, and along a corridor of faulted ground extending from the caldera through Norris and Mammoth (Fig. 1).

Table 1 - Chemical analyses in mg/kg of selected thermal waters from Yellowstone National Park. Data from Thompson and others (1975).

	Norris Basin (1)	Upper Basin (2)	Lower Basin (3)	Hot Springs Basin (4)	Mammoth (5)
t°C	92	95	95	89	65
pH	8.0	8.9	8.3	2.7	7.3
SiO_2	678	401	242	317	59
Mg	0.05	0.01	0.02	3.8	83
Ca	2.7	0.5	1.1	37	378
Na	420	365	317	187	125
K	91	19	9	16	53
Li	7	6	4	0.04	1.5
HCO_3	52	191	249	0	880
SO_4	25	21	27	1530	681
Cl	709	439	331	0.1	157
F	7	27	33	0.8	2.8
B	10	5	4	5	4

(1) Unnamed spring at base of east end of Porcelain Terrace (YF554)
(2) Giantess Geyser (YF534)
(3) Ojo Caliente Spring (YF351)
(4) Unnamed perpetual spouter (YF448)
(5) Spring flowing from Elephant Back (J7303)

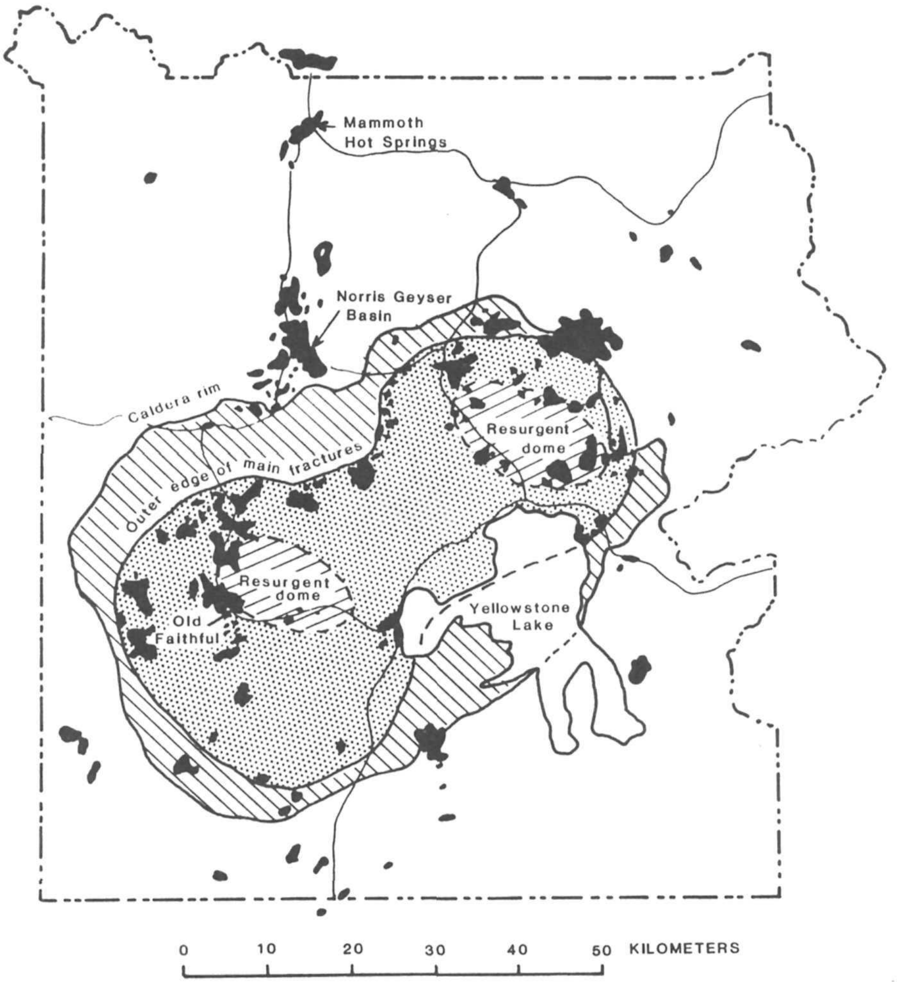

FIGURE 1 - Yellowstone National Park showing outline of 0.6-m.y. caldera, outer edge of main fractured zone, resurgent domes, and distribution of hydrothermal features (black). After Christiansen (1984).

CONCEPTUAL MODELS OF INTERACTION OF METEORIC WATER WITH A MAGMATIC BODY

In most current models of magmatic-hydrothermal systems (Lister, 1974, 1983; Hardee, 1982; Sleep, 1983; Fournier and Pitt, 1985), relatively dilute meteoric water circulates along fractures above and to the sides of a magmatic heat source (Fig. 2). The water is separated from very hot crystalline rock or magma by an impermeable zone where quasi-plastic deformation prevents brittle fracture and maintains low permeability. Heat extracted by the circulating water slowly cools the system, allowing thermal cracking and faulting to progress inward so that water steadily migrates deeper into the heat source while attaining about the same maximum temperature.

Studies of fluid inclusions in minerals in fossil hydrothermal systems show that relatively dilute waters are commonly underlain by brines in the deeper parts of these systems. Therefore, more than one convecting cell may be present, with more dilute waters floating upon more dense brines and confined at the sides by cold, relatively dense water. Figure 3 shows a situation in which two hydrothermal cells are present.

A self-sealed zone also may develop, separating fluid at hydrostatic pressure from fluid at greater than hydrostatic pressure (Fig. 4). The fluid trapped at high pressure may come from various sources, connate pore water, mineral dehydration reactions, and aqueous fluids expelled during crystallization of magma. The maximum pore-fluid pressure that can be attained within the self-sealed region is about equal to the least principle stress within the rock, which may be equal to the lithostatic load. Where lithostatic pore-fluid pressure is attained, thin, discontinuous lenses of water-rich liquid may develop perpendicular to the direction of least principle stress.

At Yellowstone good estimates can be made of the temperature and depth of point B in Figures 2 and 3, the heat flux that results from the hydrothermal activity, and the thermal gradient beneath the convecting hydrothermal system (line DB in Fig. 2 and DF in Fig. 3) required to maintain that heat flux. With the data available for the Yellowstone system we can only speculate about the existence of brine beneath the dilute hydrothermal system, the possibility of fluid trapped at greater than hydrostatic pressure, and present-day crystallization of magma at a relatively shallow depth (4-6 km) as the primary source of thermal energy.

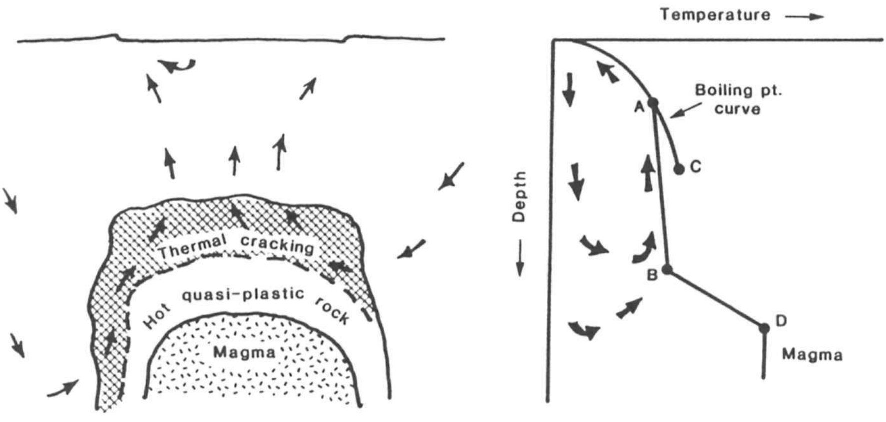

FIGURE 2 - Conceptual model of interaction of circulating water at hydrostatic pressure with a magmatic heat source (see text discussion). After Fournier (1985).

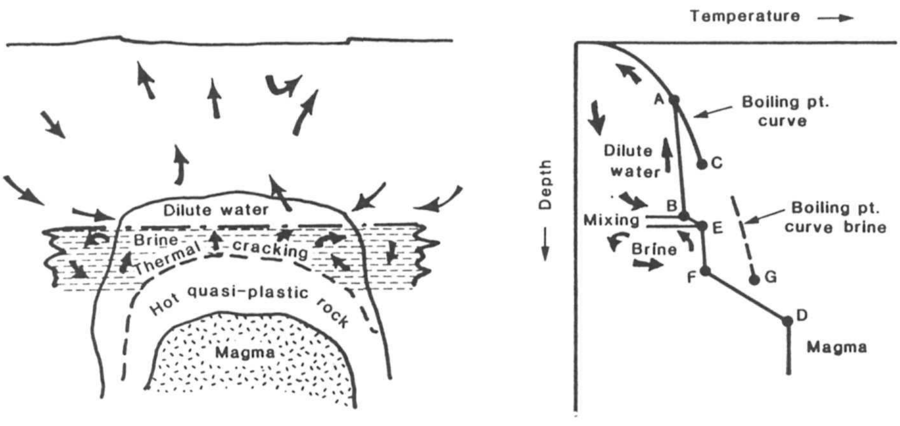

FIGURE 3 - Conceptual model of interaction of circulating water at hydrostatic pressure with a magmatic heat source with highly saline brine between the dilute water and quasi-plastic rock (see text discussion). After Fournier (1985).

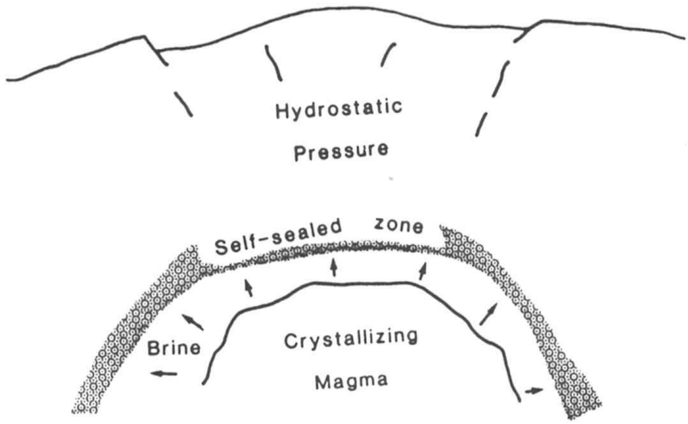

FIGURE 4 - Schematic diagram showing a situation in which mineral deposition and quasi-plastic flow have created a self-sealed zone that separates brine at lithostatic pore-fluid pressure from dilute, hydrothermal fluid at hydrostatic pressure. The brine may be all or in part derived from crystallizing magma.

UNDERGROUND TEMPERATURES WITHIN THE HYDROTHERMAL SYSTEM

Temperatures of local subsurface reservoirs that feed water to hot springs and geysers have been estimated using chemical and isotopic geothermometry, and measured in relatively shallow holes drilled for scientific purposes; about 270°C at Norris, 215°C at Geyser Hill in Upper Basin, 170-200°C at Lower Basin, and 80°C at Mammoth (White and others, 1975; Fournier, 1981). The minimum temperature likely to be attained by the convecting water deep in the system at the base of hydrothermal circulation is about 340-370°C, estimated using mixing models that take account of underground boiling and mixing relations, such as the enthalpy-chloride model (Fig. 5). The maximum temperature likely to be attained by the deeply convecting water, 400-430°C, is constrained by physical-chemical relations (Fournier and Pitt, 1985).

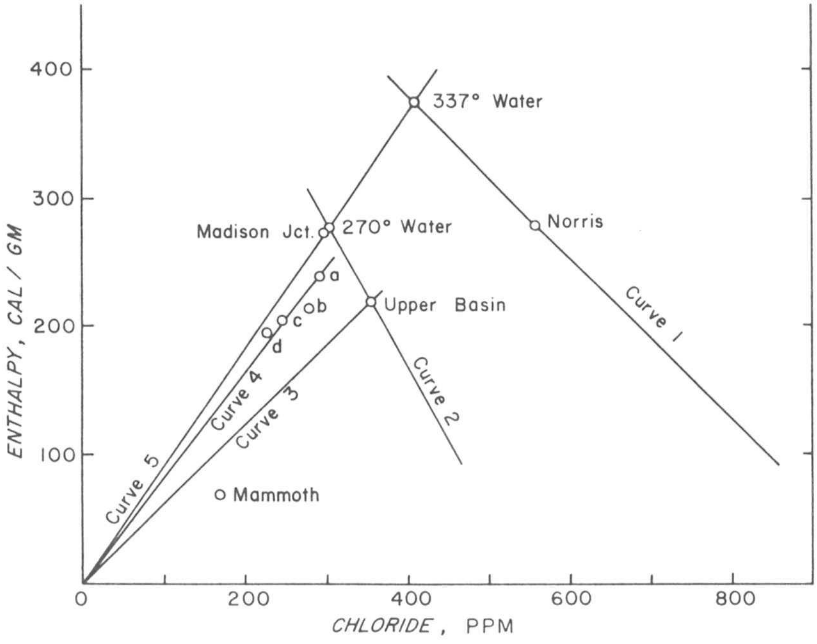

FIGURE 5 - Enthalpy-chloride diagram for Yellowstone thermal waters. Underground boiling with steam separation results in data points that lie along lines radial to the steam point. Mixing with dilute water results in data points that lie along lines radial to the origin. By this model the minimum temperature attained by the convecting waters is about 340°C (337°C) and the chloride concentration is about 400 mg/kg. From Fournier and others (1976).

MINIMUM HYDROTHERMAL MASS AND HEAT FLUX

The chloride concentration of the water deep in the hydrothermal system before decompressional boiling and before near-surface mixing is about 400 mg/kg (Fig. 5). Nearly all of the chloride discharged by the hot-spring waters eventually enters the major rivers that drain the Park. Therefore, measurements of the rates of discharge of the rivers and the chloride carried by those river waters provide a means of determining the total rate of discharge of the deep component of the hot-spring water. The determination is conveniently carried out with the aid of a log-log plot of river discharge rate versus river chloride, and extrapolating to 400 mg/kg chloride using theoretical mixing curves that have fixed shapes (Fig. 6). A summation of the results for all the major rivers gives a value of 10^{11} kg/yr for the deep component of the hydrothermal water (not including the additional water that mixes with the deep water before emerging at the surface) and 4×10^7 kg/yr for the chloride carried by that water (Fournier and others, 1976; Fournier and Pitt, 1985). For a minimum initial water temperature of 340°C, the total amount of heat discharged by that water is 4×10^{16} cal/yr (5.5×10^9 watts), and the heat flux averaged over the entire 2500 km^2 of the Yellowstone caldera is 1800 mWm^{-2} (40 HFU), about 30 times greater than the average continental heat flow.

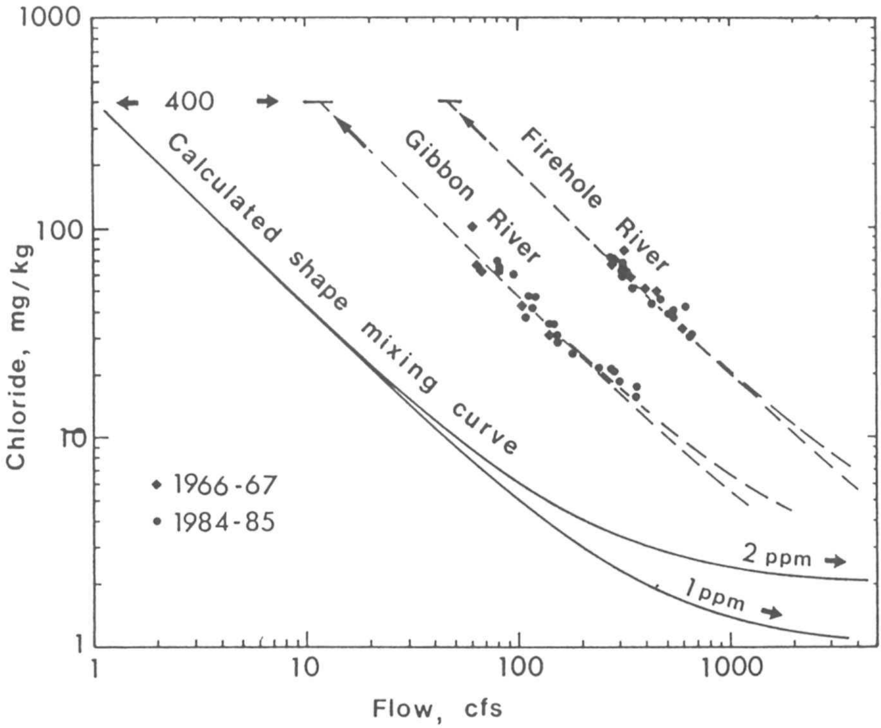

FIGURE 6 - Logarithmic plot of flow rate versus dissolved chloride for the Gibbon and Firehole Rivers. The hot-spring end-member component contains 400 mg/kg chloride. Nonthermal water contains about 1-2 mg/kg (ppm) chloride. The estimated flow of thermal water into the Gibbon River is about 11 cfs, and into the Firehole about 47 cfs.

DEPTH OF CIRCULATION OF THE HYDROTHERMAL WATER AT YELLOWSTONE

Deep drilling in presently active hydrothermal systems has shown that permeability at temperatures above about 300°C is controlled mainly by fractures. Precipitation of minerals and quasi-plastic flow decrease permeability by closing fractures at temperatures above about 350-400°C (Fournier and Pitt, 1985). Therefore, sustained circulation of hydrothermal fluids at these high temperatures is likely to take place only where the rocks are subjected to repeated brittle fracture that counteracts the processes that decrease permeability. Focal depths of well-located earthquakes are deeper than 15 km outside the Yellowstone caldera, but within the caldera seldom exceed 4-5 km, the probable depth of the transition from brittle fracture to quasi-plastic flow (Fournier and Pitt, 1985). Therefore, the maximum depth of sustained fluid flow at hydrostatic pressure is probably about 4-5 km within the caldera and deeper at the sides.

THE THERMAL GRADIENT BENEATH THE CONVECTING HYDROTHERMAL SYSTEM

If the assumption is made that thermal energy is transferred uniformly by conduction from the heat source across a 2500 km^2 surface, through hot dry rock to the base of circulation of the hydrothermal system, a thermal gradient of about 700° to 1000°C/km is required to sustain the average convective thermal output (Morgan and others, 1977; Fournier and Pitt, 1985). To account for both the large advective heat flux and lack of earthquakes below about 4-5 km, it is likely that magmatic temperatures are attained beneath some portions of the caldera at depths as shallow as about 4.5-5.5 km.

LONGEVITY OF THE HYDROTHERMAL SYSTEM

An investigation of the silica budget in the Upper and Lower Geyser Basins showed that hot-spring activity at about its present rate, and lasting from the end of the last glacial period to the present, would be required to deposit the amount of observed sinter (Truesdell and others, 1968). Studies of secondary fluid inclusions found in vein minerals obtained from drill core in the geyser basins show that shallow temperatures within the hydrothermal system at given depths were higher during the glaciation and have not been cooler than presently measured temperatures (Fig. 7).

The thick ice cover effectively raised the water table which, in turn, allowed the boiling-point curve to rise. Therefore, hydrothermal activity at about its present rate is likely to have operated for a minimum of 10,000 years and possibly much longer, starting before or shortly after the last major volcanic eruption in the Park about 70,000 years ago.

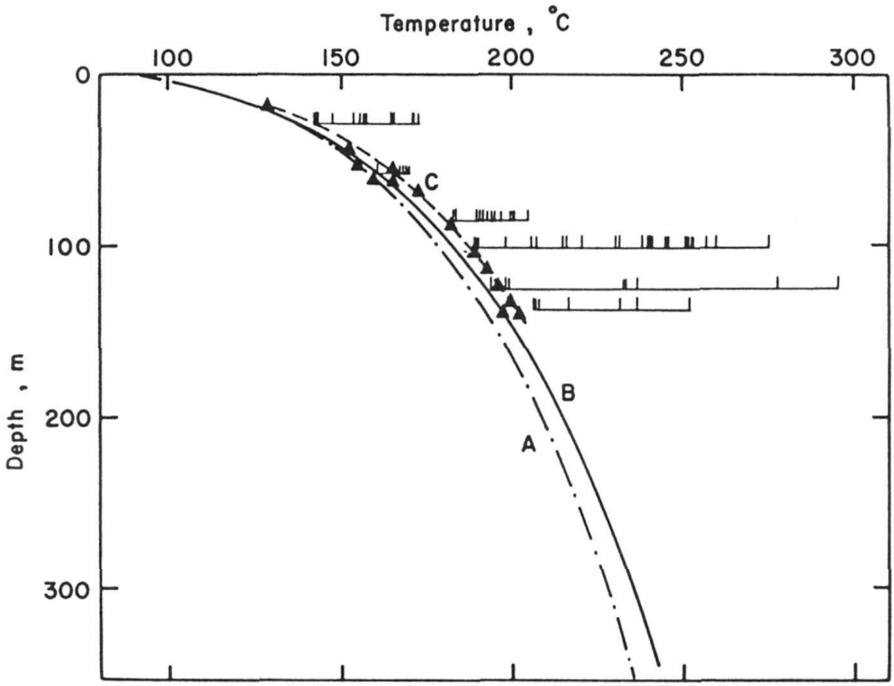

FIGURE 7 - Temperature-depth diagram for the Y-13 scientific drill hole in Lower Basin, Yellowstone National Park. Triangles show measured temperatures as drilling progressed. Short vertical lines show homogenization temperatures of secondary fluid inclusions in quartz obtained from indicated depths. Theoretical boiling-point curves are shown for reference, assuming hydrostatic pressure controlled by weight of overlying column of boiling water (A) and by weight of cold recharge water (B). The actual boiling-point curve measured as drilling progressed is shown by curve C. From Bargar and others (1985).

MAGMA AS A SOURCE OF HEAT AND VOLATILES AT YELLOWSTONE

If the heat carried in the advective flow of water from the system was supplied entirely by the latent heat of crystallization of rhyolite magma, about 5×10^{11} kg/yr of magma (about 0.2 km^3/yr) would be required to furnish that heat (Fournier and Pitt, 1985). A lack of water-bearing minerals in the rhyolite erupted at Yellowstone coupled with the presence of the mineral fayalite suggest that the initial magma contained not more than 1 to 2 wt percent dissolved water (Hildreth and others, 1984). The chloride concentration in fresh obsidian glass shows that the minimum initial chloride concentration in the magma was 1500 mg/kg (Fournier and Pitt, 1985). If most of the chloride is partitioned into the aqueous magmatic fluid that separates upon slow crystallization of the magma, that evolved fluid will contain a minimum of about 12 to 25 wt percent salt. The maximum quantity of water that could be liberated by crystallizing 0.2 km^3/yr of magma initially containing 2 wt percent water is 8.8×10^9 kg/yr, and a minimum of about 7×10^8 kg/yr of chloride would be liberated with that water. For comparison, about 10^{11} kg/yr water (not including water incorporated by near-surface dilution) and 0.4×10^8 kg/yr chloride are discharged by the hot-spring system. Thus, a maximum of about 9 wt percent of the deep hot-spring water could be magmatic, but, only about 6 wt percent of the available chloride is discharged. The deficiency of chloride in the discharged thermal water may be interpreted in two ways: (a) thermal energy is supplied mainly by cooling already crystalline rock with little thermal input from the latent heat of crystallization of magma, or (b) brine evolved from presently crystallizing magma is ponding beneath the dilute hydrothermal system.

CONTRASTING THERMAL AND TECTONIC MODELS

The heat extracted by the hydrothermal system in 10,000 years could be supplied by (a) subsolidus cooling by 350°C (for example, from 750° to 400°C) a crystalline body of rock 0.8 km thick beneath the entire caldera (2500 km^2), (b) the latent heat associated with crystallizing a body of magma 0.8 km thick beneath the entire caldera with no change in temperature of the system, or (c) crystallizing a body of silicic magma 0.4 km thick and then cooling by 350°C.

Cooling of hot but already crystalline rock should lead to thermal contraction and a subsidence of the caldera floor. However, a significant uplift of the caldera has been measured over the period 1923-1984 (Pelton and Smith, 1979, 1982; Dzurisin and Yamashita, 1986; Dzurisin and others, 1986) and studies of raised and submerged shoreline terraces show that there has been episodic uplift interspersed with local deflation of the caldera throughout the Holocene (Hamilton, 1985; Meyer and Locke, 1986). The uplift could be the result of injection of basaltic magma from the mantle into the crust at a depth of about 10-15 km. Meertens and Levine (1985) have suggested that the uplift is the result of horizontal compressive strain, but this does not appear to agree with focal mechanisms of earthquakes within the caldera. The very large and long-sustained flux of thermal energy from the caldera coupled with the apparently shallow penetration of hydrostatic water into the system (shown by the depth of seismic activity) suggest that the latent heat of crystallizing silicic magma is an important source of energy. Crystallization of water-bearing silicic magma could lead to a net increase in volume of the system (accommodated by uplift) if the liberated magmatic fluid is trapped underground where pore-fluid pressures equal lithostatic pressure (Fig. 4).

The calculated total volume change associated with the crystallization of a given amount of rhyolitic magma is strongly influenced by the amount of water that is assumed to be liberated during that crystallization, the salinity of that water, and the temperature and fluid pressure. For a crystallization temperature of 800°C at 150 MPa (lithostatic fluid pressure at about 5 km depth), the total volume change that would result from the crystallization of 0.20 km^3/yr of rhyolite with the liberation of 2 wt percent dissolved water as a 10 wt percent NaCl solution would be about +0.035 km^3/yr. The calculated average rate of volume increase determined from the measured rate of uplift at Yellowstone is about 0.012 km^3/yr (Dzurisin and others, 1986). Therefore, the volumetric change associated with crystallization of an amount of magma that could supply the heat discharged by the hydrothermal system is within the range of the volume of the uplift. These calculations do not demonstrate conclusively a causal relationship between the uplift and liberation of fluid from crystallizing magma. However, the calculations do show that the volumetric effects of liberating a magmatic fluid could be important if the latent heat of crystallization of magma is an important source of energy for the hydrothermal system.

Episodic hydrofracturing and injection of pore fluids that have accumulated at lithostatic pressure into the hydrostatically pressured system might account for episodic deflation of the caldera. Also, rupturing of self-sealed rock that separates regions of lithostatic and hydrostatic pore-fluid pressures could account for some of the seismic swarms that occur within the caldera. A change from 0.012 km^3/yr inflation of the caldera to no inflation would require an increased flow of about 5-10 percent of hot-spring water from the system; about within the uncertainty of measurement of the method employed by Fournier and others (1976) to determine the total convective flow.

It is generally agreed that continuing injection of basaltic magma (1200-1300°C) from the mantle into the crust over a long period of time supplies the thermal energy to melt crustal material, forming large volumes of silicic magmas at 800-900°C (Christiansen, 1984). Crystallizing and cooling (1200° to 860°C) about 0.08 km^3/yr of basalt could furnish the heat for the present-day Yellowstone hydrothermal system. This yearly volume of basalt is about 7 times more than the historic measured average rate of volumetric inflation of the Yellowstone caldera. If mass (either cooled basaltic magma or dense crystalline material) is not convecting downward into the lower crust and mantle beneath the Yellowstone caldera to counterbalance the buoyant upflow of hotter basaltic magma, the Yellowstone volcanic system, as a whole, is cooling at present and the amount of silicic melt (if any) in the shallow part of the system is probably steadily decreasing. But, associated volcanic hazards may be increasing owing to accumulation of aqueous magmatic fluids.

CONCLUSIONS

Water at hydrostatic pressure convects to a depth of about 4-5 km within the Yellowstone caldera and attains a maximum temperature of about 350-450°C. The heat discharged by the hydrothermal system is about 4×10^{16} cal/yr, and the hydrothermal activity appears to have been continuous for 10,000-70,000 years. It is not known whether the magmatic-hydrothermal system, as a whole, is presently cooling down or heating up. The thermal energy that drives the hydrothermal convection can come entirely from cooling already crystalline rocks, entirely from the latent heat of crystallization of silicic magma at a depth of about 4-5 km, or a combination of the above. The recent uplift of the Yellowstone caldera suggests that the injection of magma into the system and/or liberation of fluid from a crystallizing magma are processes that are presently active. At this time the most plausible model is one in which the thermal energy carried to the surface by the advecting hot-spring water comes in part from crystallizing silicic magma and in part from cooling already crystalline rock. It is likely that crystallization and cooling are occurring at some levels while new magma accumulates at others. If water is becoming concentrated in residual silicic melt that is slowly crystallizing, and/or if expelled magmatic fluid is becoming trapped in regions where the pore-fluid pressure is lithostatic, there could be a high potential for future explosive volcanic activity.

REFERENCES

Allen, E. T., and Day, A. L., 1935, Hot springs of the Yellowstone National Park: Carnegie Institution of Washington Publication 466, 525 p.

Bargar, K. E., Fournier, R. O., and Theodore, T. G., 1985, Particles in fluid inclusions from Yellowstone National Park-Bacteria?: Geology, v. 13, p. 483-486.

Christiansen, R. L., 1984, Yellowstone magmatic evolution: Its bearing on understanding large-volume explosive volcanism, in Explosive volcanism: Inception, evolution, and hazards: Studies in geophysics: Washington, D.C., National Academy Press, p. 84-95.

Dzurisin, D., and Yamashita, K. M., 1986, Preliminary results of leveling and trilateration surveys in Yellowstone National Park, Wyoming, 1983-1985: U.S. Geological Survey Open-File Report 86-265-A, 33 p.

Dzurisin, D., Yamashita, K. M., and Johnson, D. J., 1986, Preliminary results of leveling and trilateration surveys in Yellowstone National Park, Wyoming, 1985: U.S. Geological Survey Open-File Report 86-265-B, 28 p.

Fournier, R. O., 1981, Application of water geochemistry to geothermal exploration and reservoir engineering, in Rybach, L., and Muffler, L. J. P., eds., Geothermal systems: Principles and case histories: New York, John Wiley, p. 109-143.

Fournier, R. O., 1985, Continental scientific drilling to investigate brine evolution and fluid circulation in active hydrothermal systems, in Raleigh, C. B., ed., Observation of the continental crust through drilling I, of Behr, H.-J., and Raleigh, C. B., eds., Exploration of the deep continental crust: New York, Springer-Verlag, p. 98-122.

Fournier, R. O., and Pitt, A. M., 1985, The Yellowstone magmatic-hydrothermal system, in Stone, Claudia, ed., Geothermal Resources Council 1985 International Symposium on Geothermal Energy [transactions]: International Volume, p. 319-327.

Fournier, R. O., White, D. E., and Truesdell, A. H., 1976, Convective heat flow in Yellowstone National Park, in Second United Nations Symposium on the Development and Use of Geothermal Resources, San Francisco, 1975, Proceedings: Washington, D.C., U.S. Government Printing Office, v. 1, p. 731-739.

Gooch, F. A., and Whitfield, J. E., 1888, Analyses of waters of the Yellowstone National Park, with an account of the methods of analysis employed: U.S. Geological Survey Bull. 47, 84 p.

Hamilton, W. L., 1985, Deformation models for interpreting warped Holocene terraces of Yellowstone Lake and the Yellowstone River at the Yellowstone Caldera, Wyoming: EOS, Trans. American Geophysical Union, v. 66, no. 46, p. 853.

Hardee, H. C., 1982, Permeable convection above magma bodies: Tectonophysics, v. 84, p. 179-195.

Hildreth, W., Christiansen, R. L., and O'Neil, J. R., 1984, Catastrophic isotopic modification of rhyolitic magma at times of caldera subsidence, Yellowstone Plateau volcanic field: Journal of Geophysical Research, v. 89, p. 8339-8369.

Kennedy, B. M., Lynch, M. A., Reynolds, J. H., and Smith, S. P., 1985, Intensive sampling of noble gases in fluids at Yellowstone: I. Early overview of the data; regional patterns: Geochimica et Cosmochimica Acta, v. 49, p. 1251-1261.

Lister, C. R. B., 1974, On the penetration of water into hot rock: Royal Astronomical Society Geophysical Journal, v. 39, p. 465-509.

Lister, C. R. B., 1983, The basic physics of water penetration into hot rock, in Rona, P. A., Bostrom, K., Laubier, L., and Smith, K. L., Jr., eds., Hydrothermal processes at seafloor spreading centers: New York, Plenum Press, p. 141-168.

Meertens, C., and Levine, J., 1985, Compressive tectonic strain as a possible mechanism for long-term vertical deformation of the Yellowstone caldera: EOS, Trans. American Geophysical Union, v. 66, no. 46, p. 853.

Meyer G. A., and Locke, W. W., 1986, Origin and deformation of Holocene shoreline terraces, Yellowstone Lake, Wyoming: Geology, v. 14, p. 699-702.

Morgan, P., Blackwell, D. D., and Spafford, R. E., 1977, Heat flow measurements in Yellowstone Lake and the thermal structure of the Yellowstone caldera: Journal of Geophysical Research, v. 82, p. 3719-3732.

Pelton, J. R., and Smith, R. B., 1979, Recent crustal uplift in Yellowstone National Park: Science, v. 206, p. 1179-1182.

Pelton, J. R., and Smith, R. B., 1982, Contemporary vertical surface displacements in Yellowstone National Park: Journal of Geophysical Research, v. 87, p. 2745-2751.

Rowe, J. J., Fournier, R. O., and Morey, G. W., 1973, Chemical analysis of thermal waters in Yellowstone National Park, Wyoming, 1960-1965: U.S. Geological Survey Bull. 1303, 31 p.

Sleep, N. H., 1983, Hydrothermal convection at Ridge Axes, in Rona, P. A., Bostrom, K., Laubier, L., and Smith, K. L., eds., Hydrothermal processes at seafloor spreading centers: New York, Plenum Press, p. 71-82.

Thompson, J. M., Presser, T. S., Barnes, R. B., and Bird, D. B., 1975, Chemical analysis of the waters of Yellowstone National Park, Wyoming, from 1965-1973: U.S. Geological Survey Open-File Report 75-25, 59 p.

Truesdell, A. H., Fournier, R. O., White, D. E., and Muffler, L. J. P., 1968, Preliminary silica budget for the Upper and Lower Geyser Basins of Yellowstone National Park, Wyoming, U.S.A.: International Geological Congress, Czechoslovakia, 1968, Report of the 23rd Session, Abstracts, p. 389.

Truesdell, A. H., Nathenson, M., and Rye, R. O., 1977, The effects of subsurface boiling and dilution on the isotopic compositions of Yellowstone thermal waters: Journal of Geophysical Research, v. 82, p. 3694-3704.

White, D. E., Fournier, R. O., Muffler, L. J. P., and Truesdell, A. H., 1975, Physical results of research drilling in thermal areas of Yellowstone National Park, Wyoming: U.S. Geological Survey Prof. Paper 892, 70 p.

INTEGRATED STUDIES OF SOIL PROCESSES IN SEQUOIA NATIONAL PARK

M. A. Lueking, A. D. Brown, and L. J. Lund[1]

ABSTRACT

Sequoia National Park is the site of an integrated watershed study designed to evaluate the effects of acidic deposition on aquatic and terrestrial ecosystems in the Sierra Nevada. Soils play a major role in ecosystem sensitivity and thus, estimates of the magnitudes of soil processes consuming or producing acidity must be known. Objectives of this ongoing study are to (1) identify major soil processes affecting nutrient cycling and the soil solution in the Emerald Lake Watershed (ELW), and (2) determine sensitivity of ELW soils to anthropogenic acidic deposition. Nitrogen (N) and S mineralization rates as measured in the field were very low and were related to soil temperature, moisture, and total soil C and N contents. Throughfall was enriched in most chemical constituents relative to bulk deposition. Pinus monticola and Castanopsis sempervirens throughfall contained higher levels of Al, NO_3^-, and SO_4^{2-} but lower levels of PO_4^{3-} relative to Salix oreochila. Decomposition of leaf litter resulted in 47% weight loss for Salix versus 25% for Pinus and Castanopsis under the winter snow cover. Concentrations of Ca and Mg in soil solutions and surface waters reflected mineral weathering patterns. Mineralization of N and S in the laboratory decreased with acid additions and sulfate adsorption capacity is low in soils of ELW. As a result, soils of ELW are inferred to be potentially sensitive to acidic deposition.

INTRODUCTION

The Emerald Lake Watershed (ELW) in Sequoia National Park (118°41'W,36°36'N) is the site of an integrated watershed study which includes this investigation of soil processes and their interactions with vegetation and surface waters. Soil systems are much more resistant to changes in pH than are aquatic ecosystems. Buffering processes in soils can modify the chemistry of water passing through them and thus influence the composition of surface waters. Vegetation also has a major influence on soil properties and solution composition. These processes mediate the potential effects of acidic deposition to watersheds feeding poorly buffered streams and lakes such as Emerald Lake.

Soils serve as both internal sources and sinks of hydrogen ions within an ecosystem (Van Breeman et al., 1984; Driscoll and

---

[1]Postgraduate Research Soil Scientist, Postgraduate Research Soil Chemist and Professor of Soil Science, respectively, Department of Soil and Environmental Sciences, University of California, Riverside, CA (714) 787-5116

Likens, 1982). Soil processes which can result in the production of acidity include mineralization, respiration, decomposition, uptake of cations by the biota, and cation exchange on soil surfaces. Soil processes which consume acidity include mineral weathering, sulfate adsorption, denitrification, and uptake of anions by the biota. Many soil processes that consume or produce acidity are closely related to nutrient cycles of nitrogen (N), sulfur (S), phosphorus (P) and the hydrolysis of aluminum (Al).

The objectives of the ongoing soil processes research at ELW are (1) to identify soil processes which affect nutrient cycling and soil solution composition at ELW, and (2) to determine sensitivity of soil processes to acidic deposition. Eventually, biogeochemical budgets will be produced as more data becomes available for the Emerald Lake Watershed.

MATERIALS AND METHODS

Emerald Lake is a high elevation (2800 m) lake in the subalpine to alpine landscape of Sequoia National Park, California. Like most of the Sierra Nevada, the bedrock is granitic with occasional over-lying ash deposits derived from past volcanic activity. The primary source of water is snow which is present nearly year-round. In the long winter, the snow accumulates to depths of 2 to 5 m, insulating the soil below and preventing it from freezing. The summers are usually very short and dry. The soils which have developed under these conditions are shallow and rocky, but do support alpine and subalpine vegetation.

Three predominant soil types at ELW were selected for analyses. They were located in the inlet meadow, Alta Cirque and the joint (Figure 1). These corresponded with a wet meadow (Lithic Histic Cryaquept); a well drained, sparsely vegetated site (Typic Cryorthent) and a dry meadow site (Entic Cryumbrept), respectively. The three soils were sampled in September 1984, and analyzed for particle size distribution, total Kjeldahl N, total C, total P, and inorganic levels of N, S, and P (all by standard techniques; Page, et al., 1982). Soil pH was determined in a 1:1 soil: water suspension. Reserve S (organic plus reduced inorganic S) was determined by the technique of Bardsley and Lancaster (1960).

In situ N and S mineralization rates were determined for a 30-day period in July 1985 by use of buried bags (Eno, 1960). Simultaneously, gravimetric soil moisture and integrated soil temperatures (sucrose inversion technique, Lee, 1969) were determined. Effects of acid additions on N and S mineralization were determined from a 16 week laboratory incubation (Stanford and Smith, 1972). Soil samples were leached biweekly with 0.01 M KCl which was maintained at pH 4.75 with H_2SO_4. The pH 4.75 value represents the pH of ambient precipitation of the region (Lawson and Wendt, 1982). A control consisted of a 0.01 M KCl extracting solution with a pH of 5.4 (the approximate pH of rain in a non-polluted atmosphere) (Tabatabai, 1985). The leachates were analyzed for ammonium (NH_4^+), nitrate (NO_3^-) and sulfate (SO_4^{2-}).

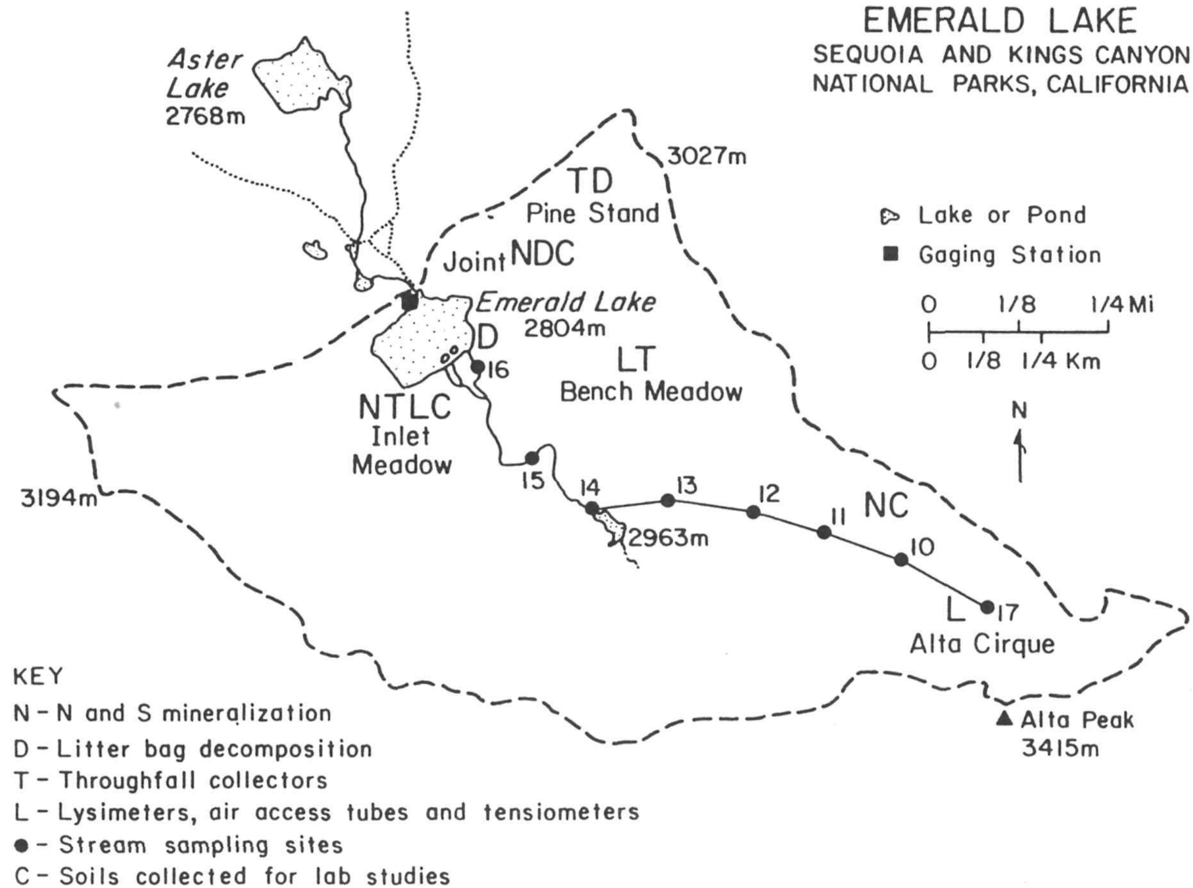

Figure 1. Map of the Emerald Lake Watershed in Sequoia National Park.

The SO_4^{2-} adsorption capacity of the Entic Cryumbrept was determined by treating soil samples with solutions containing 0, 1, 5, or 10 $\mu eq \cdot L^{-1}$ HNO_3 (to control pH of the solution) and 0, 40, 100 or 140 $\mu eq \cdot L^{-1}$ H_2SO_4 (Nodvin et al., 1986). After 24 hours of incubation, solution pH and SO_4^{2-} concentrations were determined.

A litter decomposition study was initiated by placing nylon mesh bags of senescent leaf litter from the three predominant plant species (Pinus monticola, Castanopsis sempervirens, and Salix oreochila) under the respective canopies. Litter bags were collected biannually and analyzed for weight loss (Weider and Lang, 1982). Throughfall funnel collectors were placed beneath the canopies of the three primary plant species. Throughfall and bulk precipitation samples were collected for each of the four summer precipitation events in 1985 and analyzed for chemical composition.

Tension lysimeters were installed in the field in the three representative soils to extract soil solutions from various depths. The tension lysimeter collectors consist of a 10 cm diameter plate covered by a nylon reinforced filter membrane. A single vacuum system connects the four lysimeter plates at each location. Samples of soil solution were collected on a biweekly schedule as long as soil moisture potential remained higher than -0.2 bar. Tensiometers and soil air access tubes were installed next to each lysimeter to allow the determination of soil moisture status and CO_2 content of the soil air at the time of soil solution extraction.

A transect of the major stream feeding Emerald Lake (Figure 1) was sampled biweekly and analyzed for chemical composition to isolate potential areas in the watershed where soil processes resulted in major changes in surface water chemistry. Cations in all extracts and stream samples were determined by atomic absorption or emission spectroscopy. Anions were determined by ion chromatography. Ammonium and NO_3^- were determined by automated colorimetric analyses by indophenol blue and cadmium reduction, respectively. Dissolved organic carbon (DOC) was determined by an automated persulfate oxidation method.

Mineral weathering rates were determined from a four week laboratory incubation in which soil samples were shaken continuously in 0.1 M NaCl which was maintained at pH 3, 4, 4.5, 5, 5.5, 6 or 7. The extractants were analyzed for silica (Si), calcium (Ca) and magnesium (Mg) by argon plasma emission spectroscopy. The release of these bases serves as the ultimate source of acid neutralization (Garrels and Mackenzie, 1967).

RESULTS AND DISCUSSION

Soil Characterization

Soil particle size analyses indicated that the Lithic Histic Cryaquept had the highest silt and clay contents (Table 1). This

Table 1. Physical and chemical characteristics of 3 predominant soils at Emerald Lake Watershed.

Soil Subgroup classification (location)	Depth	Particle size distribution Sand	Silt	Clay	pH 1:1	Organic C	Total Kjeldahl N	Inorganic N NH_4^+-N	NO_3^--N	Reserve S	Inorganic S	Total P	Bray Extr. P
	cm	- - - % - - -				- - - - - - - - - - - - - - - mg·kg^{-1} - - - - - - - - - - - - - - -							
Typic Cryorthent													
(ridge at	0-6	81	13	6	4.39	8200	470	1.92	1.40	37	0.26	270	6
top of	6-44	78	17	5	4.52	2900	310	0.71	0.32	32	0.50	192	3
watershed)	44-68	86	7	7	4.58	1100	150	0.57	0.20	7	0.12	133	8
Lithic Histic Cryaquept													
(inlet	0-15	42	39	19	4.48	135000	11300	14.20	1.15	827	0.37	574	1
meadow)	15-30	58	26	16	4.53	88400	4680	4.41	0.61	362	0.16	175	1
	30-45	67	24	9	4.52	36800	2590	2.84	0.25	--	0	180	0
Entic Cryumbrept													
(joint NE	0-6	60	25	15	4.71	45000	4500	8.54	1.41	238	0.25	223	44
of lake)	6-28	64	24	12	4.47	26600	2060	10.40	1.27	148	0	344	43
	28-55	68	26	6	4.51	24100	1980	4.27	0.96	156	0	384	9
	55-70	69	21	10	4.64	26400	1820	10.00	1.22	148	0	332	2

is important since it indicates a higher moisture holding capacity which is critical for microbial activity and mineral weathering. Soil pH ranged from 4.4 to 4.8 and was not significantly different among soils. These low pH values not only affect nutrient availability but slow many microbial processes, including nitrification (Alexander, 1977).

The Lithic Histic Cryaquept contained the highest organic levels of C, N, S and P (Table 1), a result of the cold, wet condiions in the inlet meadow which slow the decomposition process. The Entic Cryumbrept from the dry meadow also had high levels of total N and C and inorganic N, S and P. The Typic Cryorthent had consider-ably less N and C, a reflection of the lack of plant life in the high cirque resulting in very little organic matter accumulation.

Major Soil Processes Affecting Nutrient Cycling

In situ N and S mineralization and nitrification

Nitrogen and S mineralization rates in the field were generally very low or negative indicating that microbial assimilation was tying up inorganic N and S in these soils (Table 2). Of the $mg \cdot kg^{-1}$ N mineralized in the Typic Cryorthent, 72% was present in the NO_3^- form indicating the importance of the nitrification process. Nitrogen mineralization was found to be highly correlated to soil moisture and temperature as well as the quantity of organic matter present for the month of July. However, before conclusions can be valid, more data needs to be collected.

Table 2. *In situ* N and S mineralization for July 1985 with average soil temperature and water content.

	Mineralization		Soil	Soil
	N	S	temp.	moisture
	---$mg \cdot kg^{-1}$---		°C	wt. %
Typic Cryorthent 0-10 cm	1.71	0.01	14.4	17.2
Lithic Histic Cryaquept 0-15 cm	-0.31	-1.84	12.1	90.0
Entic Cryumbrept 0-10 cm	-1.08	-0.13	13.3	18.4

Sulfate adsorption

The ELW Entic Cryumbrept adsorbed only small quantities of sulfate in comparison to a Typic Haplorthod from the Hubbard Brook Watershed in New Hampshire (Lund et al., 1986). With small additions of sulfate, the amount of sulfate removed from or released to the solution by the soil was linearly related to the initial amount added to the soil-water systems. The linear relationship applies only to the very narrow range of pH values maintained in this experiment. The slope of the relationship is an indicator of the sulfate retaining ability with greater slopes reflecting greater adsorption. In compari-son to the Hubbard Brook soil with a slope of 0.52, the Entic Cryumbrept exhibited a slope of 0.11. This indicates that the ELW soil has a relatively low capacity for adsorbing sulfate additions.

Soil respiration

The respiration of microbes and plant roots in the soil produces carbon dioxide (CO_2). This is important as a control of soil solution acidity since CO_2 reacts with water to form carbonic acid. The concentration of CO_2 in the soil at any time will be a function of both respiration and diffusion rates of CO_2 from the soil (deJong and Schappert, 1972). The partial pressure of CO_2 in the Entic Cryumbrept soil solution increased from 0.19% on July 25, 1985 to 4.66% on August 10. This increase in CO_2 concentrations caused a decrease in soil solution pH for the Entic Cryumbrept from 6.26 in July to 4.91 in August. This large change in pH no doubt had an effect on the solubility of Al, N, S, P and other elements.

Mineral weathering

The extent of mineral weathering in ELW soil surface horizons at pH 4.5 in 0.1 M NaCl was highest for the Entic Cryumbrept, intermediate for the Typic Cryorthent, and lowest for the Lithic Histic Cryaquept (34, 18 and 15 $mmol \cdot kg^{-1} \cdot yr^{-1}$ Si released, respectively). These values are relatively high compared to soils from the northeastern U.S. (Cronan and Aiken, 1985). Cronan and Aiken (1985) found values of 3 and 6 $mmol \cdot kg^{-1} \cdot yr^{-1}$ Si released for a Typic Dystrochrept and Typic Haplorthod, respectively. Calcium and Mg released was also highest for the Entic Cryumbrept (732 and 342 $pmol \cdot kg^{-1} \cdot s^{-1}$, respectively) and lowest in the Lithic Histic Cryaquept (190 and 3 $pmol \cdot kg^{-1} \cdot s^{-1}$, respectively). This indicates the presence of a higher quantity of reactive minerals in the Entic Cryumbrept compared to the Lithic Histic Cryaquept. The observed differences can not be explained by the expected quantities of exchangeable bases since the finer textured Cryaquept should have the highest quantity of exchangeable cations. Cation exchange capacities and base saturations have not yet been determined and that data is critical to a further evaluation of the observed mineral weathering rates.

Other Processes Occurring in Soils, Vegetation and Surface Waters

Litter decomposition

Most of the weight loss from decomposition occurred during the first winter. *Salix* leaves decomposed faster than those of *Pinus* or *Castanopsis* in the first year. Only 53% of the original dry matter from the *Salix oreochila* placed in the litter bags in the fall of 1984 remained when collected in the spring of 1985. There was no weight loss during the summer of 1985. For the *Pinus* and *Castanopsis*, 76 and 79% of the original litter weight remained after the winter, respectively. Another 3% weight loss occurred during summer 1985 for both *Pinus* and *Castanopsis*. The fate of decomposition products released under the snow is thought to be microbial assimilation, or they are lost to surface waters in the spring snowmelt (Lewis and Grant, 1980).

Throughfall

The evergreens (*Pinus* and *Castanopsis*) contributed many substances to throughfall. Aluminum, NH_4^+, NO_3^-, and SO_4^{2-} concentrations in bulk deposition were 1, 97, 100, and 39 $\mu mol \cdot m^{-2}$, respectively. In *Pinus* throughfall, these values were 25, 616, 779, and 122 $\mu mol \cdot m^{-2}$ for Al^{3+}, NH_4^+, NO_3^- and SO_4^{2-}, respectively. *Salix* throughfall seemed to remove N compounds from intercepted precipitation, having NH_4^+ and NO_3^- concentrations of 45 and 30 $\mu mol \cdot m^{-2}$, respectively. The sum of cation charges minus the sum of anion charges indicated anion deficits of -112, -441, -690, and -740 $\mu mol \cdot m^{-2}$ for bulk deposition, *Salix*, *Castanopsis*, and *Pinus* throughfall, respectively. Organic acids probably account for the anion deficit of throughfall solution chemistry.

Soil solution sampling

Soil moisture decreased throughout the summer until September when snow and rain events occurred. Concentrations of Al^{3+}, Ca^{2+}, Mg^{2+}, H^+, NO_3^- and DOC all tended to increase during the season due to concentration by evaporative water loss. Nitrate concentrations were notably lower in the Entic Cryumbrept compared with the Lithic Histic Cryaquept. This is probably related to seasonal plant and microbial activity. Phosphorus was undetectable in soil solutions. This may be due to both the relative insolubility of P compounds and the efficiency of plant and microbial uptake of P.

Calcium and Mg concentrations in soil solutions indicated the influence of mineral weathering on soil solution chemistry, being highest in the Entic Cryumbrept soil solution and lowest in the Lithic Histic Cryaquept. These results agreed with laboratory studies of mineral weathering.

Stream sampling

The concentrations of dissolved substances in samples from the stream transect demonstrate that soil-stream interactions were occurring. Sulfate concentrations declined downstream from below Alta Cirque to the small pond inlet at mid-elevation apparently due to SO_4^{2-} adsorption by soils. Nitrate concentrations also decreased in this same reach of stream possibly due to microbial and plant uptake of N from the surrounding soils. Phosphate was undetectable in surface waters.

Calcium and Mg concentrations in stream waters reflect the same relative concentrations as the soil solution samples. This indicates the importance of mineral weathering in controlling surface water chemistry.

Soil Sensitivity to Anthropogenic Acidic Deposition

Nitrogen and S mineralization rates decreased as a result of the acid leaching experiment. Nitrogen mineralization decreased from 206 $mg \cdot kg^{-1}$ in the control to 191 $mg \cdot kg^{-1}$ ($LSD_{\alpha=.20}$, = 3.9) as a result of acid leaching. Sulfur mineralization decreased from 12.8 to 10.0 $mg \cdot kg^{-1}$ ($LSD_{\alpha=.10}$, = 1.2). Nitrification of mineralized N was not affected by acid treatment and ranged from 30 to 34% in all treatments. It is likely though that many other soil microbial processes such as respiration may also be adversely affected by acidic deposition.

Sulfate adsorption is low in soils of ELW relative to soils from the eastern United States as represented by a Hubbard Brook Typic Haplorthod. This indicates that the ability of ELW soils to neutralize acidic deposition in the form of H_2SO_4 through SO_4^{2-} adsorption is also low.

Soils from ELW have a higher rate of acid neutralization due to mineral weathering than forest soils of the northeastern U.S. (Cronan and Aiken 1985). This implies that these soils may be sensitive to acidic deposition in the short term (microbial and adsorption processes) but that long-term weathering reactions may compensate for this.

CONCLUSIONS

Anthropogenic acidic deposition at ELW is modified by several soil processes which have been observed at this site. Nitrate, NH_4^+ and SO_4^{2-} from acidic deposition will interact with leaves as they fall through the vegetative canopy. Willows (*Salix oreochila*) absorb N compounds in precipitation; whereas, evergreens (*Pinus monticola* and *Castanopsis sempervirens*) release N. Aluminum and other cations and organic acids leach from the leaves and move to the soil surface in throughfall. Litter decomposition in the winter months is more rapid than in summer and produces Al, N, S, P, organic cations and anions which may be utilized in microbial assimilation, plant uptake, or are lost to surface waters.

Once water has entered the soil, it may be modified by a large number of processes. The microbial decomposition of organic matter (mineralization) produces N and S compounds. These nutrients are then assimilated by plants or soil microbes or enter soil or surface waters. Soil minerals derived from the granite and volcanic ash of the watershed contribute to the dissolved cations (and thus the acid neutralizing capacity) of the soil solution. Cation composition in both soil and surface waters is related to mineral weathering.

Carbon dioxide concentrations observed in air trapped in the pore spaces in the soil were high enough to affect the composition of soil solutions. This is an important process determining natural fluctuations in soil pH, which in turn affects organic matter decomposition (mineralization) and weathering rates of soil rocks and minerals.

Adsorption of SO_4^{2-}, believed to be a major mechanism of removal of anthropogenically derived sulfur deposition, is very low in ELW soils. However, effects of SO_4^{2-} adsorption are reflected in surface waters where SO_4^{2-} levels decrease along an elevational gradient.

Our research has shown that soils of ELW may be sensitive to anthropogenic acidic deposition. The microflora are influenced by acid additions as shown in decreased mineralization rates. Sulfate adsorption capacities are low, hence the capacity of the soils to immediately neutralize acidic deposition may be limited. Mineral weathering rates are relatively high though, and may replace cations lost in the adsorption/exchange processes.

Continuing studies will allow us to develop biogeochemical budgets for ELW. Data is presently being collected for a second year. Soil physical and chemical properties such as bulk density, infiltration, water holding capacity, cation exchange capacity and base saturation will all be defined.

LITERATURE CITED

Alexander, M. 1977. Introduction to Soil Microbiology. 2nd ed. pp. 251-277. John Wiley & Sons, New York, NY.

Bardsley, C. E. and J. D. Lancaster. 1960. Determination of reserve sulfur and soluble sulfates in soils. Soil Sci. Soc. Am. Proc. 24: 265-268.

Cronan, C. S. and G. R. Aiken. 1985. Chemistry and Transport of Soluble Humic Substances in Forested Watersheds of the Adirondack Park, New York. Geochim. Cosmochim. Acta 49:1697-1705.

de Jong, E. and H. J. V. Schappert. 1972. Calculation of Soil Respiration and Activity from CO_2 Profiles in the Soil. Soil Science 113:328-333.

Driscoll, C. T. and G. E. Likens. 1982. Hydrogen Ion Budget of an Aggrading Forested Ecosystem. Tellus 34:283-292.

Eno, C. F. 1960. Nitrate Production in the Field by Incubating the Soil in Polyethylene Bags. Soil Science Society of America Proceedings 24:277-279.

Garrells, R. M. and F. T. Mackenzie. 1967. Origin of the chemical com-position of some springs and lakes. Equilibrium concepts in natural water systems. Am. Chem. Soc. Adv. Chem. Sci. 67:222-242.

Lawson, D. R. and J. G. Wendt. 1982. Acid Deposition in California. Society of Automative Engineering Technical Paper No. 821245.

Lee, R. 1969. Chemical Temperature Integration. Journal of Applied Meteorology 8:423-430.

Lewis, W. M., Jr. and M. C. Grant. 1980. Relationships Between Snow Cover and Winter Losses of Dissolved Substances from a Mountain Watershed. Arctic and Alpine Research 12:11-17.

Lund, L. J., A. D. Brown, M. A. Lueking, S. C. Nodvin, A. L. Page and G. Sposito. 1986. Soil Processes at Emerald Lake Watershed. Final Report to California Air Resources Board, Sacramento, CA.

Nodvin, S. C., C. T. Driscoll and G. E. Likens. 1986. The Effect of pH on Sulfate Adsorption in a Forest Soil. Soil Science (in press).

Page, A. L., R. H. Miller and D. R. Keeney (Editors), 1982. Methods of Soil Analysis. Part 2: Chemical and Microbiological Properties. 2nd edition. Agronomy Monograph 9. American Society of Agronomy, Madison, Wisconsin, 1159 p.

A Study of Selected Ecosystem Processes Potentially Sensitive to Airborne Pollutants

Gail A. Baker[1], Mark E. Harmon[1], Sarah E. Greene[2]

ABSTRACT

Natural variation of ecosystem processes must be documented in order to assess the impact of airborne pollutants. The Hoh Rain Forest in Olympic National Park offers an opportunity to study ecosystem processes in a relatively pollutant free environment. The processes we selected for study are sensitive to airborne pollutants and important contributors to long-term ecosystem productivity. They included lichen and moss productivity, litter fall and decay rates and conifer needle population structure and retention times. Current seasonal patterns and characteristics of these processes were quantified. Each process is evaluated with regard to its utility as an index for the effects of pollutant stress.

---

1. Forest Science Dept., Oregon State University, Corvallis, OR 97331; 2. Forestry Sciences Lab., Pacific Northwest Research Station, 3200 Jefferson Way, Corvallis, OR 97331

BACKGROUND

In response to concerns about the spread of air borne pollution and its potential effects on the environment, baseline data collection has been initiated in many areas of the western United States. Documenting current ecosystem conditions provides data against which future comparisons can be made. In many areas now subjected to pollution these data are lacking. Without historical comparison determining the response of ecosystems to increasing pollutant input is hampered.

Complex ecosystem interactions and the variability associated with biological systems add other confounding factors to determining ecosystem response to pollutants. The range of natural variability is an important aspect of an ecosystem parameter because it represents the limits of utility of the parameter is a pollution index. During extreme environmental conditions, short time periods or early stages of pollutant input it may be difficult to distinguish between natural variation and pollutant induced change. In this case parameters with predictable fluctuations would aid in making that distinction.

OBJECTIVE

The objective of this study was to document the current state of five ecosystem processes in a relatively pollutant free area. In a pollutant free site the variability associated with the processes should reflect natural patterns. The range of natural variation determines if parameters can be sensitive enough indices of pollutant stress.

Olympic National Park, Washington was chosen as a study site because it has the cleanest air on the North American continent (Herrmann 1986). Despite this distinction the Park will not remain entirely free from future atmospheric pollutant deposition. The kinds of pollutant threatening this area, and other remote regions, are those capable of long range transport. There is increasing evidence that long range transport of trace elements, gases and manmade organics is a valid phenomenon (Henderson et al. 1985). Sources of these pollutants are the industrial centers of the eastern U.S., Europe, Japan, China and the U.S.S.R. (Rahn 1981).

The five processes chosen were lichen and moss productivity, canopy litter fall and decay rates and conifer needle retention times. These processes have all responded to increased pollution in other ecosystems or in the laboratory, and are important to longterm ecosystem productivity.

SITE DESCRIPTION

The study plot is a 1 ha area located at 176 m elevation near East Twin Creek in the Hoh River Valley, Olympic National Park, WA. The site is a temperate rain forest representative of the Picea sitchensis-Tsuga heterophylla plant community (Franklin and Dyrness 1973). There are 221 trees over 5 cm diameter at breast height and a total basal area of 74.4 m^2 ha^{-1} in the plot. Tree diameter class distribution show an abundance of small and large P. sitchensis (Sitka spruce), intermediate sized T. heterophylla (western hemlock) and 2 large Pseudotsuga menziesii (Douglas fir). Understory trees and shrubs include Acer circinatum, Vaccinium alaskaense and V. parvifolium. Ferns and herbaceous perennials are seasonally abundant. The forest floor is almost completely covered by a luxuriant layer of moss.

The maritime climate of the Hoh Valley is temperate with mean rainfall of 355 cm yr^{-1}. The rainfall has a distinctly seasonal pattern with 75 % of the precipitation falling between November and April. The coolest temperatures coincide with the wettest months (Fig. 1). Daily temperatures and rainfall are monitored at the NADP weather station 5 km from the study plot. Concentrations of NO_3, SO_4 are considerably lower than other regions of the USA and mean rainfall pH from 1980 to 1984 was 5.42 (NAPD 1985).

METHODS

Needle Population Structure: Needle Retention and Loss Rates

Needle population structure was studied on the two dominant conifer species, Tsuga heterophylla and Picea sitchensis. The main objective was to estimate how long needles were retained on twigs. Branches were collected from recently windblown trees at three canopy levels: lower, middle and upper. Needle loss rates were determined by counting needles and/or measuring branch length for each year of growth up to

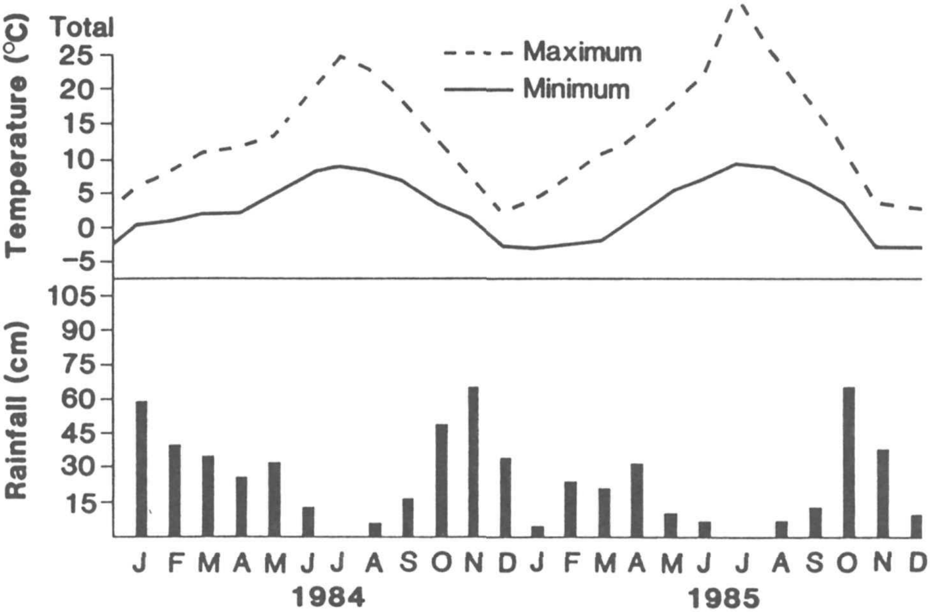

Fig 1. Total monthly rain fall and mean minium and maximum air temperatures recorded at the NADP station 5 km from the sudy plot.

9 yr. Twigs <3 years old retain most of their needles and had visible needle scars which facilitated counting the original number of needles. On older twigs needle scars were not readily apparent; therefore a regression that predicted the number of needles initially present from twig length was developed using 1-3 year old twigs. This regression was used to estimate the original number of needles retained on twigs $\geq$3 years old. The end product was a survivorship table of needles.

Moss Biomass and Productivity

Moss species composition and biomass were measured by harvesting mosses in 50 randomly placed 8.2 cm diameter cores. Ten cores were randomly distributed over each of five 35 m transects within the 1 ha plot. Total moss biomass was sampled from the forest floor but not from fallen logs which covered approximately 10% of the forest floor. The harvested mosses were separated from litter and vascular plants and then sorted into the following species: *Hylocomium splendens*, *Eurhynchium oreganum*, *Rhytidiadelphus loreus*, *Sphagnum girgensohnii* and miscellaneous moss species. Samples were oven dried at 50 °C for 41 hours and weighed immediately after removal from the oven.

Seasonal growth patterns and estimates of annual productivity can be made for H. splendens because it posseses clearly recognizable annual growth increments (Tamm 1953, Binkley and Graham 1981). Each month 25 individual H. splendens stems were harvested from the study plot. The length of the current growth (< 1yr) was measured on each individual. They were then sectioned into 6 growth classes; current, 1, 2, 3, 4, and ≥5 yrs. The growth class sections were pooled, oven dried for 48h at 50°C and weighed. The proportion of biomass in each growth class was then calculated and an age structure-biomass relationship was determined.

A second method to estimate moss production is currently being employed. This method will allow us to test our original H. splendens measurements and to estimate the production of the three other moss species. Production was measured by placing a known mass of living moss in the field and weighing it after growth. Air dried samples of moss were weighed and placed in 11 cm diameter x 7 cm deep plastic cups. Ten replicates were made for each species and placed at the study plot in a randomized block design. The cups were sunk in the moss turf. The experiment began in June 1985 and cups will be collected in November 1986 in order to encompass one complete season of uninterrupted growth.

Lichen Productivity

Lichen productivity experiments followed a methodology developed by Dr. W. Denison of the Oregon State University Botany Department (manuscript in progress). Twenty thalli of Lobaria oregana were strung on each of 30 monofilament lines to make a lichen string. The strings were air dried, weighed, and hung in the field on a PVC frame. Lichen strings were collected at 3 mo intervals, air dried and weighed to determine biomass increases. All thalli were returned to the field except for two strings at each weighing. These thalli were removed and their air dry and oven dried weights were determined. New thalli replaced the harvested ones and were returned to the field.

Occassionally thalli died. If greater than 50% of a single thallus had turned brown it was removed from the string but not replaced. If over 50% of the thalli on the string were dead all were replaced with healthy thalli.

Litter Production and Decomposition

Rates of fine litter production from the forest canopy were determined using 25 buckets randomly placed throughout the study site in June 1984. Material falling into the buckets was caught in nylon liners and collected at monthly intervals. The area of a single bucket is .066 m^{-2}, combined area of 25 buckets was 1.65 m^{-2}. The samples were oven dried, sorted into ten major components and weighed. Seasonal patterns of absolute litter fall and component proportions were then calculated. The needle component was pooled for every 2 month period beginning with Nov-Dec 1984 continuing through 1985. These seven sample groups were analyzed for lignin and nitrogen composition.

Annual decay rates of leaf litter for *Abies procera*, *Acer circinatum*, *A. macrophyllum*, *Alnus rubra*, *Cornus nutallii*, *Picea sitchensis*, *Thuja plicata*, *Populus trichocarpa*, *Pseudotsuga menziesii* and *Tsuga heterophylla* were estimated using standard litter bag methodology (Singh and Gupta 1977). Leaves were gathered just prior to abscission in the fall and air dried. Subsamples of the leaves were analyzed for initial lignin and nitrogen content. In addition the proportion of readily leachable matter was estimated by soaking the leaves in distilled water at room temperature for 48 hours.

Approximately 10 g of leaves were inserted into each of the numbered, 20 X 20 cm polyester bags with a 1 mm mesh size (Crossley and Hoglund 1962). Litter bags were placed on the forest floor in November 1984 for 12 months to determine the annual decay rate. Bags were randomly located through the plot in 5 blocks consisting of 20 bags, 2 bags for each species.

To determine if decay rates change through time, 48 bags of *Acer macrophyllum* and *Pseudotsuga menziesii* were set out. Each month two bags of each species were collected. Monthly collections will continue through November 1986, providing 24 months of data.

After the litter bags were removed from the field, the remaining tissue was oven-dried at 50 °C for 48 hr. The sample was weighed and the loss of litter was expressed as a percentage and as the decay rate constant, k (Jenny et al. 1949, Olson 1963).

RESULTS AND DISCUSSION

Needle Population Structure

Our preliminary work indicated the original number of needles on twigs was well correlated with twig length for T. heterophylla (r^2 = 0.93, Fig. 2). Picea sitchensis had an identical r^2 value. Given the fact the number of needles and internodes is fixed during bud development, these results indicated internodal distance on many twigs is relatively constant. Severe stress induced by pathogens, drought, pollution or mechanical injury may lead to shorter internode elongation than observed in our preliminary sample; therefore these equations are only appropriate to predict needle numbers for healthy trees. Needle retention patterns

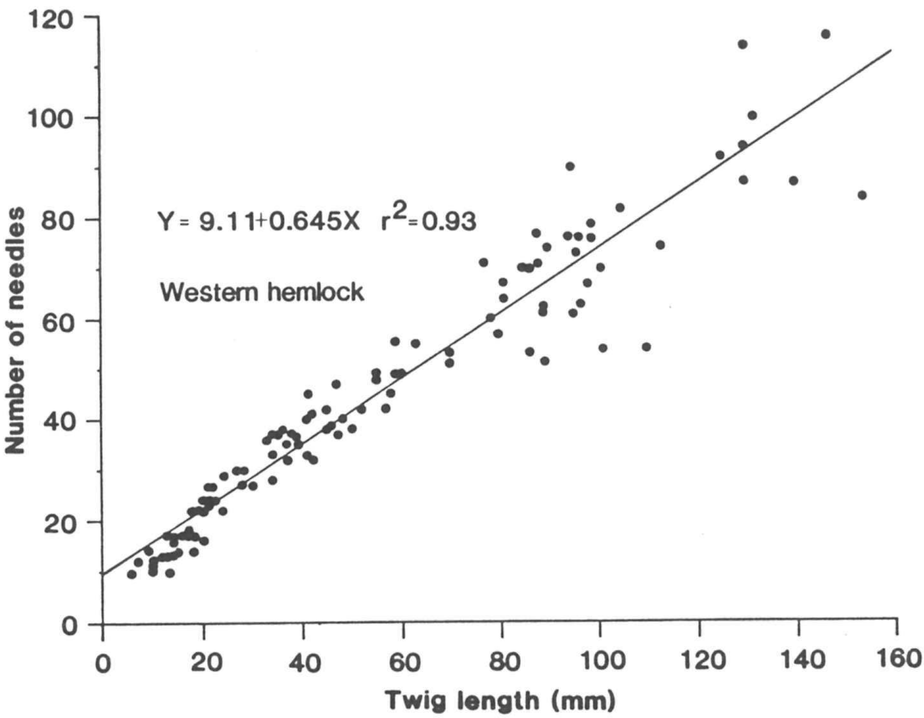

Fig. 2. Relatioship between twig length and the number of needles for one year old twigs of Tsuga heterophylla.

in *P. sitchensis* and *T. heterophylla* varied slightly. Both species lost needles in significant number after 3 years and approximately 60% of their needles were missing from 6 yr old branches (Fig. 3). However, the total length of needle retention in *P. sitchensis* appeared to be a year or two longer than for *T. heterophylla*.

The length of time needles are retained by twigs directly influences the quality of the litter that falls to the forest floor and determines the amount of leaf area in a forest canopy. If needle survivorship decreases stand primary productivity would be affected (Waring 1985). The importance of needle population structure to primary productivity and its predictability suggest that this parameter is a useful indicator of ecosystem stress.

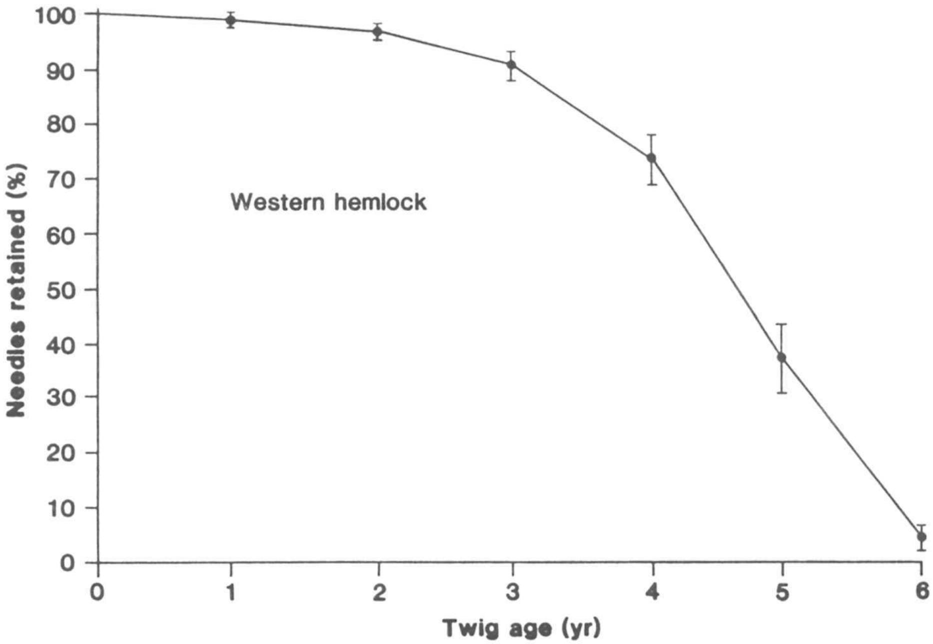

Fig 3. *Tsuga heterophylla* needle retention as a function of time.

Moss Inventory and Productivity

The four dominant forest floor moss species in the study plot were *Hylocomium splendens*, *Eurhynchium oreganum*, *Rhytidiadelphus loreus* and *Sphagnum* girgensohnii with a combined mean biomass of 186.23 gm^{-2}. Hylocomium splendens and S. girgensohnii had the greatest mean biomass values, 76.11 and 77.02 g m^{-2} respectively, and represented 82% of the forest floor moss biomass. A marked difference between H. splendens and S. girgensohnii was their distribution on the forest floor. The latter forms distinct monospecific patches, growing in thick, tightly packed mats. Hylocomium splendens is a feathery moss carpeting the forest floor, intermingling with the less abundant species. This may reflect different moisture requirements and/or growth patterns of the two species. Eurhynchium oreganum and R. loreus were almost as widespread as H. splendens but were much less abundant, 9.51 gm^{-2} and 12.68 gm^{-2} respectively. The remainder of the moss cover was made up of a variety of species that include Plagiomnium spp. and Isothecium stoloniferum.

There were two distinct growth periods associated with phenological development of H. splendens; January to June and September thru November (Fig. 4). New stems were visible at the apex of the previous years growth by November. The stem lengthens 30 to 40 mm during the wet spring months.

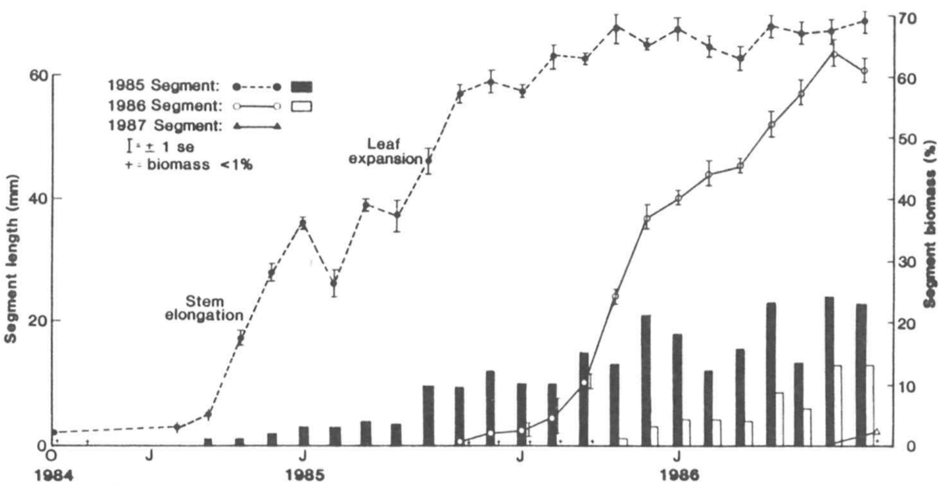

Fig 4. Seasonal growth patterns and biomass increase in the 1985 and 1986 segments of Hylocomium splendens.

During the dry summer period biomass remained constant with some shrinking of the desiccated stem. Growth resumes and leaf expansion begins in the autumn. Biomass increase of the youngest segments progresses slowly at first with the greatest increase coming at the time of leaf expansion. The new growth accounts for up to 20% of the biomass after 19 months of growth. Tamm (1953) observed that this segment continues increasing in biomass through its second year. Annual productivity must then include new growth on both current and year old segments.

An age structure- biomass relationship constructed each month showed segments ≤3 yr old make up 75% of the H. splendens standing crop. The proportion of biomass allocated to each of those segments is approximately equal except for the current segment which is a small proportion initially and increases over the year. Segments ≥4 yr old were over-topped by the younger segments and lost biomass due to decay.

The biomass and length variations seen in the 1985 segment as it entered its second year of growth (Fig. 4) may be due to natural variation. However, they are more likely due to the influence of the 1986 segment and the difficulties in measuring a feathery leaf as opposed to a lengthening stem. The answer to this question is being pursued during the 1986 measurement.

A mechanism explaining pollutant toxicity to lichens has been suggested by Fields and St. Clair (1984). The physiological aspects of pollutant toxicity are not as well known for mosses. Hylocomium splendens shows consistent seasonal growth and productivity patterns. This species and others similar to it are also found in industrial countries (Barclay-Estrup and Rinne 1978, Rühling and Tyler 1970, Rieley et al. 1979, Nakamura 1984). Monitoring moss growth rates in addition to accumulation of heavy metals and other pollutants in tissue may be an indication of atmospheric quality.

Lichen Productivity

Lobaria oregana thalli gained at least 20% of their dry weight biomass during a 3 month period (Table 1). However large portions of biomass were lost due to thallus mortality. During early winter, 17% of the thalli on the strings died. Temperatures during that time were typical for the season, but there was a more persistent snow cover than usual. We do not know if snow collected and remained on the lichen strings. Denison (unpublished) found this lichen species stored in a lab over 100 days loses viability. The thalli used in this experiment were strung and set in the field within 48 hr of collection. The cause of mortality remains uncertain.

Table 1. Biomass measurements of Lobaria oregana thalli over a 12 month period.

Interval	Mean Biomass Change (%)
Mar-Jun 1985	22
Jul-Sep	20
Oct-Dec	-15*
Jan-Mar 1986	26

*17% of the thalli had died by this date.

The growth of healthy thalli was highly variable. Lichen strings gained from 1% to 75% of their dry weight during any three month interval, dead thalli excluded. Keeping this variability in mind we estimate the mean annual productivity to be 50%. Using the same methodology and species Denison (unpublished) found annual growth rates between 13% and 30% in the drier climate of central Oregon, with less variability between strings.

Typical habitat for L. oregana is in the canopy of conifer trees in Pacific Northwest forests. On the east side of the Cascade Mountains in central Oregon, Rhoades (1977) found that L. oregana populations in the crowns of old-growth Douglas fir are in a state of dynamic equilibrim. Often dry weight gained by thallus growth is off-set by loss of whole thalli and fragments to decomposition, consumption and litter fall. The thalli that do survive however are estimated to have a net annual production of 31.1% of the standing biomass (Rhoades 1983).

Mosses and lichens have been widely used as indicators of air borne pollutants (Barkman 1969, Brodo 1966, LeBlanc and DeSloover 1970). The majority of studies quantified species diversity declines and/or accumulation of pollutants in tissue (Tuominen and Jaakkola 1973, Rühling and Tyler 1970). Estimates of lichen productivity are highly variable and may not be adequate indicators of pollutant stress, especially over time spans less than 5 years.

Litter Production

Annual canopy litter fall during 1985 was 2790 kg ha. This value is within the range of litter fall for similar forest communities in Oregon and Washington (McShane et al. 1983). Monthly amounts of litter fall were variable and showed no distinct seasonal pattern (Fig. 5). However when monthly inputs of separate components were considered on a proportional basis, seasonal fluctuations were suggested. Three dominant components of litter fall were conifer needles, cones and fine branches (Fig. 6). Minor components include deciduous leaves and "Other" comprised of reproductive tissue, moss, lichens, and miscellaneous indistinct organic matter. Needles, cones and deciduous leaves show seasonal fluctuations.

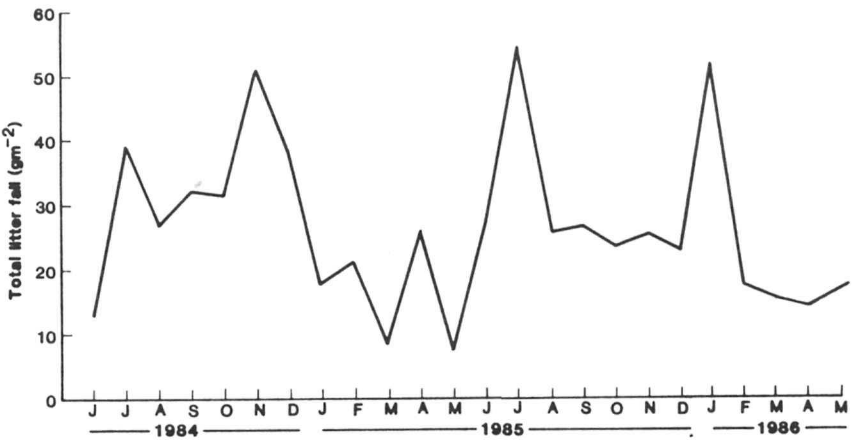

Fig 5. Total monthly canopy litter fall.

Needles from all three conifer species made up the most important litter component. The period of greatest needle fall was during the dry summer season when needles comprised from 65% to 85% of the litter fall. There was also a seasonal fluctuation in the lignin and nitrogen composition of the needle litter (Table 2). Both lignin and nitrogen decreased during the months of July and August. However, the lignin:nitrogen ratio remained fairly constant through the year with a mean value of 31.9. The predicted decay rate, k, for this value is 0.3 yr^{-1}.

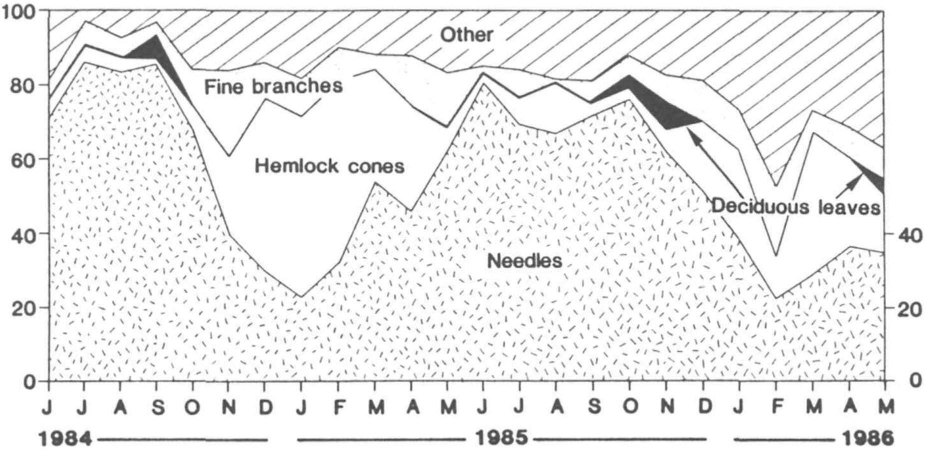

Fig 6. Monthly proportions of four litter fall components. Dark portion represents deciduous leaves. See text for description of the "Other" category.

Table 2. Initial lignin and nitrogen content of the confier needle component of canopy litter fall. Samples pooled over 2 month periods through 1985.

MONTHS	MEAN* % LIGNIN	MEAN % N	LIGNIN:NITROGEN
Nov-Dec 1984	26.2	.81	32
Jan-Feb 1985	29.1	.88	33
Mar-Apr	26.3	.95	28
May-June	22.6	.70	31
Jul-Aug	18.6	.57	33
Sept-Oct	21.3	.72	30
Nov-Dec	26.6	.73	36

*N=3

Ninety-nine percent of the cone component was from T. heterophylla trees with only occassional P. sitchensis cones and none from P. menziesii. The cone component peaked in the winter of 1985 and showed another increase 13 months later.

Acer circinatum and the two species of Vaccinium made up the deciduous component. Their input may have been underestimated because the buckets were 1 to 1.5 m above the ground which exceeds the height of some of the Vaccinium shrubs. They showed the expected seasonal peak in autumn. This is a good reference point for determining the variable timing of autumn leaf abscission in relation to climatic patterns.

Fine branches had a constant input through the year and never fluctuated much below or above the range of 5 to 10%. The "Other" component represented a small percentage of the litter input and had a constant low input.

Bark and wood fragments comprised less than 5% of the annual litter fall and fell irregularly. They are both dense and when present their weight obscures the proportions of the remaining components. For these reasons they were excluded when component percentages were calculated.

The annual amount of litter input is an indication of the biomass added to the detrital pool on the forest floor. The proportions of individual litter components are a measure of litter quality. Conifer needles are the major component of litter at our study site and alteration in their input and/or decay rates may affect the forest nutrient cycles.

Litter Decomposition

Decomposition of leaf and needle litter is related to the initial concentrations of lignin and nitrogen in the tissue (Melillo et al. 1982). The 10 species used in our experiment represented a gradient of lignin:nitrogen ratios ranging from 5 for Cornus nuttalii to 53 for Thuja plicata. Decay rate constant, k, was well correlated (r^2 = .83) with initial lignin:nitrogen ratios (Fig. 7). The deciduous leaves of Alnus rubra did not conform to the model. Alnus rubra, a nitrogen-fixer, decays slower than predicted, indicating factors other than nitrogen limit decay in this species.

Data from monthly collection of litter bags suggested decay rates were not constant through time; Decompositon during the first 3 months was faster than subsequent months; decay of Acer macrophyllum leaves and Pseudotsuga menziesii needles

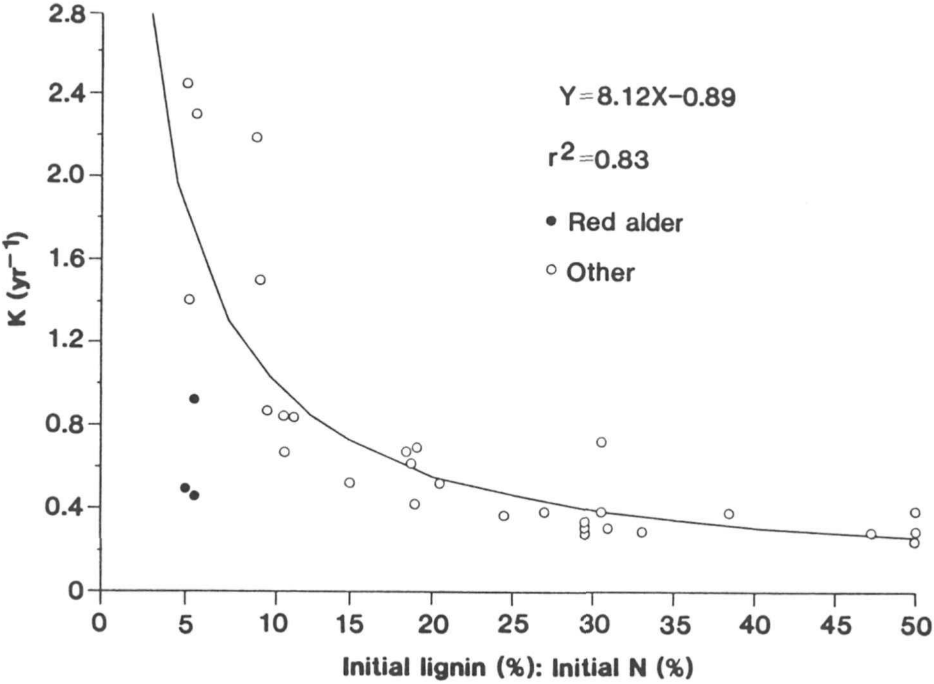

Fig 7. Relationship between the annual decay rate constant, k, and the ratio of initial lignin and nitrogen content of leaf litter.

was modelled with a double-exponential curve (Fig. 8). The main distinction between species was the proportion of fast and slow decay components. In contrast, the rates of each component were quite similar between the two species.

The initial content of readily leachable fraction in fresh litter differed significantly between species (Table 3). We felt that there might also be significant year to year variation within a species because phenological and nutrient status at the time of collection may differ from year to year. It was surprising to find similar readily leachable fraction values in both 1983 and 1984 in all but one species.

Litter decay includes both physical and biological removal of materials. The physical process of leaching by rain increases the proportion of lignin in the remaining tissue. Biological decay of remaining tissue is slower. Incubation time must be standardized (ie. 1 yr) to encompass biological

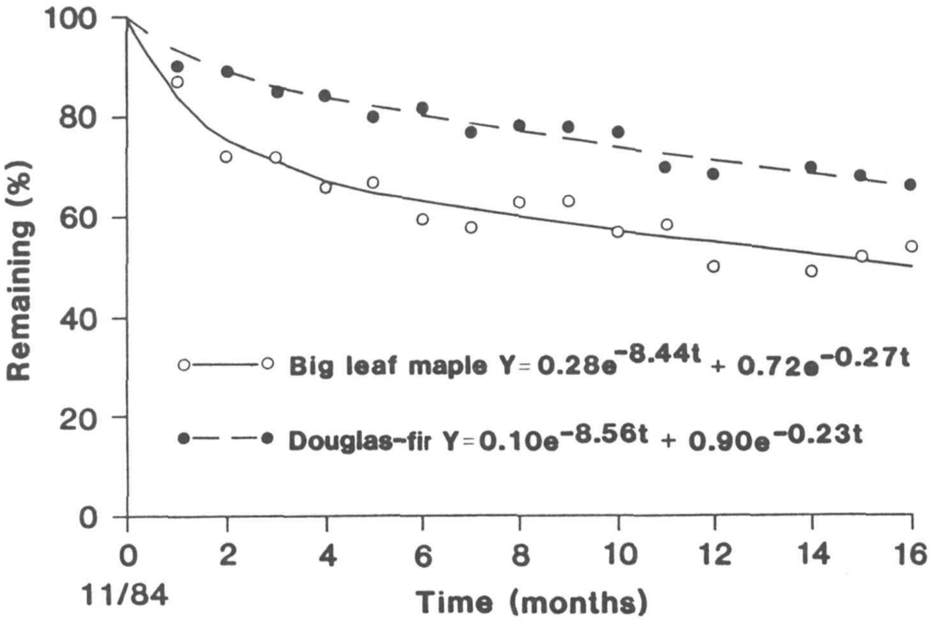

Fig 8. Decay of *Acer macrophyllum* and *Pseudotsuga menziesii* leaves modelled with a double-exponential curve.

Table 3. Variation in readily leachable fraction of fresh leaf litter.

Species	Readily Leachable Fraction (%) 1983	1984
Acer circinatum	31.4	20.9
Acer macrophyllum	14.3	12.4
Cornus nutalii	28.9	26.5
Populus trichocarpa	25.4	24.6
Pseudotsuga menziesii	7.3	8.1
Thuja plicata	5.3	4.0

decomposition processes. The physical process of leaching by rain proceeds quickly, and is probably not as sensitive to pollution effects as biological processes. The separation of the readily leachable and unleachable compounds in the leaf tissue may aid in distinguishing the decay rates associated with the physical and biological decay processes.

SUMMARY

A framework for monitoring ecosystem conditions has been suggested by McShane et al. (1986). They believe that parameters used to measure environmental conditions should reflect an ecosystem process which is measureable through time. In addition, the natural variability of the process should be established and be predictable enough to allow detection of deviation from the norm. Rapport et al. (1985) have stated that the parameters should represent several general categories including nutrient cycling, primary productivity, species characteristics (diversity, composition and size distribution), and the frequency of certain factors like disease incidence and fluctuations of component populations. Ideally one process or parameter from each category would be chosen to establish an ecosystem profile (Odum and Cooley 1980). In this way more perspectives are considered. For example, in a grassland ecosystem primary productivity may remain constant over the years while species composition fluctuates (Rapport et al. 1985). Monitoring only one of these parameters could lead to different conclusions.

The processes we have studied fulfill most of the criteria suggested for ecosystem monitoring. However we lack a long-term data base. Two to three years of documentation is not enough time to sample the range of variability that undoubtably exists. Nevertheless, it is enough time to begin to establish the factors controlling ecosystem processes.

Litter fall, needle retention times and litter decay are a related group of ecosystem processes which stand out because of their predictable seasonal patterns and application to the majority of forest ecosystems. Variability within and between seasonal fluctuations can be associated with climatic patterns and/or species characteristics which are readily distinguished. More precise indications of the sensitivity of these processes will come from data sets which extend over longer periods of time and a broader geographic range.

ACKNOWLEDGMENTS

We are grateful to D. Sharp for field assistance and H. Sharp and the National Park Service for logistic support.

References

Barclay-Estrup, P. and R. Rine. 1978. Lead and zinc accumulation in two feather mosses in northwest Ontario, Canada. Oikos 30:106-108.

Barkman, J. 1969. The influence of air pollution on bryophytes and lichens. In Air Pollution: Proceedings of the First European Congress on the Influence of Air Pollution on Plants and Animals. Wageringen, 1968. p. 197-209.

Binkley, D. and R. Graham. 1981. Biomass production and nutrient cycling of mosses in an old-growth Douglas-fir forest. Ecology 62: 1387-1389.

Brodo, I.M. 1966. Lichen growth and cities. A study on Long Island, New York. The Bryologist 69:427-449.

Crossley, D. and M. Hoglund. 1962. A litter bag method for the study of microarthropods inhabiting leaf litter. Ecology 43:571-573.

Fields, R. and L. St. Clair. 1984. The effects of SO_2 on photosynthesis and carbohydrate transfer in the two lichens: *Collema polycarpon* and *Parmelia chlorochroa*. Am. J. Botany 7:986-998.

Franklin, J. and C. Dyrness. 1973. Natural vegetation of Oregon and Washington. Forest Service General Technical Report. PNW-8, Pacific Northwest Forest and Range Experiment Station, Portland, Oregon. 417 pp.

Henderson, D., M. Liu and D. Stewart. 1985. Long distance transport of man-made air pollutants. Park Science 5:6-8.

Herrmann, R. 1986. Acid Precipitation Research and Monitoring in the National Park Service. Park Science 6:31-32.

Hoortsman, J., W.C. Denison, W.B. Silvester. 1982. $^{15}B_2$ fixation and molybdenum enhancement of acetylene reduction by *Lobaria* spp. New Phytol. 92:235-241.

Jenny, H., S.P. Gessel and T. Bingham. 1949. Comparative study on decomposition rates of organic matter in temperate and tropical regions. Soil Sci. 68:419-432.

LeBlanc, F. and J. DeSloover. 1970. The relationship between industrialization and the growth of epiphytic lichens and mosses in Montreal. Can. J. Bot. 48:1485-1496.

Likens, G. 1983. A priority for ecological research. Bulletin of the Ecological Soc. Am. 64:234-243.

McShane, M., D. Carlile and W. Hinds. 1983. The effect of sample size on forest literfall collection and analysis. Can. J. For. Research 13:1037-1047.

McShane, M., D. Carlile and W. Hinds. 1986. Needlefall in Pacific Northwest Forests: An evaluation of its use for detecting stress-related changes. J. of Environmental Monitoring (accepted).

Melillo, J., J. Aber and J. Muratore. 1982. Nitrogen and lignin control of hardwood leaf litter decomposition dynamics. Ecology 63:621-626.

Mitchell, R.G. 1977. Estimation of needle populations. USDA Forest Service Research Paper PNW-181.

Nakamura, T. 1984. Development of terricolous moss communities in subalpine coniferous forests on Mt. Fuji. J. Hattori Bot. Lab. No. 56:65-77.

National Atmospheric Deposition Program. 1985. NADP/NTN Report: Precipitation Chemistry: Fourth Quarter 1983. Natural Resource Ecology Laboratory, Colorado State Univ., Fort Collins, CO. 280 p.

Odum, E. and J. Cooley. 1980. Ecosystem profile analysis and performance curves as tools for assessing environmental impact. In Biological evaluation of environmental impacts, p. 94-102. U.S. Fish and Wildlife Service, Washington, D.C.

Olson, J.. 1963. Energy storage and the balance of producers and decomposers in ecological systems. Ecology 44:322-331.

Rahn, K.A. 1981. The Mn/V Ratio as a Tracer of Large Scale Sources of Pollution Aerosol from the Arctic. Atmospheric Environment 15(8):1457-1464.

Rapport, D., H. Regier and T. Hutchinson. 1985. Ecosystem behavior under stress. Am. Nat. 125:617-640.

Rhoades, F. 1977. Growth rates of the lichen Lobaria oregana as determined from sequential photographs. Can. J. Bot. 55:2226-2233.

Rhoades, F. 1983. Distribution of thalli in a population of the epiphytic lichen Lobaria oregana and a model of population dynamics and production. Bryologist 86:309-331.

Rieley, J., P. Richards and A. Bebbington. 1979. The ecological role of bryophytes in a North Wales woodland. J. of Ecol. 67:497-527.

Rühling, A. and G. Tyler. 1970. Sorption and retention of heavy metals in the woodland moss Hylocomium splendens. Oikos 21:92-97.

Singh, J. and S. Gupta. 1977. Plant decomposition and soil respiration in terrestrial ecosystems. Bot. Rev. 43:449-528.

Tamm, C. 1953. Growth, yield and nutrition in carpets of a Forest Moss (Hylocomium splendens). Meddelanden Fran Statens Skogsforskningsinstitut 43:1-140.

Tuominen, Y. and T. Jaakkola. 1973. Absorption and accumulation of mineral elements. In The Lichens, eds. V. Ahmdjian and M. Hale. p. 185-224. Academic Press, New York and London.

Waring, R. 1985. Imbalanced forest ecosystems: Assessments and consequences. For. Ecol. and Mgt. 12:93-112.

RELATING NATIONAL ATMOSPHERIC DEPOSITION PROGRAM DATA WITH A STUDY ON THE EFFECT OF EXTENDING THE ACTIVE GROWTH PERIOD OF AN ALPINE SEDGE

Richard B. Keigley[1] and Robert E. Porter[2]

ABSTRACT

An experimental treatment study of Kobresia myosuroides (Vill.) Fior et Paol. indicates that the ecologic importance of nitrate and sulfate deposition may exceed that of hydrogen ion deposition. The negative effect is hypothesized to result from the inhibition of natural dormancy at the end of the growing season. The NADP dataset provides an excellent baseline for comparing the results of experimental treatments with potential changes in the real world. However, in using the NADP dataset, loading rates may be underestimated if sample volume is used for calculation the calculation of deposition rather than values from the associated Belfort rain gauge. In Rocky Mountain National Park, maximum deposition and minimum pH occurs late in the growing season of alpine plants- a time that may have maximum adverse impact. The highest concentration of nitrate is associated with periods of low precipitation, a situation that may maximize uptake by shallow-rooted plants. The pH reported by the Central Analytical Laboratory may underestimate acidity in low pH samples.

INTRODUCTION

The objective of this paper is to discuss the implications of certain aspects of hydrogen, nitrate and sulfate deposition at Rocky Mountain National Park on Kobresia myosuroides (Vill.) Fior et Paol., a common alpine tundra sedge in the Colorado Front Range. Kobresia was selected for study because of its ecologic importance and because its populations are primarily maintained by vegetative reproduction (Bell 1979)- a characteristic that would would provide limited ability to recover from mortality caused by acid deposition.

Hydrogen, nitrate, and sulfate ions are the most important constituents of acid deposition. At high concentrations, hydrogen ions may produce lesions on plants (eg. Evans and Curry 1979) and at lower concentrations may influence physiological processes by inhibiting the availability of nutrients (eg. Shriner and Johnson 1981). However, Colorado Front Range soils are well buffered against changes in pH (Litaor in press) and modest increases in hydrogen ion deposition may not pose the most immediate environmental threat.

Instead, the increased deposition of nitrate and sulfate associated with acid deposition may have the most significant impact on vegetation. Both nitrate and sulfate are limiting factors in the Colorado Front Range alpine tundra, and plants would likely respond to increased deposition of those ions with an increase in growth. However, growth late in the growing season may adversely affect survival. Sakai and Otsuka (1970) found that plants collected while actively growing showed little ability to withstand freezing, while plants collected after entering dormancy were freeze resistant. The increased deposition of nitrate and sulfate late in the growing season may encourage growth when plants should be preparing for dormancy.

The effect of a potential change in the atmospheric deposition of nitrate and sulfate can be predicted, once the response of the plant to those variables is determined under controlled conditions using existing deposition rates as the experimental baseline. Weekly data, such as those published by the National Atmospheric Deposition Program (NADP) give the researcher an excellent opportunity to relate experimental treatments with meaningful environmental data.

The specific objectives of this paper are to discuss:

1. how the efficiency of sample collection influences the calculation of deposition,

2. seasonal periodicity of the deposition of strong acid ions,

3. the the relationship between nitrate deposition and the weekly level of precipitation, and

4. the difference between the pH measured by the field operator and the pH reported by the NADP Central Analytical Laboratory (CAL) that performs the chemical analysis of the precipitation samples.

RESPONSE BY KOBRESIA TO EXPERIMENTAL TREATMENT

As part of the University of Colorado Long Term Ecological Research program, the author investigated the effect of treatments that may encourage the growth of Kobresia late in the growing season (Keigley unpub). The field experiment was conducted on Niwot Ridge at the University of Colorado Mountain Research Station.

Nitrate and sulfate were applied weekly as KNO_3 and K_2SO_4 at multiples of 2.5, 5.0, and 10.0 times the mean loading rates reported by Grant and Lewis (1982) (Table 1). Potassium nitrate was also applied once early in the growing season at levels of 0.5, 5.0, and 50.0 g/m^2.

Table 1. Nitrate and sulfate applied as KNO_3 AND K_2SO_4 in experimental treatments. Data in (mg/m^2/wk).

	TREATMENT LEVEL		
	LOWEST	INTERMEDIATE	HIGHEST
NO_3^-	35.9	95.8	215.4
$SO_4^=$	42.1	112.2	252.5

In general, fertilization at a single time, early in the growing season produced an increase in net productivity that was sustained over the four years of the study. In contrast, plants fertilized weekly at the intermediate and highest levels in Table 1 responded with a change in net productivity that implies future mortality.

The precipitation chemistry data are from the Rocky Mountain National Park, Beaver Meadows NADP site located at an elevation of 2490 meters approximately 13 km east of the Continental Divide. The precipitation samples are collected by an Aerochem Metrics Model 301 Automatic Sensing Wet/Dry Precipitation Collector. A moisture sensor controls the position of a sheet of anodized aluminum covering one of two buckets. By exposing one or the other of the buckets, a sample can be taken of either dry deposition or deposition occurring during a precipitation event. The data described in this paper are from wet samples only.

RESULTS AND DISCUSSION

Calculation of Deposition Rate

The accurate determination of baseline deposition is essential in determining the potential environmental impact of changes in deposition. Deposition is calculated by multiplying the concentration of an ion by the amount of precipitation occurring during the sample period. The Preliminary Report distributed by the Central Analytical Laboratory gives two values of precipitation: one based on the sample volume caught in the wet bucket and one based on a standard Belfort rain gauge that is located adjacent to the Aerochem sampler. The deposition values presented in the Preliminary Reports are based on sample volume rather than on the rain gauge value.

If precipitation measured by the Belfort rain gauge is accepted as accurate, the ratio established by dividing the sample volume in the Aerochem collector (converted to inches of precipitation) by the inches of precipitation measured by the Belfort rain gauge provides a means of evaluating sample collection efficiency. Small values of the ratio would indicate that the Aerochem sampler underestimated precipitation. The ratio over the sample period is plotted in Figure 1. Values of less than 1.0 are common, especially during the winter. Use of sample volume, rather than Belfort rain gauge values may significantly underestimate deposition.

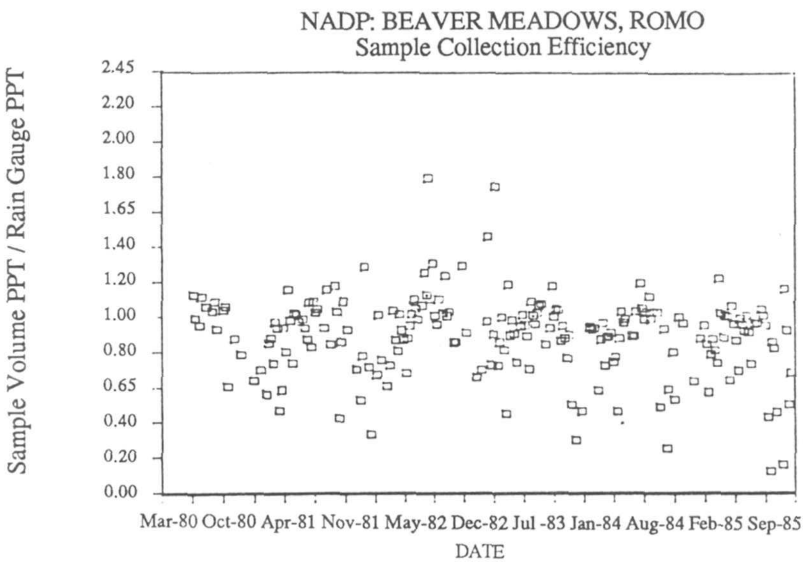

Figure 1. Ratio of sample volume precipitation to Belfort rain gauge precipitation plotted against time.

The mean deposition rate for each of the reported cations and anions was calculated using rain gauge precipitation (Table 2). The pH values were transformed to concentration before averaging and back transformed to mean pH.

Table 2. Deposition rates based on rain gauge precipitation. Data are in ($mg/m^2/wk$).

PERIOD: JUNE 10, 1980 THROUGH SEPTEMBER 23, 1985

Ca	Mg	K	Na	NH_4	NO_3	Cl	SO_4
2.33	0.42	0.50	0.72	2.15	9.91	1.12	9.49

MEAN ANNUAL PRECIPITATION: 36.9 cm

MEAN pH: 4.99

Seasonal Periodicity of pH and Nitrate

Graphs of both pH and nitrate deposition show a seasonal periodicity (Figures 2 and 3). Lowest pH and highest nitrate deposition tend to occur at mid-to-late summer. Mean hydrogen ion concentration was calculated from pH values and was significantly higher during the growing season months of June, July, and August than at other times of the year ($P<.001$). The mean pH during the growing season was 4.78 compared to 5.11 at other times of the year.

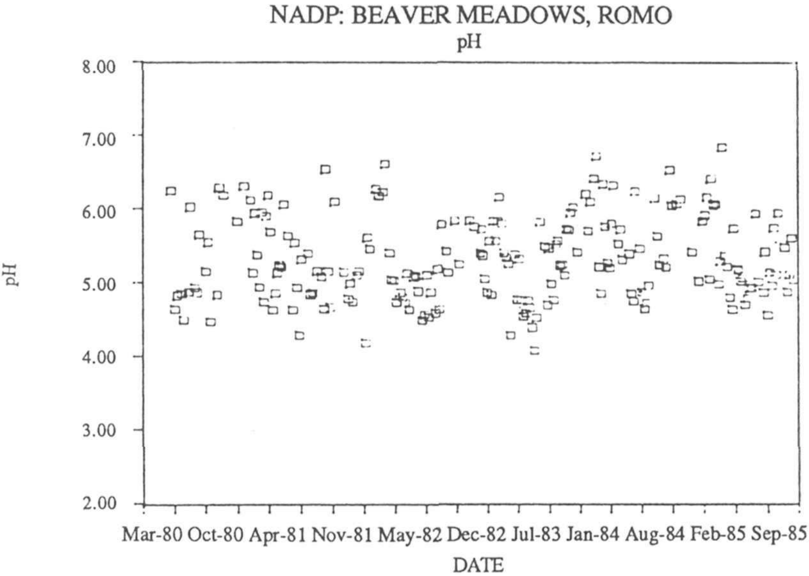

Figure 2. Seasonal variation in pH.

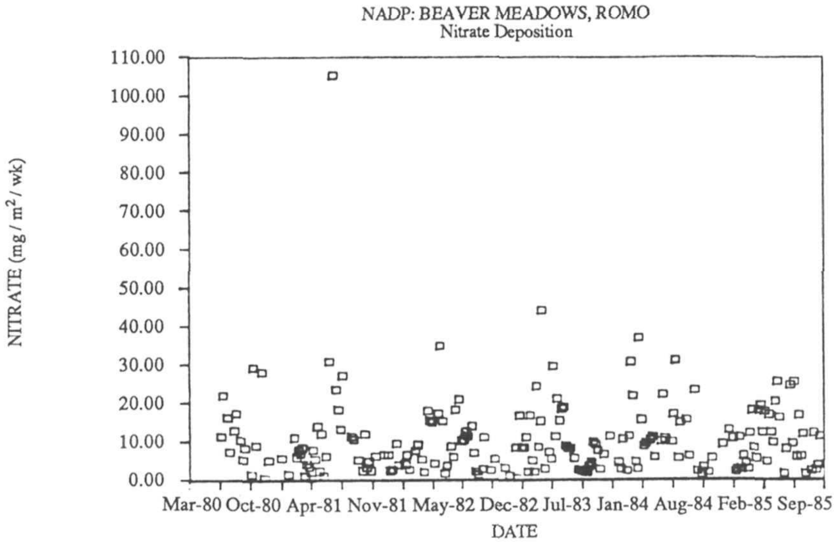

Figure 3. Seasonal variation in nitrate deposition.

Similarly, the mean nitrate deposition of 15.21 $mg/m^2/wk$ during the growing season months was significantly greater than the mean deposition of 7.51 $mg/m^2/wk$ occurring at other times of the year. Table 3 summarizes nitrate and sulfate deposition during June, July, and August for each of the years of the sample period.

Table 3. NADP nitrate and sulfate deposition rates during the growing season months of June, July, and August. Data are in ($mg/m^2/wk$).

	1980	1981	1982	1983	1984	1985
NO_3^-	14.5	26.0	12.4	14.8	13.0	12.6
$SO_4^=$	12.5	23.8	12.1	12.4	13.0	11.1

Weekly Precipitation Level and Nitrate Deposition

Kobresia has fine fibrous roots that are concentrated near the surface of the soil. Nitrate in precipitation would not be available when carried below the surface zone by infiltration or lost in surface runoff. The retention of precipitation near the soil surface would be maximized by frequent, light events. The highest nitrate concentrations are associated with weeks of low precipitation, a combination that maximizes the availability of the nutrient (Figure 4).

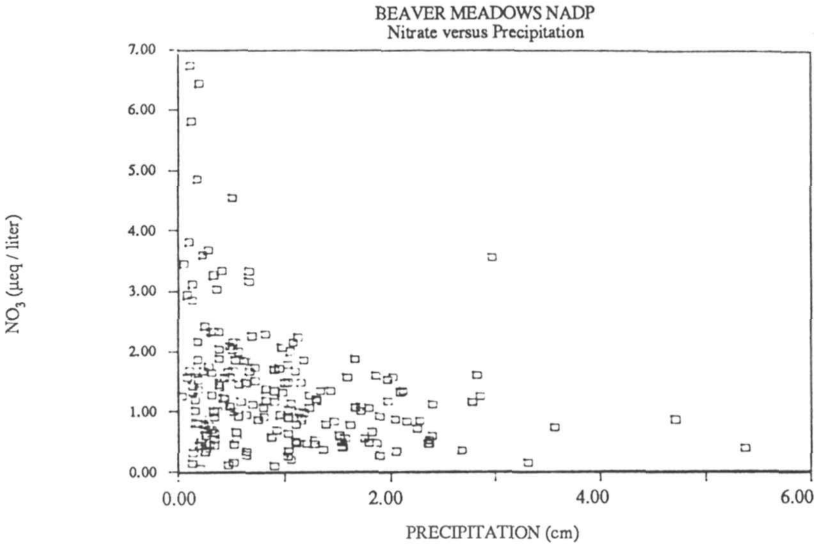

Figure 4. Association of high nitrate concentrations with low weekly levels of precipitation.

Accuracy of pH Determination

The NADP Preliminary Report gives two pH values: one is measured by the field operator immediately after collection of the sample and the other is determined by NADP Central Analytical Laboratory (CAL). The pH values were often substantially different; most frequently the field pH was lower than that reported by CAL. The difference between the two pH values (CAL pH minus field pH) was negatively correlated with the field pH ($r=-0.69$, $P<.01$, Figure 5). At high field pH values, CAL reported relatively lower values, while at low field pH values, CAL tended to report higher values. The Central Analytical Laboratory may underestimate acidity at low pH- a situation that is probably the most environmentally significant.

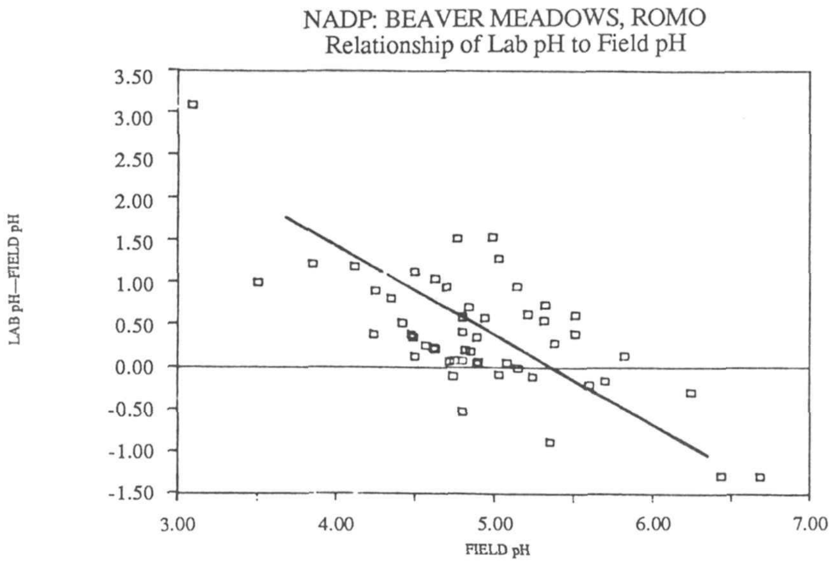

Figure 5. Correlation of pH measured in the field with the difference between pH measured in field and pH measured by the Central Analytical Laboratory.

LITERATURE CITED

Bell, K. and L.C. Bliss. 1979. Autecology of Kobresia bellardii: Why winter snow accumulation limits local distribution. Ecological Monographs. 49(4): 377-402.

Evans, L.S. and T.M. Curry. 1979. Differential responses of plant foliage to simulated acid rain. Botanical Review. 50(4): 449-490.

Grant, M. and W.M. Lewis Jr. 1982. Chemical loading rates from precipitation in the Colorado Rockies. Tellus. 34:74-88.

Litaor, M.I. The influence of eolian dust on the genesis of alpine soils in the Front Range, Colorado, U.S.A. Soil Science. (in press).

Sakai, A., K. Otsuka. 1970. Freezing resistance of alpine plants. Ecology. 51: 665-671.

Shriner, D.S. and J.W. Johnston. 1981. Effects of simulated acid rain on nodulation of leguminous plants. Environmental and Experimental Botany. 21(2): 199-209.

---

[1] Rocky Mountain National Park, Estes Park, Colorado.
[2] 24194 Sumac Dr., Golden, Colorado.

NOTES